Holocene Environmental History of Lake Chamo, South Ethiopia

Inaugural-Dissertation

zur

Erlangung des Doktorgrades

der Mathematisch-Naturwissenschaftlichen Fakultät

der Universität zu Köln

vorgelegt von

Tsige Gebru Kassa

Aus Äthiopien

Köln 2015

Berichterstatter: Prof. Dr. Frank Schäbitz

Prof. Dr. Helmut Brückner

Prof. Dr. Michael Bonkowski

Tag der mündlichen Prüfung: January 2015

Abstract

East African Rift Valley Lakes hold a rich source of information for palaeoclimate change. Specifically, the sediment archives of Lake Chamo, one of the Ethiopian Rift Valley Lakes, reveal short-term climatic fluctuations and environmental instability during the Holocene, since it is located in a temporary endorhëic system. Currently there are no substantial studies yet that investigate palaeoenvironmental history of Lake Chamo. The objective of this thesis is to reconstruct the Holocene climatic and environmental history of Lake Chamo at high temporal resolutions. The specific aim of the project is to estimate climate-driven and anthropogenic environmental change during the Holocene, and to test a hypothesis that there were rapid climate fluctuations during the termination phase of the "African Humid Period" (AHP).

Initially, the first continuous and high-resolution geochemical and geophysical core data from the sediments of Lake Chamo using X-Ray Fluorescence (XRF) core scanner and Geotek Multi-Sensor-Core-Logger (MSCL) respectively, is presented. Using these techniques palaeoclimatic conditions of the region during the Holocene are reconstructed. Additionally, the core chronology is established using Accelerator Mass Spectrometry (AMS) radiocarbon analysis, the results of which show that the core dates back to 9000 cal yr BP. Early-Holocene can be seen to be characterised wetter climatic conditions as recorded from the relative lower lightness values, high Silicon to Titanium ratio (Si/Ti), and minimum calcium concentration in the sediment. Pronounced peak in calcium and Strontium content, which are the main features of the early-mid Holocene transition period, are ascribed to a high evaporation to precipitation ratio, implying the aridity of the region in this time frame. In addition, the peak values of magnetic susceptibility (MS), Potassium (K), Titanium (Ti), Silicon (Si), and Iron (Fe) during 1500–800 cal yr BP are found to be associated to a change in intensity of anthropogenic land use in the area surrounding the lake.

Subsequently, the charcoal counting and detection of benzene polycarboxylic acids (BPCA) methods are implemented to estimate paleofire occurrence in relation to climatic and anthropogenic impact of Lake Chamo. These results are used to correlate the long term trends in fire occurrence in relation to climate, vegetation and human activities at different spatial and temporal scales. Fire occurrence was found to be higher during the early Holocene, typically identified through black carbon (BC) from woody or shrub vegetation sources. The occurrence of fire was found to be lower during the mid-Holocene, due to the presence of predominantly grass savannah which usually results in reduced biomass burning in response to drier condition. Climate and vegetation were found to be the main factors for fire occurrence during the early and mid Holocene, whereas the increased fire intensity since 2000 cal yr BP record is potentially attributed to anthropogenic forcing.

Finally, ostracod analyses are used to gain evidence about climatic and hydrological instability of southern Ethiopia during the Holocene. The ostracod study focuses on the taxonomy, stratigraphy and the use of ostracod assemblages to interpret the palaeoenvironments established during Holocene period. Ostracod assemblages were found to be infrequent and of limited diversity in the sediment profile, implying a period of wetter conditions. The highest abundance and more diverse ostracod assemblage were found to be associated with periods of drier climatic condition in the Lake Chamo records.

To summarize, the geophysical, geochemical, charcoal, and ostracod data analysis, alongside core chronology results of this thesis have been used to reconstruct Holocene climatic and environmental history of Lake Chamo region, and of the East Africa region as a whole. The main results of this study provide significant input for the understanding of climate variability in the Holocene, as well as identifying termination of the African human period was gradual in Lake Chamo region.

Zusammenfassung

Seen aus dem Ost-Afrikanischen Grabenbruch enthalten reichhaltige Informationen zu Klimaveränderungen in der Vergangenheit. Insbesondere das Seesedimentarchiv des temporär endorëhischen Entwässerungssystems des Chamo Sees, der zu den Äthiopischen Riftseen zählt, bietet die Möglichkeit, kurzzeitige Klimafluktuationen und Umweltveränderungen während des Holozäns zu identifizieren. Bisher gibt es noch keine Untersuchungen, die die Umweltgeschichte des Chamo Sees mithilfe seiner Sedimente klären. Deshalb ist das Ziel dieser Doktorarbeit, die Klima- und Umweltgeschichte des Chamo Sees in großer zeitlicher Auflösung für das Holozän zu rekonstruieren. Insbesondere soll der Frage nachgegangen werden, wie groß der natürliche und anthropogene Einfluss auf die Umweltveränderungen im Holozän war und ob die Hypothese eines abrupten Endes der sogenannten, Afrikanischen Feuchtphase“ (AHP) für diese Region Gültigkeit hat.

Zunächst werden die kontinuierlichen und geophysikalischen Sedimentkerndaten des Chamo Sees vorgestellt, die mit der Röntgenfluoreszenzmethode (XRF) und dem Geoteck Multi-Sensor-Core-Logger (MSCL) gemessen wurden. Mithilfe dieser Methoden gelingt es, die paläoklimatologischen Bedingungen für das Holozän zu rekonstruieren.

Das Alter der Sedimente von ca. 9000 Jahren wurde mittels der AMS-Radiokohlenstoffanalyse ermittelt und anschließend kalibriert. Das Früh-Holozän zeigt durch die Kombination von relativ niedrigen Helligkeitswerten, einem hohen Silizium/Titanverhältnis und minimalen Ca-Gehalten der Sedimente feuchtere Klimabedingungen an. Deutlich erhöhte Gehalte an Kalzium- und Strontium, die als wichtiges Merkmal in der Übergangsphase zum Mittel-Holozän auftreten, werden als Zunahme des Verdunstungs-/Niederschlagsverhältnisses interpretiert und deuten auf größere Trockenheit in diesem Zeitraum hin. Darüberhinaus zeigen hohe Werte der magnetischen Suszeptibilität, des Kaliums (K), des Titans (Ti), des Silikats (Si) und des

Eisen (Fe), die im Zeitraum von 1500 bis 800 Jahren vor heute auftreten, einen größeren Einfluss des Landwirtschaft betreibenden Menschen in der Umgebung des Sees an.

Weiterhin werden die Anzahl der Holzkohlepartikel und das Vorhandensein von Benzen Polycarbonsäure (BPCA) genutzt, um das Auftreten von Feuern in der Vergangenheit zu dokumentieren und ihre klimatischen oder anthropogenen Ursachen zu differenzieren. Diese Ergebnisse werden genutzt, um eine Korrelation zwischen dem Langzeittrend der Feueraktivität sowie der Klima- und Vegetationsentwicklung, aber auch des menschlichen Einflusses auf verschiedenen räumlichen und zeitlichen Skalen herzustellen. Danach lässt sich ein größeres Auftreten von Feuerereignissen während des Früh-Holozäns feststellen, das sich durch, Black Carbon“ (BC) von Bäumen und Sträuchern zu erkennen gibt. Im Mittel-Holozän dagegen nimmt die Feuerhäufigkeit ab, es herrschen verbrannte Savannengräser vor, die auf eine reduzierte Biomasse aufgrund größerer Trockenheit hindeuten. Das Klima und die Vegetation sind die wichtigsten Faktoren für das Auftreten von Feuern im Zeitraum vom Früh- zum Mittel-Holozän, während die Zunahme der Feuerintensität in den letzten 2000 Jahren vor heute wohl hauptsächlich dem zunehmenden menschlichen Einfluss zuzuschreiben ist.

Schließlich wurde die Analyse von Ostrakoden genutzt, um Hinweise auf klimatische und hydrologische Instabilitätsphasen während des Holozäns für Südäthiopien zu gewinnen. Zur Interpretation der Paläoumweltbedingungen wurden die Ostrakoden taxonomisch analysiert, Ostrakodengemeinschaften identifiziert und stratigraphisch eingeordnet. Während feuchter Klimabedingungen sind Ostrakodengemeinschaften seltener und zeigen eine geringere Diversität. Dagegen treten große Ostrakodenvorkommen und eine höhere Diversität in trockeneren Phasen des Chamo Sees auf.

Zusammenfassend kann man sagen, dass die geophysikalischen und geochemischen Befunde sowie die Holzkohle- und die Ostrakodenergebnisse zur Rekonstruktion der Klima- und Umweltgeschichte der Region um den Chamo See sowie Ostafrikas genutzt werden können. Dadurch wird das Verständnis zur Klimavariabilität des Holozäns dieser Region erweitert und nachgewiesen, dass das Ende der AHP allmählich erfolgte.

Acknowledgements

Firstly, I express my gratitude to my primary supervisor Prof. Dr. Frank Schäbitz, for his unreserved and continuous advices which enabled me to complete my studies. Also I extend my thanks to Dr. Finn A.Viehberg for his advice on ostracod analysis, as well as Prof. Dr. Michael E.Weber, Dr. Asfawossen Asrat, Prof. Henry Lamb, Dr.Mohammed Umer†, Prof. Dr. Janet Rethemeyer, Dr. Giday WoldeGabriel, and Dr. Tamrat Endale who's feedback has been vital for this study's progress.

I also want to thank Oliver Langkamp and Wolfgang Frank for their contributions during coring, Johannes Jakob and Andreas Holzapfel who were involved in MSCL data processing; Nicole Mantke for sample preparation; Frederik von Reumont for graphics; Hanna Cyszienski for the SEM work; Prof. Koen Martens for his advices and providing his literatures; Dr. Eva Lehndorff and Dr. Mareike Wolf for the analysis of black carbon; and finally Dr. Ute Frank and Dr. Maxwell Brown for palaeomagentic analysis.

The German Science Foundation in the framework of the Collaborative Research Center 806 "Our way to Europe" deserves recognition for funding this project. I am grateful to the School of Earth Sciences of Addis Ababa University, authorities of the Nechisar National Park and the community around, and Department of Geology and Mineralogy of University of Cologne for their technical and material supports during the research period.

Finally, I am indebted to Pro. Valery J. Terwilliger and Dr. Hailu Gebru Kassa for their unconditional advices and suggestions. I thank my colleagues Jean-Pierre Francois, Karsten Schittek, Verena Foerster, Jonathan Hense, Kostas Panagiotopoulos, Diana Becker, Jan Wowrek, and Jonas Urban for they created peaceful and stimulating working atmosphere. Their contributions improved the quality of this work meaningfully.

Abbreviations

ACB	Abaya-Chamo Basin
AHP	African Humid Period
AMS	Accelerator Mass Spectrometry
BC	Black Carbon
BP	Before Present
BPCA	Benzene PolyCarboxylic Acid
Ca	Calcium
CAB	Congo Air Boundary
$CaCO_3$	Calcium Carbonate
Cal yr BP	Calendar Year Before Present
CRC	Collaborative Research Centre
EA	Elemental Analyzer
EARS	East African Rift System
ENSO	El Niño- Southern Oscillation
ERVL	Ethiopian Rift Valley Lake
Fe	Iron
ITCZ	Intertropical Convergence Zone
LIA	Little Ice Age
K	Potassium
MER	Main Ethiopian Rift
MS	Magnetic Susceptibility
MSCL	Multi-Sensor-Core-Logger
MCA	Medieval Climate Anomaly
NNP	Nechisar National Park
SEM	Scanning Electron Microscopy
Si	Silicon
SOM	Soil Organic Matter

Sr	Strontium
SST	Sea Surface Temperature
Ti	Titanium
TIC	Total Inorganic Carbon
TOC	Total Organic Carbon
XRF	X-Ray Fluorescence

Table of Contents

Table of Figures

Figure 5.16. *Stenocypris minuta* (A-B); *Hemicypris intermedia* (C-F); *Sclerocypris Clavularis* Sars (G-H); *Psedocypris bouvieri* (I-L); ***S. minuta***: A. left valve, external view; B. right valve, internal view. ***H. intermedia***: C. left valve, external view; D. right valve, external view; E. left valve, internal view; F. right valve , internal view. ***S. Clavularis* Sars**: G. juvenile, right valve, external view; H. juvenile, left valve, external view. ***P.bouvieri***: I. right valve, external view; J. left valve, external view; K. left valve, external view; L. right valve, external view. Scale A-F = 100 µm; G-H = 300µm; I-J=100 µm. .. 104

List of Tables

Chapter 1

1. Introduction

1.1 General introduction

The structure and evolution of East Africa's rift during the younger Quaternary are thought to have led to the region having a high sensitivity to climatic changes, particularly the many alternations between wet and arid periods which have occurred. The climatic alternations may have, in turn, influenced human societies. Understanding and reconstructing environment and its interactions with human society in this tropical region has been complex because of frequent fluctuations in climate. Determining the impact of major climatic influences on the environmental dynamics for long time scales is crucial to understand the impact of humans in highly populated regions, such as those found in East Africa.

The reconstruction of regional climate and environmental dynamics is predominantly dependant on reliable and well-constrained proxy archives, such as the hydrological sensitive lakes of equatorial East Africa. Morphological and stratigraphic data, along with extensive radiocarbon datings from Ethiopian Rift Valley Lakes (ERVL), have been acquired during the last decades (Grove et al., 1975; Gasse, 1977; Gasse and Street, 1978; Street and Grove, 1979; Gillespie et al., 1983; Gasse and Fontes, 1989). These data can be used as valuable archives for the investigation of past climatic, environmental, tectonic, volcanic, and evolutionary changes over long time scales (WoldeGabriel et al., 1991; Le Turdu et al., 1999; Yirgu et al., 2006). WoldeGabriel et al. (2000) initially identified that ERVLs have volcaniclastic sediments containing faunal and floral remains which can be used to identify hominid habitation, palaeoanthropological, and archeological evidence sites. Recently, the potential for this use of ERVLs has led to a research focus in these areas.

Lake Chamo, the chosen study site, is one of these Main Ethiopian Rift (MER) lakes. Situated within the southern Ethiopian Rift Valley, and part of the tectonically active East African Rift System (EARS) (Figure 1.1), Lake Chamo and its sediment record have great potential to reconstruct palaeoclimate and palaeoenviromental conditions of the region. Additionally, Lake Chamo is found in a temporary endorhëic system. Of particular note is that, even though Lake Chamo is located in a tectonically active region, the influence of tectonic processes during the Holocene period is minimal. Hence, as a result, the sediment from Lake Chamo is well preserved and can give reliable climatic information. In addition, the proximity of the lake to the well known archeological site called “Moche Borago” and to the lower Omo valley, where the oldest known Homo sapiens fossils were found, meaning the Lake Chamo region holds a promising source of information on the history of human settlement and dispersal through the region.

As mentioned earlier, Lake Chamo as one of the ERVLs is an interesting palaeoenvironmental research site. One such research project is a collaborative, multidisciplinary research project entitled: CRC-806 “Our Way to Europe”, which aims to investigate the role of climatic and environmental changes in the last 200,000 years on population dynamics, mobility, and cultural development of early modern humans from a key part of Africa, specifically the source area of human dispersal into Europe and Asia. Moreover, this thesis, embedded in A3 project, which is subproject of CRC-806, intends to obtain quantifiable records from Ethiopian lake sediments to investigate climatic and environmental changes, as well as its interactions with human society for longer time scales. In the first phase, Project A3, planned to find the most suitable place for deep drilling to take place to obtain sediments covering the past 200,000 years. Lake Chamo was among the many lakes tested for this purpose, but the lake sediments only record the last 9,000 years. But the results of this thesis, which come out of the history of the Holocene age, can meaningfully contribute to the far-reaching objective of the CRC project. To gain a comprehensive understanding of the environmental history of East Africa through the Holocene, a brief summary of previous research is presented in the following section.

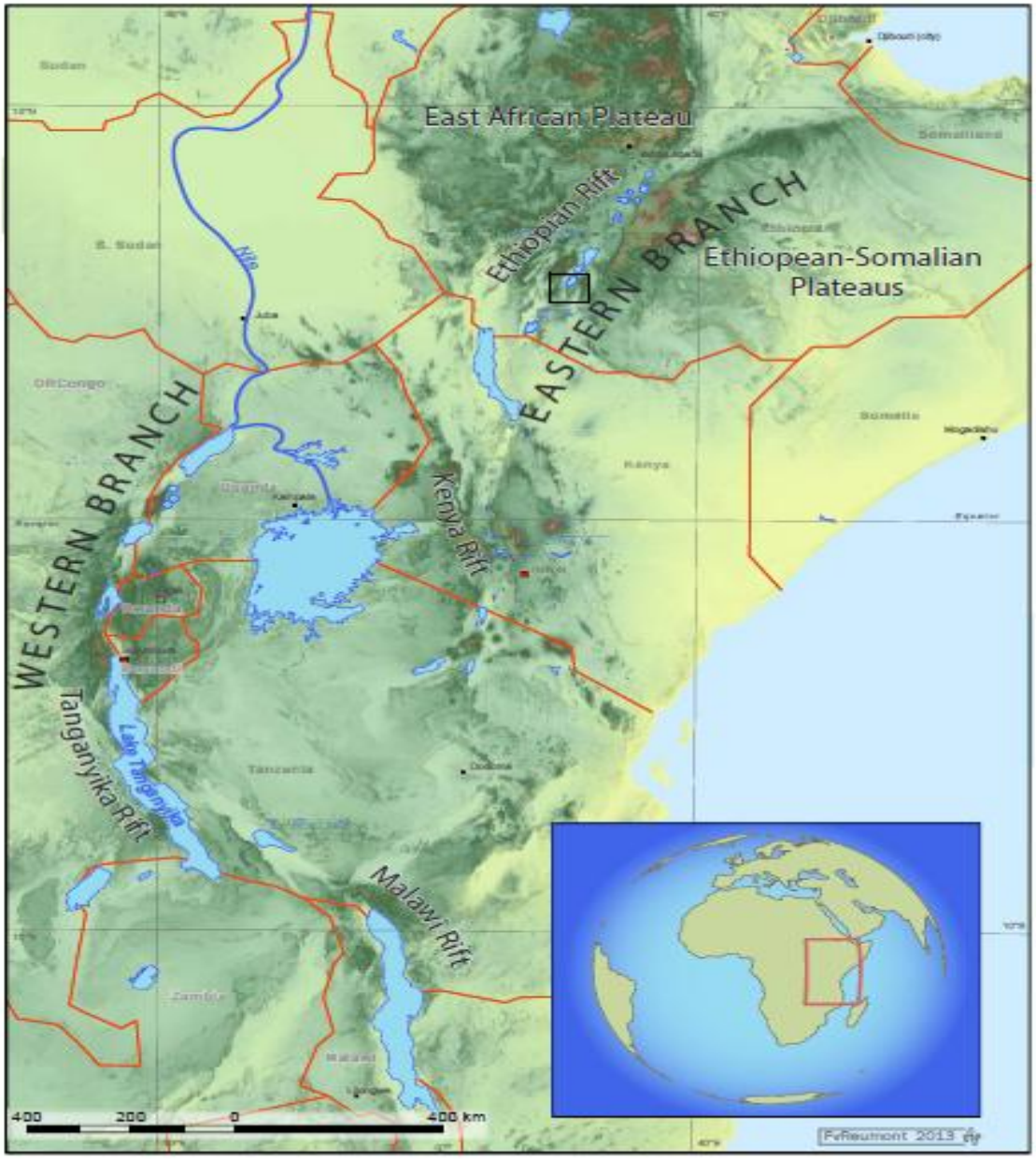

Figure 1.1. A map of the East African Rift System, showing the main Rifts of Eastern and Western branches. The study area, Lake Chamo, is within the black rectangle in southern Ethiopia.

1.2 Environmental history of East Africa during the Holocene

During the Holocene, the climate in tropical East Africa was characterized by fluctuations between wet and dry periods, controlled by orbitally-induced monsoon variability (Gasse, 2000; Verschuren, 2002; Junginger, 2011). Most of the East African Rift Valley Lakes (EARVLs) are endorhëic and their lake level records are among the best documented and most sensitive indicators of climate change in the region (Street and Grove, 1979). In Lake Ziway–Shala basin; diatoms, geochemistry, and pollen analysis from its sediment indicated the presence of wet phases and reveal that the four lakes seen at present were one lake during the early Holocene (Grove et al., 1975; Gillespie et al., 1983). Similarly, the lacustrine sediment analyses from Lake Abhé indicate a high lake level during the early Holocene (Gasse, 1977; Gasse and Street, 1978). In addition, diatom and oxygen isotope analyses in Northern Ethiopia from Lake Ashenge sediment confirmed that the lake was overflowing and at its highest level during this period (Marshall et al., 2009). The presence of wetter conditions during the early Holocene is also indentified by the presence of a higher level of fresh water up to 5400 cal yr BP, shown in diatom evidence from Lake Abiyata (Chalié and Gasse, 2002). The lake-level records of Lake Abhé and Ziway-Shala provide the primary evidence for arid intervals which interrupted the generally humid early-mid Holocene climate in the Ethiopian Rift. More specifically, from ca 8.4 - 8 ka and 4.2 - 4 ka BP a worldwide distribution of major dry spells occurred in Africa with different regional expressions (Gasse, 2000).

In addition to lake sediments, many other studies have also identified climatic variations in the region during the early Holocene. Among these, the presence of abundant and evenly distributed rainfall in southern Ethiopia during this early to mid-Holocene has been found through an increase in arboreal pollen (Mohammed and Bonnefille, 1998). More recently, Terwilliger et al. (2013) analyzed stable hydrogen isotopic ratios (δD) of land-plant derived fatty acids (n-$C_{26–30}$) and other proxies from soil sequences, and found the record for the highest rainfall prior to ca 6000 cal yr BP from Northern Ethiopia. Buried charcoalized wood identifications and percentage of organic carbon from C_4 plants (% C4 carbon) and

from $\delta^{13}C$ values of bulk organic matter in the soils of gully walls and in the travertine dam of Tigray Plateau (Northern Ethiopia) (Gebru et al., 2009; Terwilliger et al., 2011) also suggest that prior to 5500 cal yr BP the climate was wetter than the subsequent time period. Peat and buried soil deposited in travertine dammed basins in the Tigray region (Berakhi et al., 1998; Dramis et al., 2003) and multi-proxy speleothem records from the southeast Ethiopian highlands and adjoining rift margins (Asrat et al., 2007; Baker et al., 2010) are a further line of evidence which indicates a relatively wet climate during the early Holocene.

On the other hand, variations in C/N ratio and $\delta^{13}C$ contents of bulk organic material from Lake Tilo (south-central Rift Valley) suggested that the termination of the humid climate occurred at around 5100 cal yr BP (Lamb et al., 2004). In the same lake, Lamb et al. (2000) also showed the presence of more arid condition during the mid Holocene transition and an abrupt increase in $\delta^{18}O$ values at 4800 cal yr BP. Similarly, increment of $\delta^{18}O$ and $\delta^{13}C$ records of Lake Awassa around 5500 cal yr BP (Lamb et al., 2002) and a sharp decrease in Lake Ziway-Shala water levels during 5700 – 5100 cal yr BP potentially indicate the onset of aridity (Gillespie et al., 1983). This climatic signal is broadly recorded in tropical African sites with lowering of lake levels from ~5500 cal yr BP onwards (Stager et al., 1997).

During the mid to late Holocene, dry conditions on a millennial scale are a common feature of tropical Africa. These dry conditions affected the entire East African region, identified from the sediment record of ERVLs (Gasse, 1977; Gasse and Street, 1978; Gillespie et al., 1983; Gasse and Fontes, 1989; Telford and Lamb, 1999; Lamb et al., 2000; Chalié and Gasse, 2002; Lamb et al., 2002; Lamb et al., 2004) as well as from other several East African Great lakes, including Lake Edward (Russell and Johnson, 2005), Lake Turkana (Johnson et al., 1991; Halfman et al., 1994; Ricketts and Johnson, 1996), Lake Victoria (Stager et al., 2003), and Lake Tanganyika (Cohen et al., 2005; Stager et al., 2009). Marked aridity in Ethiopian speleothem records for these periods (Asrat et al., 2007; Baker et al., 2010) also show aregional expression of this dry event.

Low lake levels existed during the whole mid and late Holocene, except some lakes with short high stands. Among these, Lake Abhe´ dried out rapidly in the mid Holocene with a

rise of lake level at around 3800 – 1600 cal yr BP (Gasse, 1977; Gasse and Street, 1978; Gasse and Fontes, 1989) and Lake Shala at around 1900 – 1400 cal yr BP (Gillespie et al., 1983), indicated a temporary reverse to wetter condition during the late Holocene.

During the Medieval Climate Anomaly (MCA) from 1000 – 1300 AD, equatorial East Africa was broadly represented by relatively drought condition (Verschuren et al., 2000; Darbyshire et al., 2003) but during the Little Ice Age, (LIA) from 1500 – 1800 AD, relatively wet conditions were found (Russell and Johnson, 2007).

All the aforementioned studies give information about the climatic history of East Africa, whilst also identifying the need for further study through the use of high spatial and temporal resolution data to better understand these highly variable environmental conditions. Based on the implication of these studies, this thesis is designed to understand environmental change and its impact on human societies during the Holocene, which will provide an insight into the influence of environmental change on human population over a much longer time scale. The sediment core from Lake Chamo provides additional results about the timing and process in East African climate changes during Holocene. This study is significant because, other than a recent investigation of the physical parameters of Lake Chamo and its adjacent Lake Abaya (Awulachew, 2006; Schutt and Thiemann, 2006; Gebremariam, 2007; Belete, 2009), there are no other continuous, high resolution, and well-dated records from Lake Chamo to reconstruct Holocene environment. Therefore, this thesis investigates the sedimentological, geophysical, geochemical, and biological climate-proxy data extracted from lacustrine sedimentary climate archives of Lake Chamo to gain information about the climatic variability, as well as anthropogenic influences on the region.

The research presented here outlines the importance of multi-proxy indicators to explore a range of potential proxies for the interpretation of climate signals registered and stored in the sediment during the Holocene. In this context, the high-resolution records used here distinguish between regional and site-specific trends, whilst also providing the key to differentiate past climatic- and anthropogenic-induced changes in southern Ethiopia. In this multi-proxy study, all proxies show significant variation which could be show sensitivity to

prevailing climatic and environmental shifts. Among these, variations in geochemical elements and the down core changes in mineral composition which are obtained from high-resolution XRF core scanner and from Geotek Multi-Sensor-Core-Logger (MSCL), respectively, indicate major climatic changes in Lake Chamo sediment. In addition, long term trends in fire occurrence in relation to climate, vegetation and human activities are estimated by two independent methods; charcoal counting and detection of benzene polycarboxylic acids (BPCA) (Brodowski et al., 2005; Wolf et al., 2013). Macroscopic charcoal counts and an organo-geochemical characterization (BC quantity and quality by the BPCA method) of fire residues studies provide preliminary evidence in this study area. Therefore, particularly as this study differentiates between human-induced and natural fires, how humans are dispersed from their origin and affected by the changing climatic condition is revealed. Furthermore, a detailed chronology of climatic and environmental shift in the Lake Chamo region is also recorded from ostracod analysis. All these analytical methods, together with core chronology established using AMS radiocarbon analysis, have allowed a succession of sedimentary units to be defined which are interpreted as a series of fluctuations in climate and human impact in East Africa.

1.3 Aim and objectives of the thesis

This study is designed to better understand millennial time-scale climatic variability, as well as to study the anthropogenic influences on the environment, in Southern Ethiopia. Ultimately the study aims to fill the gap in the knowledge on environmental changes of the Holocene in East Africa. Orbitally-induced changes in summer solar radiation account for the Holocene climatic variability (Gasse, 2000) and for the termination of “African humid period” in the region. The role of orbital forcing in climate change over the early-mid Holocene and observed environmental changes after this period is currently not well explained in this region. Our high resolution multi-proxy data sets from Lake Chamo helps to estimate the climatic fluctuation of the Holocene and contributes to resolution of the discussion on abrupt or gradual termination of the AHP in East Africa.

The overall aim of this PhD thesis is therefore to determine the response of the Lake Chamo archives in tropical East Africa to historical climate-driven and anthropogenic environmental change during the Holocene. Since little is known about the palaeoenvironment and palaeoclimate condition in the southern Ethiopia Rift Valley lakes, and in particular Lake Chamo, this study is the first in its kind which employs sedimentological, geochemical, geophysical, and palaobiological analyses of sediment cores for this purpose in this region.The data obtained from this lake will contribute in filling the gaps in knowledge on climatic variability of the Holocene in East Africa.

Therefore, the first specific objective of this thesis is to reconstruct Holocene environmental history of Lake Chamo using the first continuous, high-resolution geophysical, geochemical and sedimentological core data. In addition, this research specifically tests a hypothesis that there were rapid climate fluctuations during the termination phase of the "African Humid Period" (AHP).

The second specific objective of this thesis is to make palaeoclimate estimates for paleofire occurrence in relation to climatic and anthropogenic impact of the region. The last objective is to identify significant autecological changes of ostracod fauna to provide a preliminary base on which to reconstruct palaeoenvironmental conditions, by implementing a quantitative and high-resolution analysis of shifts in ostracod fauna and investigate the climate variability of the Holocene period.

In order to accomplish these objectives, a field campaign was carried out in November-December 2010. After undertaking a bathymetric survey of the northern area of Lake Chamo (Figure 1. 2), sediment cores (CHA-01-2010) long core and 7 short cores were obtained. Geophysical, geochemical, and palaecological analysis was undertaken for the long core.

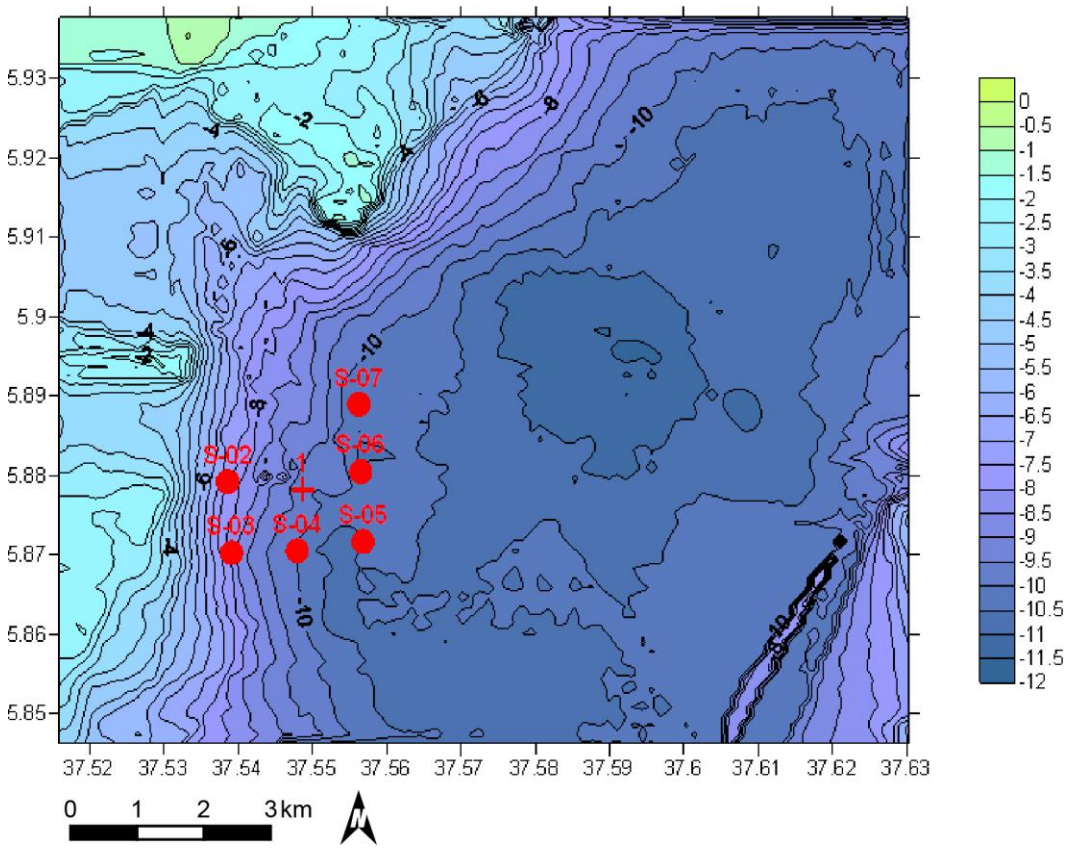

Figure 1.2. The bathymetry of Lake Chamo, collected during the field campaign of November-December 2010 showing the coring sites of long core (CHA-01-2010) and short cores (CHA-01- SC1 to SC7). Scale for both axes (Geogr. Coordinates) and the depth scale in (m).

1.4 Outline of the Thesis

This thesis is presented in six chapters. The focal points of each chapter are presented below.

In the **first chapter**, a general introduction and theoretical background about the paleoenvironment reconstruction of East Africa, and particularly Lake Chamo, are presented. In addition, the objective and the design of the study are presented in this chapter.

Chapter 2 focuses on the description of the study area. A brief description of geographical setting, geology of the area, review of regional recent climate, human settlement history,

flora and fauna, along with the chemical composition of the Lake, are discussed in order to get an overall understanding of the nature and climatic conditions of the lake and its region.

In **Chapter 3**, the lithological, sedimentological, geochemical, and physical properties from Lake Chamo core are discussed in detail, to examine climatic and environmental fluctuations of the Holocene from different sedimentary units in the record.

In **Chapter 4**, two independent methods; charcoal counting and detection of benzene polycarboxylic acids (BPCA) from Lake Chamo which enable us to analyze complex interactions among climate, vegetation and human, are presented. Both methods provide an enlightening base to understand fire activity over long time scales and to estimate the paleofire intensity and frequency in relation to climate, ecosystem structure, human use of land, and thus human development.

Chapter 5 outlines the taxonomy, stratigraphy, and the use of ostracod assemblages that are used to interpret the palaeoenvironments. Moreover, it presents Geometric morphometric analyses for *Limnocythere* species that were applied to complement the classical morphological observations during the identification phase.

Lastly, **Chapter 6** states final conclusion and synthesizes the environmental conditions of the different Holocene stages based on the main results of this research works. Suggestions for future research are outlined in particular for Lake Chamo and in a broader content for East Africa.

Chapter 2

2. Study Area

2.1 Geographical setting of Lake Chamo

Lake Chamo is found in southern Ethiopia and is part of the Main Ethiopian Rift system (WoldeGabriel et al., 2000), located specifically in the Lake Abaya-Lake Chamo basin. Lake Chamo lies at 5.82°N and 37.57°E, south of Lake Abaya, east of the Guge Mountains, and close to the city of Arba Minch (Figure 2.1), at an elevation of 1,235 m above sea level. The lake has a surface area of 551 km^2 and it is a shallow lake with a maximum depth of up to 13 m (Kebede et al., 1994). Groundwater springs (called "Arba Minch" or "forty springs") feed both the Chamo and Abaya lakes. The lakes were previously connected via surface streams (Awulachew, 2006). Currently the Kulfo river (Figure 2.1) flows from the rift margin to the west of Lake Abaya; a few kilometres before reaching Lake Abaya where it abandons its old valley joining Lake Abaya and flows south towards Lake Chamo following a recent NE-SW oriented fault. At high stands, the outflow from Lake Abaya feeds Lake Chamo via the River Kulfo. The River Metenafesha forms the outlet from Lake Chamo at its east shore, joining the Sermale stream, which flows south from the uplands south of Lake Abaya. These two streams are tributaries of the Sagan River which flows south and ultimately drain into the Chew Bahir Basin.

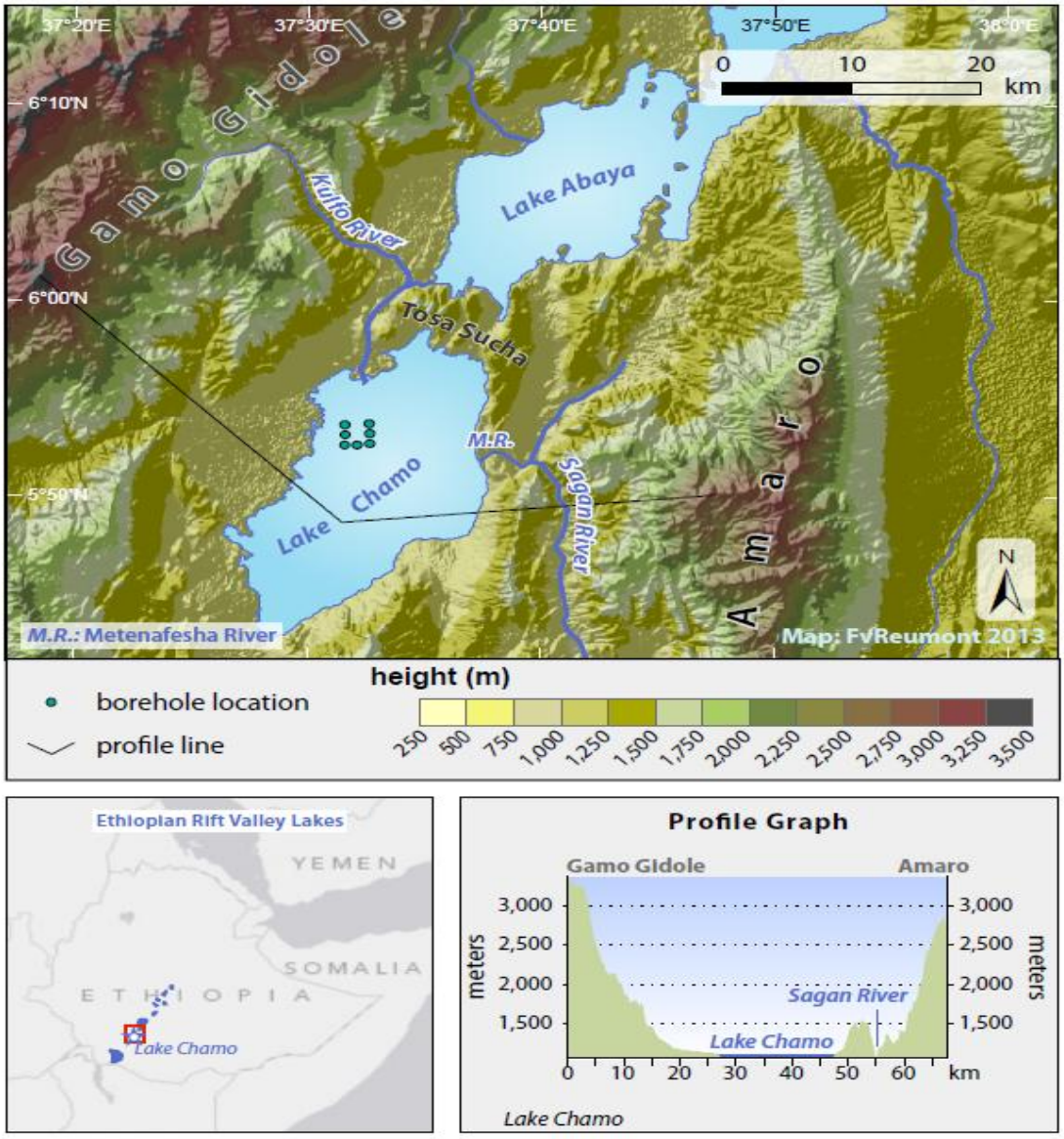

Figure 2.1. A map of Ethiopia showing the location of Lake Chamo and other Ethiopian Rift Valley lakes mentioned in this project. Lake Chamo tributaries are also shown, as well as the core site and the fault-bounded Chamo basin, between the Gamo-Gidole horst to the west and the Amaro horst to the east.

2.2 Recent climate of Lake Chamo region

East African rainfall and climatic variability depend on sea surface temperature (SST), atmospheric winds, the El Niño Southern Oscillation (ENSO), and regional climate fluctuations in the Indian and Atlantic Oceans (Gasse, 2000; Baker et al., 2007; Diro et al., 2009; Segele et al., 2009). The latitudinal variation of the Inter Tropical Convergence Zone (ITCZ) across the equator, monsoonal wind systems from the Indian and Atlantic Oceans, and complex topography also contribute to strong seasonal variation in precipitation and climatic fluctuations in Equatorial East Africa.

Seasonal to interannual variability of rainfall in Ethiopia is associated with the monsoonal wind systems from the Indian and Atlantic Ocean and ENSO events (Conway, 2000; Seleshi and Zanke, 2004; Segele and Lamb, 2005; Diro et al., 2008; Segele et al., 2009). The strong summer rain (locally known as Kiremt) which originate in the Atlantic Ocean and spring (Belg) rains from Indian Ocean are major moisture sources for Ethiopian rift lakes. The northward movement of the ITCZ from June to September dominates the atmospheric circulation, resulting in summer rainfall, bringing wet winds from the Indian and Atlantic Oceans which converge to produce a high summer rainfall in the Ethiopian highland region. Conversely, during its southward movement between November and February (Bega), dry weather leads to dry winter in most parts of East Africa. The movement of ITCZ over most parts of Ethiopia is attributed to teleconnections with ENSO (Seleshi and Zanke, 2004) and most El Nino years are found to correlate with below-average main (summer) rainfall, whereas ENSO enhances the belg rainfall (small rainfall season) in the interior of the country. Specifically, in the Chamo-Abaya basin, the annual average precipitation pattern over the thirty year period (1970-2000) showed a relationship between the ENSO events and lake level changes and served as an evidence for a general trend of low lake level during the occurrence of ENSO event (Figure 2.2) (Schutt and Thiemann, 2006).

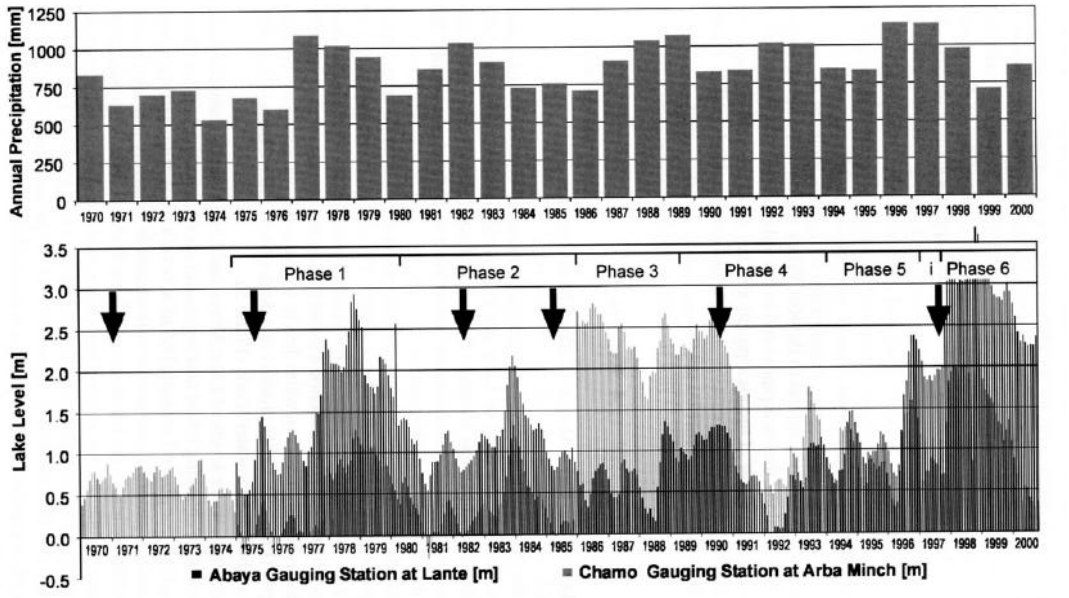

Figure 2.2. Annual average precipitations in the Abaya-Chamo Basin since 1970 (top) and monthly average lake levels of Lake Abaya (since 1977) and Lake Chamo (since 1970); arrows mark ENSO events (bottom) (Schutt and Thiemann, 2006).

The local climate of the Chamo basin ranges from semiarid to subhumid due to variations in topographical elevation. The dependence of precipitation on altitude in the basin is characterised by higher precipitation in the mountainous region when compared to the rift valley (Schutt and Thiemann, 2006). The annual oscillation of the ITCZ in Africa towards an extreme northward location of 15 °N in July and an extreme southward location of 15 °S in January lead towards a bimodal rainfall pattern in southern Ethiopia (Diro et al., 2009). Therefore, Lake Chamo basin is also characterized by a bimodal annual rainfall distribution with "big" spring (March-April-May-Mid June) rains and "small" rains in September and October. The summer (June - August) and winter months (November - January) are the driest months in the Chamo basin, according to rainfall records at Arba Minch. Average annual rainfall in the region ranges from 521 mm at Bilate, north of the Abaya-Chamo lakes, to 2105 mm at Chencha, situated on the adjoining highlands to the west. At Arba Minch station, the average minimum and maximum monthly rainfall is 34.5 mm (January) and 170 mm (April), respectively. From October to February the weather is predominantly characterized by hot and dry weather. Mean annual temperature varies between 14.5 ˚C

(September to November and April to June) and 33.2 °C (February and March) (Belete, 2009) at Arba Minch station.

Long term precipitation change was a primary cause of Holocene lake level fluctuation in tropical Africa (Grove et al., 1975) and the current lake levels of Lake Chamo and Lake Abaya still vary with the prevailing precipitation pattern of the region (Schutt and Thiemann, 2006). The annual average precipitation pattern over the thirty year period (1970-2000) from 15 weather stations showed a direct relationship between precipitation amount and lake level in these two neighbouring lakes. Therefore, the presence of increased precipitation leads to wetter condition where the lake level tends to increase. On the other hand, low lake level could as a result of lesser rainfall, indicating dreir climate (Schutt and Thiemann, 2006) (Figure 2.2).

In addition to the movement of ITCZ, the eastwards longitudinal shift of the Congo Air Boundary (CAB) over East African plateaus (Nicholson, 1996) is also thought to control the current precipitation pattern in the region. The large-scale changes in the Atlantic and Indian monsoons lead to a shift in the position of the CAB which may cause large moisture gradients across equatorial Africa (Russell and Johnson, 2007).

2.3 Geology of the study area

The EARS is characterized by continental rifting and faulting, which reshaped the earth's surface either by producing sediment filled rift lakes or by rupturing of tectonic plates. These processes have developed the topography of East Africa considerably and may have influenced past human evolution (Yirgu et al., 2006). The topographic change between the Miocene (Tertiary) and Quaternary shaped the rift valley currently seen. Tectonic activities in and near these valleys formed a series of splits, which subsequently filled with water forming the African rift lakes (Crul, 1995).

The East African Rift Valley forms part of a series of fractures in the earth's crust extending from the Dead Sea in the north, via the Red Sea and the rifts of East and central Africa, to Mozambique in the south (Crul, 1995; Chorowicz, 2005; Yirgu et al., 2006). The EARS is

broadly divided into two branches; the eastern branch includes the Ethiopian rift, the Kenyan rift and a number of shallow saline lakes in Kenya and Tanzania up to the Malawi rift and is characterized by greater volcanic activity, the western branch extends from Lake Mobutu in the north to Lake Tanganyika in the south (Figure 2.3) and is characterised by deep basins which contain large lakes.

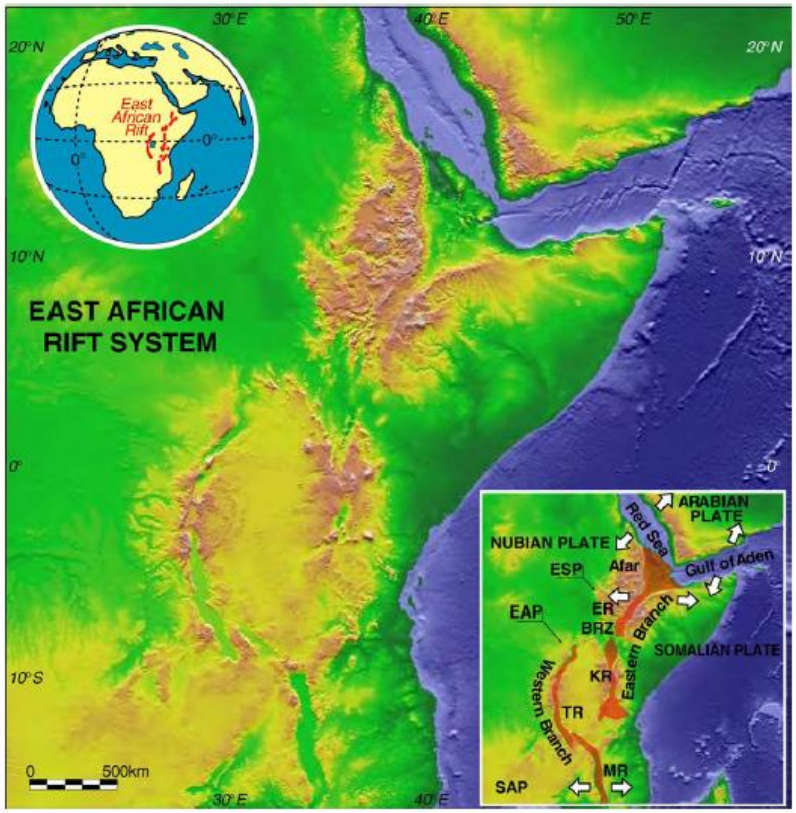

Figure 2.3. The East African Rift System. BRZ: Broadly Rifted Zone; EAP: East African Plateau; ER: Ethiopian Rift; ESP: Ethiopian–Somalian plateaus; KR: Kenya Rift; MR: Malawi Rift; SAP: Southern African Plateau; TR: Tanganyika Rift (From Corti, 2009).

From the end of the Tertiary period, the Ethiopian Rift Valley was formed by down faulting of the earth's crust which resulted in volcanism and transverse arching to the rift floor creating internal drainage basin (Grove et al., 1975; Ebinger et al., 1993). During this time, a proto-rift trough, fine grained water-laid tuffs and pumice beds were deposited continuously from Ziway- Shala basin to Awasa and then to the Abaya - Chamo basin (ACB) in the south (Grove et al., 1975). According to Grove et al. (1975), during the late

Tertiary period, all of the main Ethiopian Rift Valley lakes were joined and form one big lake, subsequently separating during down faulting of the rift and volcanism in the rift floor. During the late Pleistocene the current basin topography was created. Due to their underground interconnection by NE-SW united regional faults (Alemayehu et al., 2006) all of the ERVLs form a unique system within the rift and have similar hydrogeological settings. In the late Quaternary, both tectonic and volcanic activities in the Main Ethiopian Rift (MER) have been focused in the axial zones of the rift called the "Wonji Fault Belt" which originated in the recent Pleistocene (Grove et al., 1975; Benvenuti et al., 2002; Corti, 2009).

The MER is geographically divided in to three sections; northern, central and southern. The southern Ethiopian rift is further divided into Chamo basin to the west and Galana basin to the east, whilst they are symmetric along the Amaro horst (Ebinger et al., 1993; WoldeGabriel et al., 2000; Corti, 2009) (Figure 2.4). The land feature of the Chamo Basin shows big vertical differences over short distance between the rift floor and the basaltic highlands (Ebinger et al., 1993). The Lake Chamo rift floor is predominantly bounded by Pliocene-Holocene sedimentary rocks (Ebinger et al., 2000) which also indicates that a more recent extended Holocene fluvial deposits cover the ground at the base of the rift flank in this basin (Schutt and Thiemann, 2006).

The Chamo basin is bounded by a series of NNE-SSW oriented normal faults, forming the tectonic blocks of the Gamo-Gidole horst to the west and the Amaro horst to the east of the basin (Figure 2.4). The NE-SW elongated Chamo basin is separated from the Abaya (Ganjuli) basin to the north by the Tosa Sucha (Bridge of God ridge); a chain of Quaternary eruptive volcanic centers (Ebinger et al., 1993). To the north and northeast the lake is bordered by Quaternary basalt flows with minor trachytic tuff (the "Bridge of God" basalt), dotted by basaltic cinder and scoria cones (the "Chamo" cinder), porphyritic basaltic lava flows (the "Dagabulae" basalt), and basaltic lava cones (the "Segen" basalts) aligned along a general NE-SE direction. The faulted, cliff-forming eastern shore of the lake exposes Quaternary vesicular and porphyritic basalt (the "Nech sar" basalt) which underlies the Nech Sar plain east of the lake. The western and southern margins of the Chamo basin are

underlain by Palaeogene aphyric to porphyritic basalts forming prominent NE-SW faulted ridges. Deep normal faults at the southeastern margin of the Chamo Basin expose the Precambrian basement rocks made up of hornblende-biotite-quartz-feldspar gneiss intercalated with biotite-quartz-feldspar gneiss, which form a prominent, NNE-SSW elongated horst above the alluvium-covered floor of the Chamo basin. The western and southeastern shores of Lake Chamo are bordered by a 1 to 2 km wide plain of alluvial, lacustrine and swamp deposits. The Chamo basin formed during the mid Miocene when fluvio-lacustrine deposition began in the southern part of the basin. Fluvio-lacustrine sediments containing biostratigraphical fauna assemblages are found south of Chamo Lake in the Konso foothills (WoldeGabriel et al., 1991).

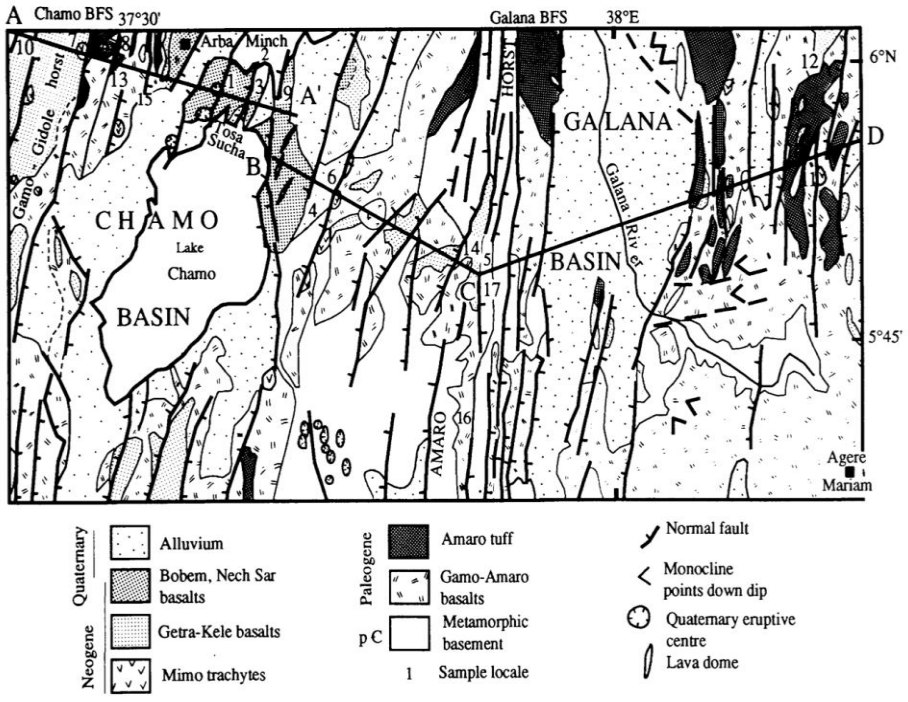

Figure 2.4. The geology of the area. Lake Chamo is surrounded by Quaternary alluvium sediment, Quaternary Bobem-Nech Sar basalts and a small part by paleogene Gamo-Amaro basalts. The rift valley floor of Lake Chamo is filled with alluvial and lacustrine sediment (From Ebinger et al., 1993).

2.4 Human settlement history and land cover/land use of the study area

Although there is considerable evidence about human population movements during Holocene times in the Horn of Africa (Lesur et al., 2014), the knowledge of early and middle Holocene hunter-gatherer population in the Horn of Africa is not adequate. However, this knowledge is very helpful to understand their impact on the environment and how population adapts rapidly to the new environments they encountered. Despite the limited archaeological work done in neighboring areas of Lake Chamo, the preliminary ethnoarchaeological and archaeological research work of Borada peoples on the highlands above Lake Abaya on the western edge of the Rift Valley (Arthur et al., 2010), give some hint about the settlement of human on the highland. The archaeological assemblages and dating along with oral history on this highland prove that the area has been settled since at least approximately 6400 years cal BP (Arthur et al. 2010). The assemblage and dating suggest that the area was occupied during the Pastoral Neolithic documented ca. 6500 cal yr BP in North Africa and 4000 cal yr BP in East Africa (Arthur et al. 2010), however, this preliminary study did not mention weather the settlers of this area were pastoralists or not. Especially, the Holocene occupation of the area in the lowland, where Lake Chamo is found, is not well documented. Therefore, more research is needed to show the settlement history of the area and to better understand the movements of population either from the highland to lowland or vice-versa.

Despite the recent archaeological and archaeozoological studies from Djibouti, Somalia, and southwest Ethiopia suggesting that pastoral societies emerged only at the beginning of the 2nd millennium BCE in the Horn of Africa (Lesur et al., 2014), the initiation of agricultural activity, and its impact, in southern Ethiopia is currently not well understood. However, the study done at Chencha–Dorze Belle, above the steep escarpment of the rift valley, has provided evidence that the stonewalled indigenous terraces have been long-lived agricultural activities in the region (Assefa and Bork, 2014). The radiocarbon ages from these terraces prove that they were built and used over the last 800 years (Assefa and Bork,

2014) and the area was cultivated during this time. The oral history from the elder people in Chencha– Dorze Belle about the history of the terraces and ancient landscape management practices infer that the terraces were as old as the agricultural activities in the area (Assefa and Bork, 2014). Therefore, their cultural heritage considered to be one of the oldest practices to manage the environment over generations for many centuries and leads to an enormous increase of land availability for cultivation. Arthur et al. (2010) also indentified many settlements on a mountain top which dated from the thirteenth to the nineteenth centuries and cattle were the dominant faunal species in association with their archeological assemblages, which implies livestock was also integrated in their agricultural system.

The study from Assefa and Bork (2014) explained about the significant changes of agricultural land use systems and forestland of Chencha and Arbaminch only during the last century. Their data indicate that cultivated land has increased by 39 % over the last four decades and about 37 % of grasslands in the highlands were converted to cultivated land from 1973 to 2006. The reports on forest cover from travelers or expeditions to the southern Ethiopia, in particular in Chencha and Arbaminch region, revealed that large-scale clearance and exploitation of forest resources first occurred in the region at the end of the nineteenth century (Assefa and Bork, 2014). According to the informants, both intensive cultivation and large-scale forest clearance started in the lowlands in the 1960s in association with recent settlement and cash crop farm expansion (Assefa and Bork, 2014). The establishment of the town of Arbaminch in the 1960s and mechanized agriculture that was launched in the Arbaminch area also exerted further pressure on the forest resources of the area. The result from satellite image analysis, field surveys, household interviews and group discussions on regional forest cover also show a 23 % decline from 1972 until 2006, with the most significant change from 1986 to 2006 (Assefa and Bork, 2014). Therefore, within the last hundred years, low agricultural production, coupled with high population growth, resulted in the massive conversion of forest and grazing land to cultivated land (Assefa and Bork, 2015). Currently, in the southern and western parts of Lake Chamo, subsistence farming has extensively altered natural woodland to cultivated land (Soromessa et al., 2004).

The farmers of the region practice both ox and hoe ploughing. Currently, hoe ploughing is dominantly exercised on the highland of the region as it is becoming inconvenient for ox ploughing as a result of increased fragmentation of land and its steep landscape. In the lowland part of the area both ox ploughing and rare mechanized farming are in use. Rain-fed agriculture is the main subsistence of the local people and small-scale irrigation is also practiced in limited part of the lowland (Assefa and Bork, 2015). Maize and sorghum are main crops in the rift floor whereas coffee, enset, and banana are cultivated through rain-fed agriculture and small-scale irrigation. The escarpment area is predominantly used for extensive pastoralism (Schutt and Thiemann, 2006).

2.5 Flora and fauna of the study area

The natural vegetation of the Rift Valley region is characterized by a savanna ecosystem. Open *Acacia* woodland in the neighborhood of the lakes, tall forest trees on the shoulders of the rift, grassland on the plateau, and tropical alpine vegetation in the high mountain areas are the main vegetation structure of the Rift valley region (Grove et al., 1975; Shibru and Woldu, 2006).

The northern shore of Lake Chamo lies in the Nechisar National park (NNP) where Acacia-dominated savanna grassland is the remnant of natural vegetation found in the rest of the Ethiopian Rift Valley region (Figure 2.5). An ecological survey carried out on the grassland plain of NNP indicated that the mean plant density cover was 31% of woody, 58% of grass, 68% of unpalatable forbs and121% of total herbaceous species per hectare of land (Yusuf et al., 2011). Yusuf et al. (2011) survey found Acacia species is the major encroaching woody species of the area. A protected natural swampy forestland of approximately 1 km width separates Lake Chamo from neighboring Lake Abaya (Schütt et al., 2002), thought to be natural savanna woodland which represents the natural vegetation of the upland areas. Gamo-Gidole and Amaro horsts are situated to the west and east of the lake respectively have relatively extensive vegetation cover. Most parts of the lake shore are covered by papyrus, which is the dominant vegetation type in a broad coastal wetland.

Figure 2.5. Natural Acacia dominated grassland in Nechisar National Park (Photo by Verena Foerster, Dec. 2010).

The lake has a natural blue color unlike Lake Abaya (Figure 2.6), which is attributed to the presence of dense papyrus wetland cover which filters the sediment input. The lake and its catchment are rich in fauna (Figure 2.7). The lake is fringed by wetlands which are used as grazing area for hippopotamus (*Hippopotamus amphibius*). The lake is rich in a variety of fish species, including tiger-fish (*Hydrocynus forskahlii),* giant Nile Perch *(Lates niloticus),* catfish *(Clarias gariepinus*) and tilaphia (*Oreochromis Niloticus)* (Admassu and Ahlgren, 2000; Dadebo and Mengistou, 2008; Dadebo, 2009; Tilahun and Ahlgren, 2010). Lake Chamo is also a sanctuary for several thousand Nile Crocodiles (*Crocodylus niloticus*). A number of bird species including Yellow wivers, white pelicans, and ibises are also found in the lake.

Figure 2.6. View of Lake Chamo from the north, Ethiopia. Top: Pelican over Lake Chamo (Photo by Verena Foerster, Dec. 2010).

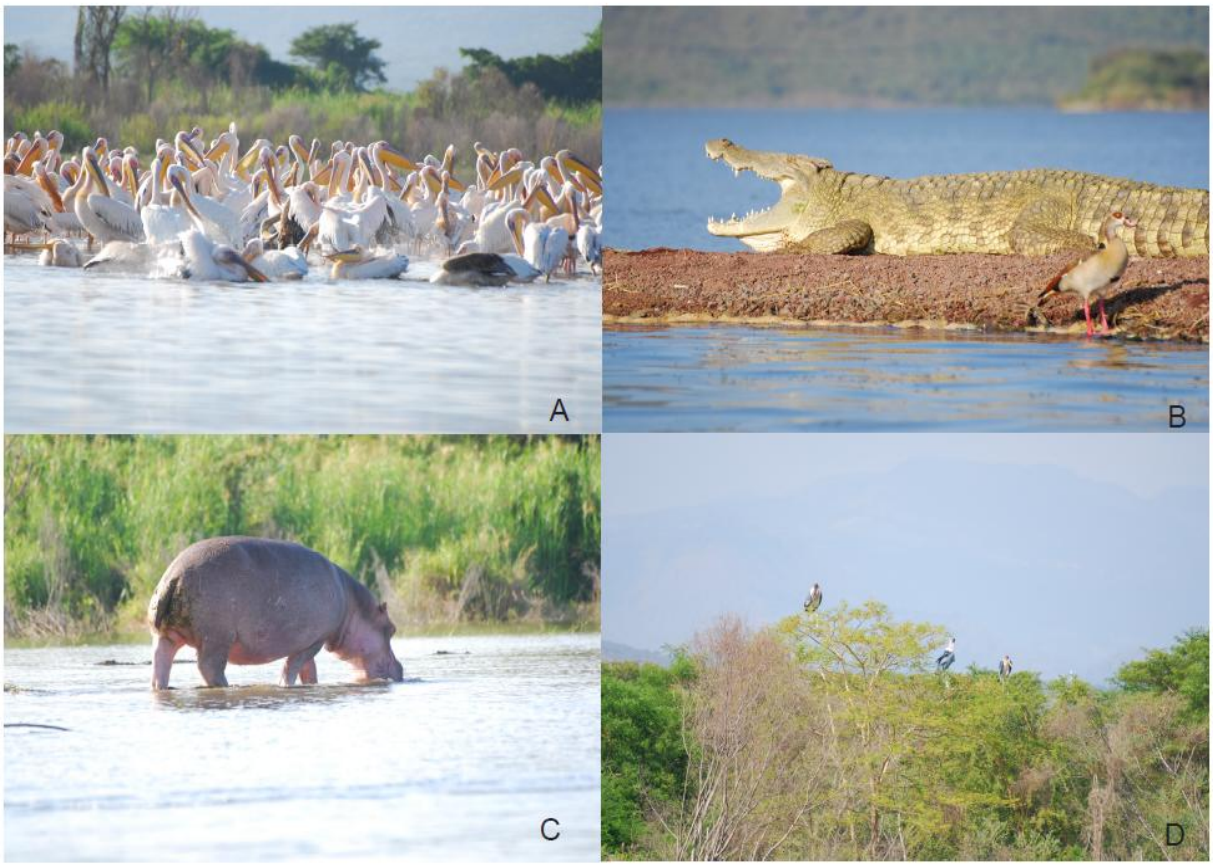

Figure 2.7. Biology of Lake Chamo. A), white pelicans B), Nile Crocodiles C), hippopotamus D), Hordes of yellow wiver birds (Photo by Verena Foerster, Dec. 2010).

2.6 The chemical composition of Lake Chamo

Ethiopian Rift valley lakes experience moist sub-humid to semi-arid climate with high evapotranspiration which has caused rainfall deficiency in the region (Kebede et al., 1994). The high evapotranspiration climatic condition lead to fluctuations in physical (lake level) and chemical (salinity and alkalinity) parameters of the lakes. The chemical compositions of lakes found in East Africa are extremely varied (Talling and Talling, 1965) and, as a consequence are important sites for investigating continuous environmental changes. The saline inflow from areas of volcanic activity and high evaporation contribute to the wide variability of total ionic concentration and alkalinity.

The alkalinity of East African lakes is monitored by the supply of carbonate and bicarbonate ions with Na, K, Ca and Mg (Lindroth, 1952; Talling and Talling, 1965; Cohen, 1983; Martens, 1990b; Mengistu, 2006). Chamo Basin shares this common feature due to its underlying basaltic rocks and in situ chemical weathering of the water shade, which are thought to enrich the amount of these ions. Most of the Rift Valley Lakes of Ethiopia are less saline and alkaline and have conductivity below 1500 µS/cm (Mengistu, 2006). They fall within a wide range of salinity-alkalinity series from fresh water (< 0.5 g/l) to mesosaline (20-50 g/l) conditions (Mengistu, 2006).

Lake Chamo has a pH of 8.9 and low values of soluble organic phosphate and soluble silicate, which could reflect their uptake by biotic communities including a high algal biomass of blue-greens and diatoms (Mengistu, 2006). Removal of silicate from solution in lakes dominated by large diatom populations also observed by Kebede et al. (1994) in lakes Zwai, Awassa, Chamo, and Abaya. Kebede et al. (1994) found that severe depletion of Si is commonly associated with increased diatom growth and lower dissolution rates of silicic acid from diatom frustules. The soluble silica in Lake Chamo was depleted over the past three decades despite the concentrations of soluble silica were generally high in other ERVLs (Kebede et al., 1994).

Chapter 3

3. Holocene environmental change recorded from geophysical and geochemical analyses of Lake Chamo sediments

Abstract

Rift valley lakes are a rich source of information on palaeoclimatic change. The sediment archives of Lake Chamo are a particularly rich archive of information on short-term climate fluctuations and environmental instability during the Holocene because they are found in a temporary endorhëic system. The sediment archive of Lake Chamo provides continuous and high-resolution lithological and geochemical evidences for dry-wet climate and lake-level fluctuations during the Holocene. Geophysical and geochemical data together with lithological analyses were used to define a succession of distinct sedimentary units. Humid conditions in the early to mid Holocene in Lake Chamo are inferred from high Si counts, poor calcite preservation, and relatively low lightness (L*) values. Small color changes of the core combined with high amounts of Ca and Sr content reveal a sequence of major dry periods during the transition from the early to mid Holocene. Carbonate deposition formed due to high evaporative concentration which result from prevailing dry conditions may indicate the low stands of the lake during this time. Frequent fluctuations between humid and dry periods reflect the changing conditions of oxidation /reduction reaction which may incur color changes during 2400 to 800 cal yr BP. High catchment inwash and deposition of terrigenous material at 1500 to 800 cal yr BP indicate periods of intensive erosion, which may vary as a function of both anthropogenic impact and climatic variability. Moderate values of geochemical data and higher values of "L*–a*–b*" color data from 800 cal yr BP to the present indicate the presence of dry conditions. As found by previous studies

conducted in the region, the records from Lake Chamo show major environmental changes during the Holocene using continuous and high resolution multi-proxy indicators.

3.1 Introduction

Ethiopian Rift Valley lakes are part of the EARS, where alteration of climatic conditions and many hominid fossils are documented. Due to frequent fluctuations in climate, reconstructing past environment in this tropical region has been complex. Wetter conditions than today prevailed during the early-mid Holocene, the so-called AHP punctuated by short arid intervals (Gillespie et al., 1983; Telford and Lamb, 1999; Lamb et al., 2000; Chalié and Gasse, 2002; Lamb et al., 2002; Lamb et al., 2004; Foerster et al., 2012). Although most of the studies in the ERVLs indicate a transition from early-mid to late Holocene, the time period for termination of the AHP in East Africa is debated. The XRF potassium record from Chew Bahir basin, the terminal drainage of Lake Chamo, indicates gradual termination of the AHP at 6000 - 5000 cal yr BP (Foerster et al., 2012). The organic geochemistry study in Lake Tilo, one of the south-central ERVLs, implies gradual vegetation changes, whilst the diatoms and $\delta^{18}O_{calcite}$ suggest an abrupt change to drier condition at almost the same time (5100 cal yr BP) of its termination (Lamb et al., 2004). Palaeotemperature data from Lake Turkana, Kenya, a nearby lake to Chew Bahir basin, also indicate a dramatic climate shift during the termination of the AHP (Berke et al., 2012). In a broader context, abrupt termination of the AHP is recorded in marine archives and climate modeling (Morrill et al., 2003; deMenocal 2005; Renssen et al., 2006; McGee et al., 2013) from Northern and Western Africa and Asia, whilst evidence from eastern Sahara indicates a gradual termination of AHP (Kröpelin et al., 2008).

Many studies from ERVLs document the presence of generally high fluctuations in climate during the Holocene period. The end of the early Holocene humid period sees a change to a more arid climate in the mid to late Holocene, recorded in diatom records (Telford and Lamb, 1999; Chalié and Gasse, 2002); C/N ratio, $\delta^{18}O$ and $\delta^{13}C$ records (Lamb et al., 2000; Lamb et al., 2002; Lamb et al., 2004) and lake level changes (Gasse, 1977; Gasse and Street, 1978; Street and Grove, 1979; Gillespie et al., 1983). All these studies have

established that the Holocene period was punctuated by several prominent and abrupt climate changes.

The present study uses high resolution, multi-proxy data sets to improve our understanding of the timing and magnitude of climate fluctuation in the region, to resolve the controversy over whether the termination of the AHP was gradual or abrupt. This knowledge will not only be of direct interest for only Lake Chamo, but will also provide basic information on palaeoclimate in East Africa during the Holocene. Despite investigation of the physical parameters of Lake Chamo and the adjacent Lake Abaya (Awulachew, 2006; Schutt and Thiemann, 2006; Gebremariam, 2007; Belete, 2009), there is no record of the Holocene environmental history of Lake Chamo. This study presents the first continuous and high-resolution geophysical and geochemical core data from the sediments of Lake Chamo. Further, it tests the hypothesis that there were rapid climate fluctuations during the termination phase of the AHP at about 5100 cal yr BP. The results show that the region remained relatively wet throughout the early Holocene and gradually responded to mid Holocene aridity.

3.2 Methods

3.2.1 Core recovery

Seven short cores and a 17 m long sediment core (CHA-01-2010) were obtained from Lake Chamo in November-December 2010, with gravity and UWITEC piston corers operated from a floating platform. The long cores were retrieved at a 10.3 m depth of the lake. Although the bathymetry of Lake Chamo (Figure 1.2) and the report of Kebede et al. (1994) indicated that the water depth reaches to a maximum of 13 m, it was not possible to core from the deepest section of the lake as it is in the restricted part of the Nechisar National park. However, the utmost effort was exerted to reach the deep site of the lake by getting close to the park as possible. The coring was sectioned in to individual core parts of 2 m length from the 17 m core overlap for about 50 cm (Figure 3.1). The cores were

retained in plastic liners and cut into 100 cm segments in the field, sealed, and shipped to the University of Cologne for further analyses. The cores were stored at 4°C until analysis.

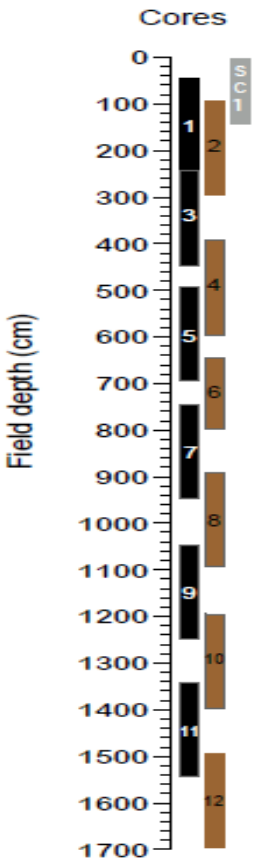

Figure 3.1. Schematic representation of the 17 m long core with an overlap of 50 cm among successive coring depths.

Sample preparation and analyses were conducted in the Institute of Geography and Institute of Geology and Mineralogy at the University of Cologne (Germany) laboratories. In order to prepare the lake sediment for analyses, core liners were grooved using a pair of vibrating medical cast saws mounted over a sliding core cradle. Utility knives and fishing line were used to complete the cuts through the liners and to split the sediment into working and archive halves. Sediment surfaces were cleaned with glass microscope slides, and then prepared for imaging and description. The lithostratigraphy was described by Munsell soil

color chart and texture was determined by a semiquantitative finger test to differentiate between finer and coarser material.

3.2.2 Core logging: Geotek Multi-Sensor-Core-Logger

The cores were scanned on a Geotek Multi-Sensor-Core-Logger (MSCL) to measure geophysical properties and obtain high-resolution down-core data from the sediments. The split and scraped clean cores were covered with thin plastic films to avoid contamination of the different sensors during scanning. The cores were then analyzed for physical sediment parameters including magnetic susceptibility, wet bulk density, p-wave velocity, and color on MSCL (Weber et al., 1997). These measurements were taken at 1 cm intervals along the entire length of the core, thus providing a continuous record of sediment changes. Color measurements were carried out with a photospectrometer using the "L*–a*–b*" color system which provides three color values for each measurement (Weber, 1998; Weber et al., 2010), whereby L* is white-black (i.e., grey scale), a* red-green, and b* yellow-blue variability. This color system covers the whole spectrum perceived by human eye and it includes the mode colors of both RGB (Red-Green-Blue) and CMYK (Cyan-Magenta-Yellow-Black) (Debret et al., 2006). Debret et al. (2011), indentified through the use of the Q7/4 diagram, which compares the ratio of the reflectance between 700 and 400 nm with sediment lightness (L*) in order to determine sediment structure and facies. Furthermore, this color system showed the presence of down-core changes in mineral composition, which were used as palaeoenvironmental tool. In this sense, L* provides an estimate for either organic carbon or carbonate; in most cases darker sediments indicate the presence of organic matter whereas lighter colors indicate carbonate materials. The a* value indicated the redox state and b* yielded information about the iron oxide content (Weber, 1998; Weber et al., 2010).

3.2.3 XRF analysis

Cores were evaluated using ITRAX X-ray Fluorescence Core Scanner after the principle of (Jansen et al., 1998) to quantify the inorganic elemental composition and down-core

chemical property variation of sediments. Split halves of cores CHA-01-2010 have been scanned with the XRF core scanner. The sediments were covered by a special (1.5 µm) thin plastic sheet in order to avoid desiccation during XRF scanning (Jansen et al., 1998). The scanner was operated at 2 cm resolution with 20 s scan time using a chromium (Cr) X-ray source set to 30 kV and 30 mA (Croudace et al., 2006). The results produced by the ITRAX scanner are outputs as counts per minute (cpm) and elemental intensities are considered to be proportional to elemental concentrations. According to Jansen et al. (1998), clay sediments provide more reliable results than silt and sandy sediments. Similarly, due to the presence of organic rich clay deposit throughout the entire core in Lake Chamo, the XRF data can give reliable results. This could be a good source of data for the down core chemical variation that give valuable information about sedimentological and diagenetic processes. The raw XRF data was converted into elemental count with the Q-spec software, which is provided with the ITRAX system (Croudace et al., 2006). The measured data was saved on the computer during the process of scanning in the form of the ".txt" files and subsequently edited with Microsoft Excel (Rothwell and Rack, 2006). The ITRAX core scanner provided many elemental scans but only those which have important palaeoclimatic significance are discussed.

The ITRAX XRF core scanning has numerous advantages and great potential for palaeo-environmental research as compared with conventional geochemical analysis. Among these XRF core scanning provides continuous, high resolution, and non-destructive elemental composition within a short period of time (Jansen et al., 1998; Croudace et al., 2006; Rothwell and Rack, 2006). Based on this, elemental intensities are obtained directly at the surface of a split sediment core. The non-destructive optical and X-radiographic images offer high resolution elemental profiles that are important for guiding sample selection for further detailed sampling. However, obtaining a semi-quantitative data and the difficulty to convert outputs to elemental concentration could be taken as limitations of the ITRAX XRF core scanning. On the other hand, the wet chemical method provides exact elemental concentrations which are basics for quantitative applications.

3.2.4 Core correlation

To select the appropriate sediment section from available overlapping core sections multiple parameters were used simultaneously to achieve an optimal match. Correlation of core sections was made based on core description, geochemical, geophysical and palaeomagnetic parameters. To analyze the sensor data from MSCL along with images of the cores (See Appendix A), CORELYZER software (www.corewall.org) was used. Among the parameters, magnetic susceptibility was used as example to show how the core correlation was done (See Figure 3.2). ANALYSERIES software version 2.0.4.2 (Paillard et al., 1996) was applied for depth-merging and integrating cores using the principle used by Weber et al. (2010). Emphasis was also given to density of geophysical parameters because Weber (1998) and Zolitschka et al. (2002) found that density is strongly affected by changes in sediment composition and could be most promising for stratigraphic correlation. In addition, geochemical data from the XRF measurement was considered during the correlation process. Furthermore, the correlation and age chronology were controlled by the results of detailed palaeo- and rockmagnetic analysis of the cores, which were performed in collaboration with the Potsdam GFZ team.

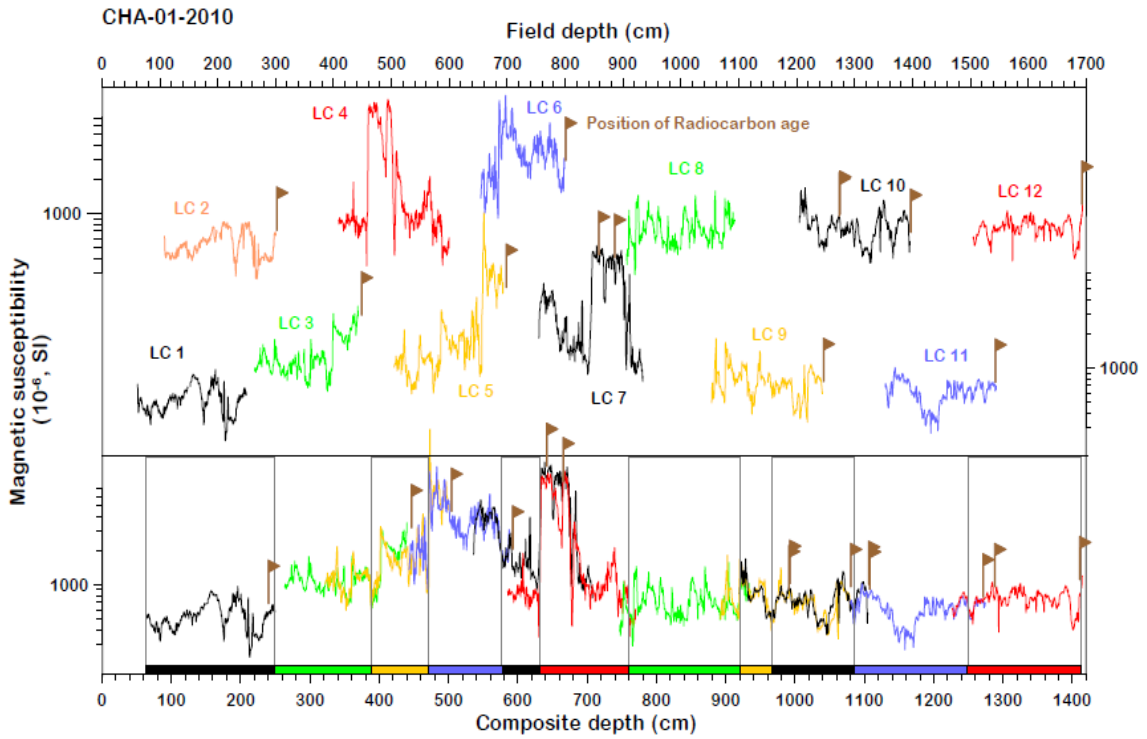

Figure 3.2. Showing the correlation of the overlapped segments of the cores using the magnetic susceptibility measurement (Plotted by Ute Frank).

Once the core correlation was done, the core was sampled continuously at 1-cm intervals over its length. Samples for charcoal and ostracods were taken based on their requirements. The detailed sample preparations of each method are presented in Chapters 4 and 5.

3.2.5 Radiocarbon analyses

The core chronology was established using AMS radiocarbon analysis of plant material (four samples), shell (two samples), bulk (two samples) and one ostracod sample. All radiocarbon ages were determined at the centre for Accelerator Mass Spectrometry (AMS) Laboratory in university of Cologne, Germany. Descriptions of the pretreatment methods used can be found in Rethemeyer et al. (2013). Briefly, plant remains were treated with diluted acid and alkali to remove inorganic carbon and humic acid, respectively. Shell and ostracod samples were treated with diluted H_2SO_4 to remove the outermost part of the shell.

Organic samples were converted to CO_2 by combustion, using an elemental analyzer. Carbonates were hydrolyzed with H_3PO_4 in septum sealed vials under a He atmosphere. The CO_2 was converted to graphite with H_2 and iron as catalyst. Radiocarbon analyses were performed with the 6 MV Tandetron AMS at the University of Cologne. ^{14}C concentrations and conventional radiocarbon ages were reported in percentage of modern carbon (pMC) and years before present (BP), respectively, calculated according to the formulas of Stuiver and Polach, (1977). Calendar ages were established by calibration with CALIB #6.0.1 (Stuiver and Reimer, 1993; Stuiver et al., 2005), and the Intcal 09 dataset (Reimer et al., 2009). The age versus depth model was performed using Bacon age-depth model (Blaauw and Christen, 2011). In order to facilitate comparison of our data with other regional studies, all the radiocarbon timescale from the original literature were changed into calibrated ages.

3.3 Results

3.3.1 Core correlation and chronology

The coring process was problematic due to the presence of high speed wind which makes the platform unstable. As a result field depths of overlapping sections were hard to define during coring. However, cores were taken in overlapping sections to avoid possible gaps between two consecutive cores. From the overlapping core sections, the sections used for the correlation and for the composite were identified (Table 3.1) based on core description, geochemical, geophysical and palaeomagnetic data. The overlapping core sections were correlated and after the depth merging and integration, a total of 14.13 m composite depth (CD) was obtained (Figure 3.3).

Table 3.1. The segments used for correlation, the total length used and the depths in composite.

	Segment used for correlation			**Depth in composite**	
Core	from (cm)	to (cm)	length (cm)	from (cm)	to (cm)
SC1	12	65	53	12	65
LC1	66	250	184	66	250
LC3	251	389	138	251	389
LC5	574	655	81	390	471
LC6	686	782	96	472	568
LC7	781	844	63	569	632
LC4	460	587	127	633	760
LC8	916	1076	160	761	921
LC9	1079	1123	44	922	966
LC10	1248	1366	118	967	1085
LC11	1359	1522	163	1086	1249
LC12	1529	1692	163	1250	1413

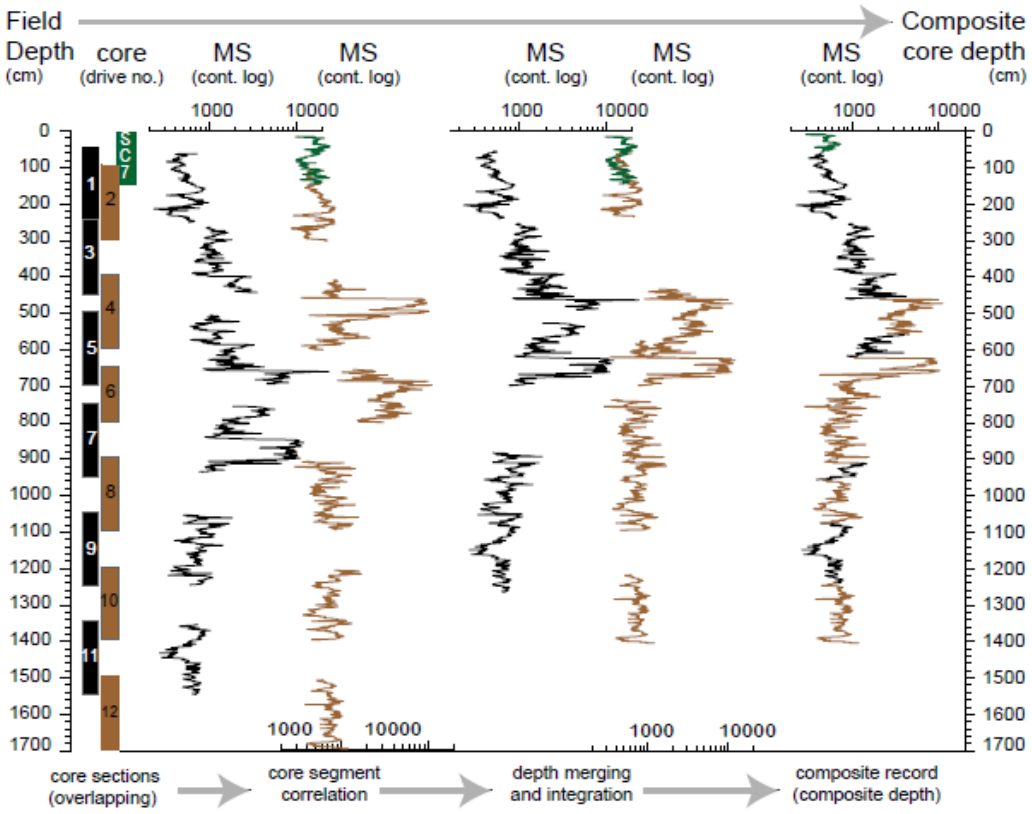

Figure 3.3. Magnetic susceptibility data from two consecutive cores were evaluated and overlapping sections were combined and correlated. A composite section was built and presented (Plotted by Ute Frank).

Following core segment correlations, the position of the dated samples were identified and correlated. The dated samples cover the time range from 1170 to 7472 cal yr BP (Table 3.2). The age model is based on four samples of wooden plant material and/or small grass charcoal fragments (unidentified plant material recovered during sub sampling), two samples of full shells of *Melanoides tuberculata* and one ostracod sample from the sediment core section. Nine total samples were dated and the two bulk samples from the upper part of the core indicate the old-carbon age offset which might be caused by old terrestrial organic matter eroded from catchments soil. Therefore, they are excluded and represented as red in the age model (Figure 3.4). These dates are individually calibrated dates without taking the other dates or accumulation model into account in the age model.

Two samples (one ostracod and one plant material) from the identical depth (8.67 m) were dated and the plant material is older by an average of 223 years than the corresponding ostracod sample. Ages from two consecutive depths (9.86 and 9.87 m) have a small reversal although they are statistically indistinguishable.

Table 3.2. AMS Radio Carbon Date from Lake Chamo. The calibrated age and age ranges were calculated using CALIB 6.0.1 and the IntCal09 data set (Reimer et al., 2009). The modelled ages are the result of Bacon age-depth model (Blaauw and Christen, 2011). The range represents the 2σ values, and the median ages are in parentheses. The first two rows in italic are not included in the age model.

Lab Code	Sample ID	Composite Depth (m)	Age (^{14}C yrs BP)	2σ Calibrated Age(Cal yr BP)	Bacon age-depth modelled age (cal yrs BP)	δ^{13}C (‰)	Dated Material
COL1892.1+2.1	*CHA-01-2010 -1.91*	*1.91*	*1876±41*	*1712-(1805)-1897*		*-19.40*	*Bulk*
COL1893.1.1	*CHA-01-2010 - 5.19*	*3.93*	*3287±52*	*3399-(3518)-3636*		*-18.10*	*Bulk*
COL1244.1.1	CHA-01-2010-7. 83	6.39	1240±31	1076-(1170)-1264	981-(1118)-1245	-12.67	Plant material
COL1246.1.1	CHA-01-2010 -8.15	6.64	1489±81	1278-(1413)-1548	1275-(1388)-1528	-53.97	Plant material
COL2454	CHA-01-2010-9.65	8.67	3083±34	3217-(3296)-3375	3261-(3403)-3567	-1.91	Ostracod
COL2455	CHA-01-2010-9.65	8.67	3304±37	3451-(3541)-3630		-18.70	Plant material
COL1240.1	CHA-01-2010-12.33	9.86	4081±24	4517-(4573)-4629	4425-(4530)-4744	-2.44	Shell
COL1241.1	CHA-01-2010-12.34	9.87	3978±48	4288-(4429)-4570	4441-(4539)-4762	4.40	Shell
COL1247.1.1	CHA-01-2010-15.38	12.89	6578±34	7428-(7472)-7515	7259-(7388)-7532	-34.83	Plant material

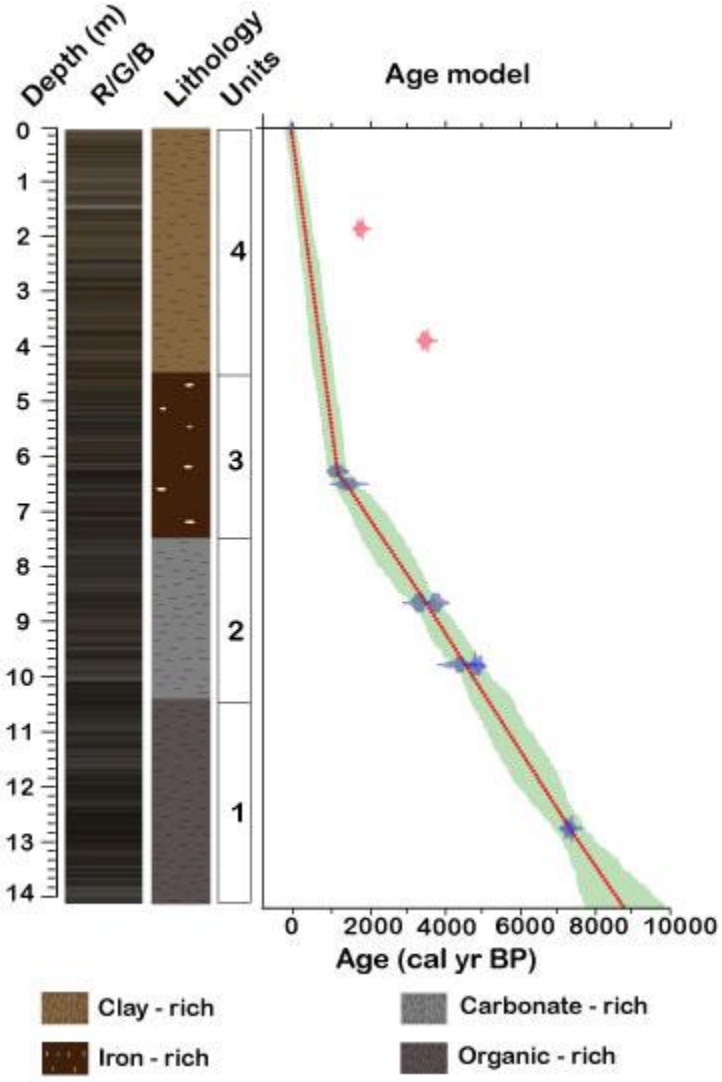

Figure 3.4. Sediment color, lithology, the different units and age-depth model of CHA- 01-2010 sample. The age–depth model is performed using Bacon age-depth model (Blaauw and Christen, 2011). Light green areas show the 95% confidence intervals of the models. The red dot line is a weighted mean of the model iterations. Blue distributions are accepted individual calibrated dates while red distributions are rejected (outlying) dates.

3.3.2 Lithostratigraphy

Core CHA-01-2010 consists predominantly of uniform organic-rich material, a typical Gyttja, varying slightly from dark to light grey at the base and dark to light brown towards the top of the core (Figure 3.4 and Appendix A). The sediment structure without any hiatus suggests a continuous accumulation since at least 8600 cal yr BP. Sedimentation rate is

nearly constant ca. 1.03 mm/yr but in the upper part of the core is much higher (5.19 mm/yr) than at the base of the core. The core shows four main lithostratigraphic units; based on geochemical, lithological and the Q7/4 diagram (Figure 3.5).

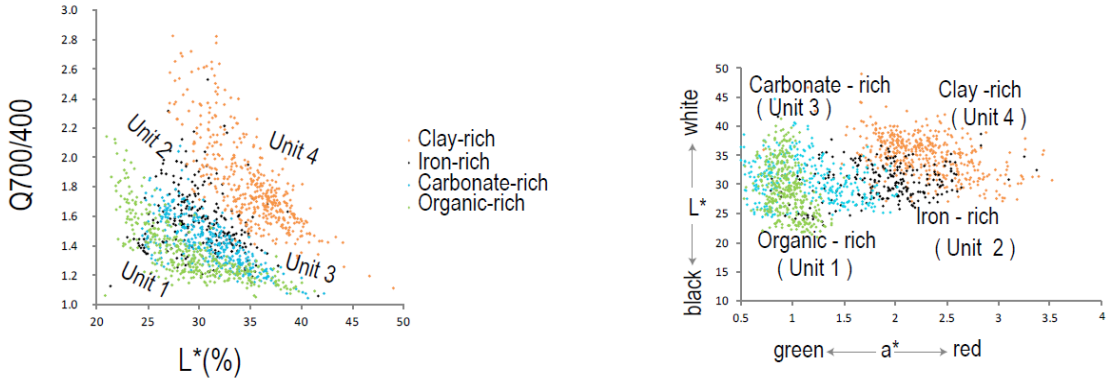

Figure 3.5. High-resolution sediment colour as lithostratigraphic description and sediment dynamic indicator. Left shows Q7/4 diagram (Debret et al., 2011), the ratio of reflectance at 700 and 400 nm on Y axis and the X-axis is sediment lightness L*(%). This distinguishes the sediment in to organic-rich, carbonate-rich, iron-rich and clay-rich faces. Right shows lightness (L*) versus red–green component (a*). Note distinguish the sediment in to organic-rich, carbonate-rich, iron-rich and clay-rich faces.

Unit 1 (14.13–10.50 m, 8646 – 5130 cal yr BP) is comprised of dark grey organic - rich sediment (Figure 3.4 and 3.5) with low density and MS values (Figure 3.6). In this unit, high resolution of L*, a* and b*color are also represented by lower values. Low amounts of Ti, Ca/Ti, Sr, K, and Fe (Figure 3.8) are characteristic for geochemical analysis in this unit, only Si and Si/Ti show higher amounts than in Unit 2 (Figure 3.8). Si and Ca are normalized by the conservative element (Ti) in order to minimize variability associated with dilution caused by clastic material of the biogenic silica, carbonates or organic matter (Brown et al., 2000; Brown et al., 2007; Burnett et al., 2011).

Unit 2 (10.50 – 7.66 m, 5130 – 2405 cal yr BP) is light grey in color (Figure 3.4), represented as carbonate - rich material based on the Q7/4 diagram and L* versus a* data (Figure 3.5). Density as well as MS have lower values while L* values show a small increment and both a* and b* values fluctuate moderately (Figure 3.6). Ca/Ti, K and Sr are

generally higher than in Unit 1 whilst the Ca/Ti and Sr counts are culminating between 10.50 – 9.50 m (Figure 3.8).

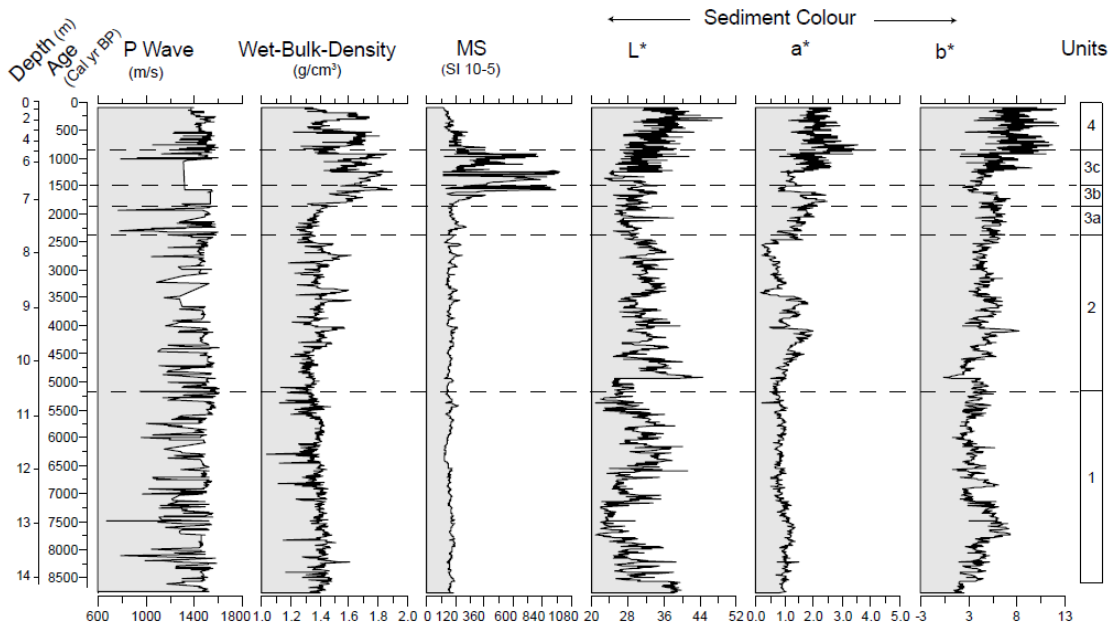

Figure 3.6. Physical parameter of the core from Geotek Multi- sensor core logger. From left to right are, P-wave velocity, wet bulk density, magnetic susceptibility (MS), sediment lightness (L*), red – green component (a*), yellow – blue component (b*) and units. Y-axis is depth (m) and age (cal yr BP).

Unit 3 (7.66 – 4.50 m, 2405 – 790 cal yr BP) is composed of dark brown iron-rich sediment (Figure 3.4 and 3.5). In this unit there is an inclusion of some volcanic clast fragments (identified with microphotos of glassy particles by Giday WoldeGabriel, personal communication). The weathered clastic material has a yellowish color and irregular shaped faces while the size differs from 4.5 mm to 1 cm length (Figure 3.7). Small pores are recognizable and are the reason for its light weight.

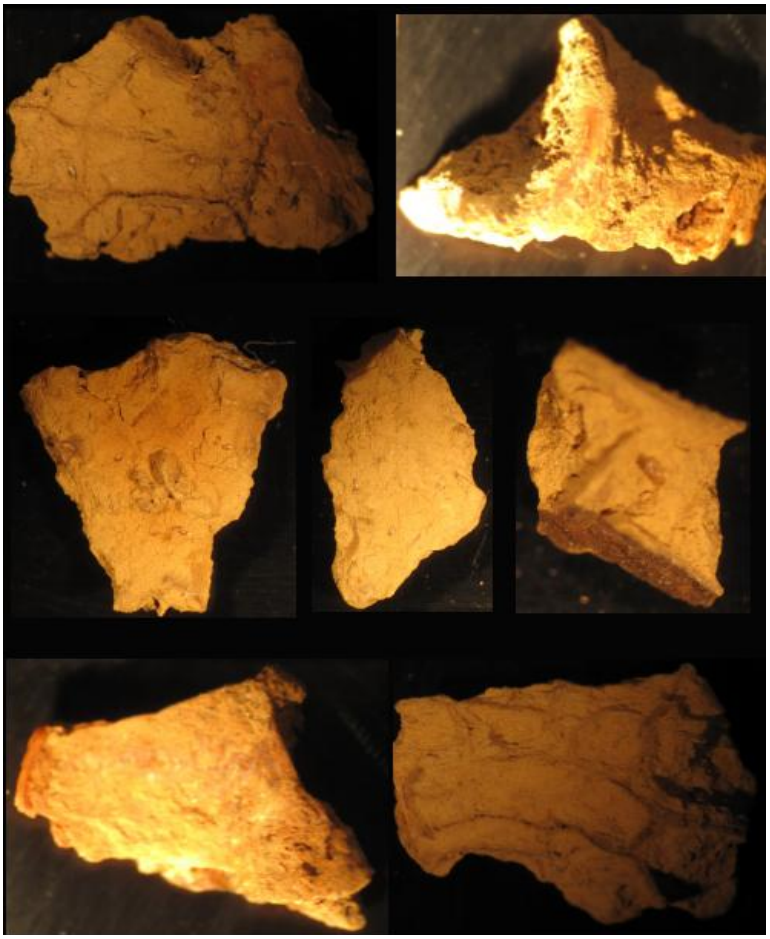

Figure 3.7. Some of the microphotos of volcanic clast fragments in unit 3 (identified by Giday WoldeGabriel).

Although the stratigraphy does not show marked changes through unit, there are variations in geophysical and geochemical parameters; hence this unit is subdivided into the following three subunits.

Unit 3a (7.66 – 7.10 m, 2405 – 1850 cal yr BP) is determined by low density and MS values, with only a minor decline in L* with a small increment for both a* – b* values (Figure 3.6). Moreover, lower Ca/Ti, Sr and K counts are characteristic for 3a.

In **unit 3b** (7.10 – 6.75 m, 1850 –1504 cal yr BP) density, MS coupled with L*– a* – b* values show a small increase. The geochemical elements also show a general tendency to increase and especially small peaks of Ca/Ti and Sr are observed (Figure 3.8).

Unit 3c (6.75 – 4.5 m, 1504 – 790 cal yr BP) exhibits highly variable density and MS values which are inversely correlated with L*– a* – b* values (Figure 3.6). Ti, Si, K and Fe attain highest values in this part of the core.

Unit 4 (4.50 – 0.12 m, < 790 cal yr BP) is brownish clay - rich deposit (Figure 3.4 and 3.5). Sediment density is high but has relatively low values of MS. L*– a* – b* values are generally high (Figure 3.6). Most geochemical elements show variations of moderate amplitude with no specific peak.

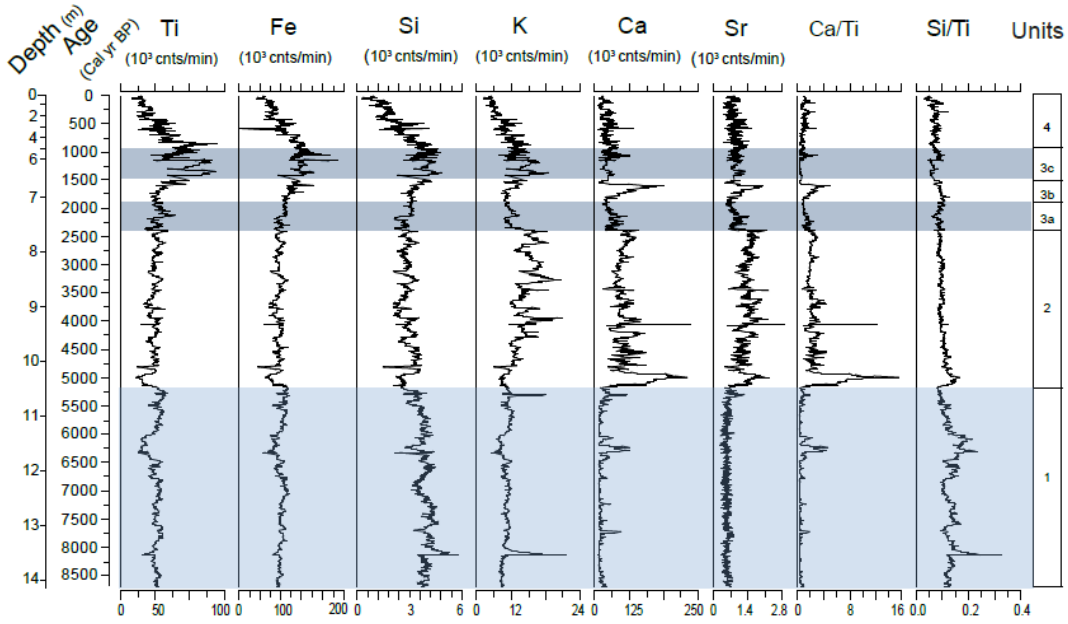

Figure 3.8. Dominant XRF elements (10^3 counts/ min) (where Ti –Titanium; Fe – Iron; Si – Silicon; K – Potassium; Ca – Calcium; Sr – Strontium; Ca/Ti–Calcium to Titanium ratio; Si/Ti – Silicon to Titanium ratio), units against depth (m) and age (cal yr BP). Light blue bar indicate the African Humid period; dark blue bars indicate relative wetter and intensive erosion phases.

3.4 Discussion

3.4.1 Core chronology

The age model is limited to seven radiocarbon dates and the sedimentation rates were almost linear between these dates. The two bulk samples, represented as red distributions in the age model (Figure 3.4), from the upper part (above 6.39 m) of the core indicate the old-carbon age offset thought to be caused by old terrestrial organic matter eroded from catchments soil. It seems obvious that radiocarbon ages obtained on bulk organic materials from sediments of Lake Chamo are most likely not a reliable chronology. Sedimentation rates increased from (1.03 mm/yr) during the time period represented by depths below 6.39 m to nearly five times higher (5.19 mm/yr) above that depth. The significant increase of sedimentation rate could be a rationale for the input of the old-carbon age terrestrial material in to the lake. It was hypothesized that the prevalence of high sedimentation rates in Lake Chamo since 1000 cal yr BP onwards may be due to the start of human settlements in the uplands (Gamo-Gidole horst and the Amaro horst) and subsequent degradation of land for expansion of agricultural use. The dramatic population growth in the region leads to farmland scarcity that enforces the cultivation of marginal land areas and fragile ecosystems (Assefa and Bork, 2014) which facilitate soil erosion processes and consequently caused an increase of the sediment yield in to Lake Chamo and Lake Abaya. This might make the correlation difficult with the well known climate events like MCA (700 to 1,000 BP / 950 to 1250 AD) and LIA (1270 to 1850 AD). However, considering only the 7 realistic dates, the age model show a credible correlation to wet and dry periods, especially during the transition towards mid/ late Holocene recorded in other East African and nearby Ethiopian rift lakes (Figure 3.10).

The reservoir effect of Lake Chamo may be small and changes in the reservoir effect over time cannot be determined due to the absence of sufficient charcoal pieces and plant material in shell-dated sediment horizons and hence not possible to undertake combined high resolution dating in order to check its effect. Only at 8.67m an attempt was done to date two samples (one ostracod and one plant material) from the same depth and the plant

material is older by an average of 245 years than the corresponding ostracod sample. We suppose that the dates of the ostracod is more closely reflect the true age of the sediment and that the older dates of the plant material may result from the inwash of older material from the surrounding. The more freshwater nature of the lake suggests that the carbonate reservoir effect may be small and its effect is taken as constant over time, although the quality of material to date is not satisfying this record. Therefore, the age model is still questionable but, at present, is the best attempt available.

3.4.2 Interpretation of proxies

High resolution data obtained from MSCL appears to be fundamental to determine sedimentological dynamics through lithographic description when considering lithologies which have been subjected to highly variable climatic and environmental conditions. In addition to visual examination, sediment lithology of Lake Chamo is described by physical properties and core imagery. Among the measured geophysical parameters, primary wave (P-wave) velocities, bulk density and magnetic susceptibility provide data about the sediment composition that enables an accurate correlation of sediment cores (Weber, 1998; Zolitschka et al., 2002). In addition, they can also be used to interpret in terms of palaeoenvriomental proxies. P-wave velocity measures the compressional wave velocity in sediment and is used to characterize sediment properties, including wet bulk density, grain size or its composition and magnetic susceptibility which provide the mineralogical nature and weathering processes of the sediment (Zolitschka et al., 2002). Sediment color is one way of describing and distinguishing sediment lithology (Debret, et al. 2006; Debret, et al. 2011). Furthermore, the sedimentary color also shows the presence of down-core changes in mineral composition. In this context, in most cases darker sediments indicate the presence of organic matter whereas lighter colors indicate less dense and carbonate materials. The total reflectance (L*) parameter was used to indicate the presence of organic matter and/ or carbonate materials (Weber, 1998; Weber et al., 2010), while a* value indicate the redox state and b* yielded information about the redox reaction of iron compounds in to iron oxides (Weber, 1998; Debret, et al. 2006; Weber et al., 2010). During a period of increased weathering intensity, Fe may undergo redox reaction and change into

iron oxides (Cohen, 2003; Weber et al., 2010), resulting in a color change in the profile, particularly during the alternating wet and dry climatic condition.

Inorganic geochemical analyses from x-ray fluorescence can provide valuable information on changes in lake trophic status and catchment environments like climate change, catchment erosion, and sediment origin. The sedimentary geochemical environment is highly sensitive to rapid changes induced by fluctuation in climate and lake level changes. In this study, high resolution semi-quantitative geochemical analyses such as Si, Ti, K, Fe, Ca, and Sr, which are significant palaeoenvironmental indicators, are presented to reconstruct past environmental changes in lake sediments as well as in the catchment.

The high mobility of Si in most tropical soils and porous volcanic lavas and the dissolution of Si compounds in saline waters of high alkalinity and pH (Talling and Tailing, 1965; Kebede et al. 1994) make the African lakes enriched with Si concentration. The Si concentration in Lake Chamo is the lowest when compared to other ERVLs (Kebede et al. 1994) but the reason for its depletion is not well understood. Mengistu (2006) and Kebede et al. (1994) obsereved that severe depletion of Si is commonly associated with increased diatom growth in Lake Chamo and other ERVLs. Further, Kebede et al. (1994) metioned that depletion of Si may also be associated with lower dissolution rates of silicic acid from diatom frustules, especially in freshwater lake environment such as Lake Chamo. Kebede et al. (1994) also suggest that the decline of Si concentration in Ethiopian rift lakes may also be influenced by reverse weathering, a process which rapidly converts diatom frustules to various forms of authigenic aluminosilicate clay mineral which ultimately remove Si from the lake water solution. Si or Si/Ti could be determined by scanning XRF from the lake sediment either in the form of biogenic or minerogenic silicon (Cohen, 2003; Brown et al., 2007; Burnett et al., 2011; Johnson et al., 2011). The biogenic silica may be added to the sediment either by the production of siliceous microorganism, primarily by diatoms or by preservation (Burnett et al., 2011). According to Burnett et al. (2011) the preservation of biogenic silica decreases at higher temperatures, higher pH and in lakes undersaturated with silica and could give a hint why Lake Chamo has lower amount of silica unlike the other ERVLs (Kebede et al., 1994).

Calcium is a major component of many watersheds of the East Africa region (Cohen, 2003). The abundance of $CaCO_3$ in the sediment can be estimated from the Ca/Ti ratio and/or from Ca profile generated by the scanning XRF. The precipitation of carbonates could increase in the lake system for several reasons, including lower lake levels or an increase in average water temperatures. Ca peaks in the records of most of East African Lakes represent periods of aridity (Halfman et al., 1994; Burnett et al., 2011; Johnson et al., 2011). Similarly, strontium (Sr) may also be found at higher value in shallow water in the form of Sr-aragonite during an arid period (Croudace et al., 2006). The high lake level and stabilization of vegetation cover in the catchment may also lead to carbonate dissolution and may be a reason for a decline in the calcium content of the sediment.

Titanium and potassium indicate the provenance of terrigenous sediments during flooding as a result of higher precipitation due to their resistance to weathering and diagenetic alterations (Cohen, 2003). In Lake Chamo, Titanium, iron, silicon and potassium supply increases during periods of rapid and intensive erosion particularly during enhanced anthropogenic erosion. The presence of good vegetation cover, deep-soil profile formation and soil stabilization (Cohen, 2003) reduces the flux of K and Ti. That is why the values of K and Ti are lower in deeper part of the core where there was a dense vegetation cover during early-mid Holocene.

Both the physical properties and bulk geochemistry of sediment from these rapid, continuous, non-destructive and high-resolution analyses from the MSCL and X- ray loggers have a good potential to get much more holistic overviews for a better and complete understanding of climate and environmental change in East Africa, in particular Southern Ethiopia. In this context, the stratigraphic variations of both the geochemical and geophysical values are conveniently interpreted based on four main zones in the following section.

Unit 1 (14.13 – 10.50 m, 8646 – 5130 cal yr BP): The dark grey color (Figure 3.4) alongside lower lightness (L*) values (Figure 3.6) are good indicators of an organic-rich (on average 20.45 g kg^{-1}) deposit as a result of high productivity of the lake in this unit. The

slight increase in b* values in Unit 1of Lake Chamo record seems to be the result of organic matter (OM) reflecting a change in the composition of the sediment. According to Debret et al. (2006), due to the sensitivity of diatoms to increased nutrient supply in the basin, b* values can be indirectly considered as a proxy for diatoms content, as well as indicator of the presence of high biogenic silica. It is hypothesized that during the early Holocene, at Unit 1 of Lake Chamo record, an increase in precipitation would have promoted a time of higher lake levels and hence dissolved silica and organic matter enter into the lake through increased runoff from the surrounding basin. Therefore, despite there are extensive diatomaceous deposits on the bed of the lake, which could sink the dissolved silica (Mengistu, 2006; Kebede et al., 1994), high levels of dissolved silica inflow from the catchment may have enriched the lake beyond the demand of diatoms. The suitable condition enabled diatoms to build their large skeletal structure and, together with the input of organic matter, enhances the productivity of the lake. In this case either detrital, biogenic silica or both might be the source of silicon in the sediment. The data from Lake Chamo obtained through the XRF measurement shows that Si or Si/Ti indicates a direct proportional relationship between Si or Si/Ti and diatom abundance. Therefore, the diatom counts and the Si/Ti ratio remain relatively high during wet climate and high precipitation, also observed in Lake Malawi (Johnson et al., 2011). Silicon may occur as biogenic silica and hence is related to highly eutrophic lakes, especially for diatom productivity. In support of this Johnson et al. (2011) and Burnett et al. (2011) found that variations in productivity of diatoms were related to the abundance of biogenic silica in Lake Malawi and Lake Tanganyika. However, the source of silica as a component of sediment needs further investigation in order to determine whether it is derived from biogenic or detrital.

Unit 2 (10.50 – 7.66 m, 5130 – 2405 cal yr BP): Unit 2 represents the driest phase of Lake Chamo as inferred from both the geochemical and geophysical proxies. Highest peaks of Ca/Ti, and Sr count (Figure 3.8) indicate prevailing arid conditions from about 5100 cal yr BP onwards. Since Ca/Ti and Sr are supposed to precipitate in the sediment during increased evaporation, their high abundance indicates arid condition in Lake Chamo sediment and hence an evidence for the low lake stand could be inferred from elevated

Ca/Ti and Sr values. Therefore, higher Ca/Ti values suggest increased lake water salinity, which in turn suggests increased evaporation under more arid climatic conditions. The precipitation of an authigenic calcium carbonate is clearly confirmed by the light grey color with relatively high L* value (see also Figures 3.4 and 3.6) in addition to the high XRF of Ca/Ti ratio. Weber (1998) and Weber et al. (2010) explained higher L* values correlated with elevated carbonate contents. Particularly at depths of 10.50 – 9.50 m the highest peak of Ca/Ti and Sr (Figure 3.8) indicate that the conditions were extremely dry. Potassium has a similar pattern as that of Ca/Ti and Sr, showing highest values in Unit 2 which can be used as an aridity proxy in this particular lake system. It has also been shown to indicate aridity in the Lake Chew Bahir record as intensively discussed in Foerster et al. (2012).

Unit 3a (7.66 – 7.10 m, 2405 – 1850 cal yr BP): Relatively lower K, Ca/Ti and Sr in this unit, indicate the return of relative humid conditions. The small decline of L* values also confirm the relative wetter condition as a result of unsaturated carbonate content.

Unit 3b (7.10 – 6.5m, 1850 – 1504 cal yr BP): Due to a small peak in the Ca/Ti and Sr record, this unit is characterized by a short dry period. This short dry interval is also accompanied by a small increments of a* and b* values in response to the alternating physical and chemical weathering. Climatic conditions control the rate of both physical and chemical weathering. During alternating wet and dry condition in different units of the sediment oxidation and reduction, along with other physical processes, could be facilitated and subsequently produce the most common iron oxides with its respective red staining as indicated by relatively high a* and b* values.

Unit 3c (6.5 – 4.5 m, 1504 – 790 cal yr BP): The highest values of Ti, Si, K and Fe are found in this unit, attributed to rapid and intensive erosion at this sub unit. Ti and K are more resistant to weathering and diagenetic alterations (Cohen, 2003) and their input to the lake indicate the provenance of terrigenous sediments during flooding as a result of higher precipitation. The high magnetic susceptibility also is a good indicator of catchment soil erosion (Figure 3.6).

After a prolonged dry period during Unit 2, which coincides with a significant lake level drop, Unit 3 represents short-term flooding events facilitating the deposition of terrigenous material. The inclusion of volcanic clasts washed into the lake between 2400 to 806 cal yr BP is a further indication of erosional processes. The clasts do not occur as a layer but as scare particles smoothly coated with clay (Figure 3.7). Therefore, it is hypothesized that these light particles were transported to the lake by fluvial processes and float to the coring site. The coating probably could have taken place when these particles were incorporated into the clay-rich sediments at the bottom of the lake. It is thought these reworked volcanic deposits were weathered and eroded from the abundant volcanic ashes occurring in the catchments of Lake Chamo. Weathering process on this accumulated terrigenous input may have led to the oxidation/reduction process and contributes to a higher and more variable a* and b* value. The fluctuating values of a* and b*could also be explained by the deposition of organic material which inhibited the oxidation of Fe^{2+} to Fe^{3+} after flooding.

Another explanation may be that these erosional processes could have been provoked by human impact, which in other Ethiopian regions was reported during this period as a result of human settlement and pastoralist activities (Lamb, 2001; Lamb et al., 2004). In addition to this anthropogenically driven environmental change and frequent and/or more intense ENSO events (Moy et al., 2002) during the late Holocene may have led to positive and strong rainfall anomalies in eastern Africa (Russell and Johnson, 2007). The inference of intensive erosion specifically between 1500 to 800 cal yr BP in Lake Chamo region may relate to the peak of ENSO event frequency occurring at around 1200 cal yr BP (Figure 3.9) in southern Ecuador (Moy et al., 2002).

Unit 4 (4.5 – 0.12 m, < 790 cal yr BP): Moderate values of all geochemical data in this unit indicate that the climate was generally dry but not as pronounced as the dry period which occurred during the time from 5100 to 2400 cal yr BP. Following the termination of flooding and relatively wetter conditions in Unit 3, there is a general positive correlation between both dry periods and the high color L*– a*– b* data. In addition to the oxidation processes identified in the organic matter imported from the catchment following the high flooding event, the significant changes in sediment color in the upper most part of the core

may have been caused by the water content of the sediment (Debret et al., 2006). The enrichment of clay deposits in this part of the core (Figure 3.5) may be a result of fluvial detrital clay input from the catchment as a function of both an increasing anthropogenic impact and climatic aridity with pronounced extreme rain events. Chemical and mineralogical analysis of levee strata from the River Kulfo, the only temporary tributary for Lake Chamo, have shown that clay minerals are the major components of the deposit (Schutt and Thiemann, 2006) and could be the source of detrital clay input for the lake. According to Yusuf et al. (2011), the topsoil of grassland plain of NNP and surrounding bush land contain high clay content and might contribute for the richness of clay at the upper part of Lake Chamo core. The intensity of that clay deposition signal may have been widely affected by human impact on the catchment area stability especially during the late Holocene. Anthropogenic pressure may have caused land use changes, which could be a reason for land degradation and erosion. During these intense land use changes, expansion of grassland may have eventually contributed to shifts in local rainfall patterns and supported frequent droughts, which may have been a reason for documented climate changes during the sedimentation of this unit.

3.4.3 Environmental changes in southern Ethiopia during the last 8600 cal yr BP

The multi-proxy record of Lake Chamo indicates marked environmental variation during the Holocene. Before 5100 cal yr BP, the climate of the Chamo region was humid as confirmed by relatively high Si counts and lower Ca concentration along with relatively lowered lightness (L*) values. The record of this study agrees well with the presence of deep, freshwater conditions as they are reported until 5100 cal yr BP in Lake Tilo (Telford and Lamb, 1999), the presence of high stand fresh water until 5400 cal yr BP in Lake Abiyata (Chalié and Gasse, 2002) and warm and wet conditions with high precipitation in the southeastern Ethiopian highlands and adjoining rift margins, as has been shown by multi-proxy speleothem records (Asrat et al., 2007; Baker et al., 2010).

Figure 3.9. Images of stromatolithes. A and B are found in 2009 during the surveying of the study area in "Elgo-bay" at the SW of the lake shore while C is found on the NE of the lake shore during 2010 field work (Photos were taken by Frank Schäbitz).

The thirty years (1970-2000) annual average precipitation data (Figure 2.2) obtained from 15 weather stations in the Abaya-Chamo basin and the surrounding area indicate that increased precipitation signals the presence of wetter condition and the prevailing of high lake level. On the other hand, low lake level could be as a result of lesser rainfall which indicates drier climate (Schutt and Thiemann, 2006). Extrapolating this relationship to the early Holocene and estimating the total precipitation of the past based on the current climate data is not possible. But the stromatolithes, Figure 3.9 (A and B) which are found in 2009 during the field survey in the "Elgo-bay" at N 05°47'01.7" and E 37°27'54.5" at the

south west of the shoreline in about 3m above the recent water level of Lake Chamo could supply indirect evidences. More recent stromatolithes, Figure 3.9 (C) which is found on the north east of the lake shore during 2010 field work, also could supply additional evidences for the recent lake level changes. Although no date was made for the moment on these stromatolithes, they could be from the early Holocene time and the lake level of Chamo might be 3m above the recent water level as a result of the prevailing of high precipitation during the early Holocene as also documented in the other regional paleoenvironmental data (Mohammed and Bonnefille, 1998).

Geochemical and geophysical evidence from Lake Chamo around 5100 cal yr BP indicate the end of the early Holocene humid period. Studies from other rift valley lakes also suggest that the end of the early Holocene humid period took place between 4500 cal yr BP (Gasse and Street, 1978) and 5000 cal yr BP (Gillespie et al., 1983). According to Chalié and Gasse (2002), the rapid shift toward an overall dry late Holocene occurred between 5700 to 5000 cal yr BP in Lake Abiyata, a similar time range as found for Lake Chamo. Palaeolimnological data from Lake Tilo (Lamb, 2001) also showed that the lake started to desiccate in a drier climatic regime, leading to a further fall of lake levels at around 5100 cal yr BP.

The presence of shallow, saline conditions after 5400 cal yr BP in Lake Abiyata (Chalié and Gasse, 2002) and the low and fluctuating water levels of Lake Nakuru (Richardson and Dussinger, 1986) and Lake Turkana (Johnson et al., 1991) and Lake Ziway-Shala (Gillespie et al., 1983) (Figure 3.10) are also clearly pronounced by in the Lake Chamo record, shown by high values of Ca/Ti and Sr. Garcin et al. (2012), which are also used to inferred a low lake level at ~5270±300 cal yr BP, using detailed palaeo-shoreline record from Lake Turkana which coincide with the beginning of major episodes of aridity at Lake Chamo. Despite there is strong evidence for an orbitally-forced change during the African Humid Period in East Africa (Gasse, 2000), the forcing mechanism for this observed regional climatic variability during this period and afterwards is not well understood. The changes in the strength and position of the ITCZ as well as east-west migration of the CAB (Nicholson, 1996; Diro et al., 2009; Russell and Johnson, 2007) govern this regional

climatic change particularly during the African Humid Period. As Junginer et al. (2014) suggested, during northern hemisphere insolation maximum, northeastwards shift in the CAB as a result of enhanced atmospheric pressure gradient between East Africa and India could be taken as one of the important forcing mechanism for this regional variability. The multi-proxy data from Lake Chamo have also corroborated and support that this forcing mechanism resulted in climatic variability during early to mid Holocene and afterwards. The progressively changing humid to arid climatic condition at early-mid Holocene transition in East Africa particularly in Lake Chamo might be due to the reduction of the East African–Indian atmospheric pressure gradient in response of changes in solar irradiation. Therefore, the overall reduction of humidity in the atmosphere and prevention of the CAB from its precipitation source could be additional reasons for this early-mid Holocene transition (Juniper et al., 2014).

The lake level changes of Lake Chamo are also inferred from relatively high lightness values, due to the elevated precipitation of calcium carbonate during this time (Figure 3.8). The carbonate deposition in Lake Turkana is used as the most reliable indicator of aridity in the region (Halfman et al., 1994) at about 5000 cal yr BP, which is around the same time as the start of highest deposition of carbonate in Lake Chamo. Burnett et al. (2011) and Johnson et al. (2011) recognized the preservation of calcite during arid times in Lake Tanganyika and Lake Malawi. Burnett et al. (2011) indicated that higher Ca concentration is a sign of dry conditions and the preservation of calcium carbonate could be the evidence for extremely dry conditions in Lake Tanganyika.

The data suggest that the end of the AHP from Lake Chamo may have been a gradual process due to the existence of the driest condition for at least 1100 years (from 5100 to 4000 cal yr BP). Most of the amplifier lakes found in EARS reacts very sensitively for long-term tectonic processes to short-term climate fluctuations and environmental instability (Olaka et al., 2010; Trauth et al., 2010) but due to its large size catchment area, Lake Chamo may have responded gradually to the termination of the AHP. The gradual termination of the AHP is also recorded at Chaw Bahir (Foerster et al., 2012) and in the eastern Sahara (Kröpelin et al., 2008), but disagrees with palaeotemperature data and

palaeo-shoreline record from Lake Turkana (Berke et al., 2012; Garcin et al., 2012) and in marine archives of Northern and Western Africa and Asia (deMenocal et al., 2000; Morrill et al., 2003; Renssen et al., 2006; McGee et al., 2013).

The geochemical record from Lake Chamo indicates the strongest aridity during a period between 5100 to 4000 cal yr BP, but generally arid conditions persisted until around 2400 cal yr BP. A short arid interval also occurred between 1850 to 1500 cal yr BP (Figure 3.8). The moderately higher value of geochemical data along with the higher value of "L*–a*–b*" color data give an insight into the relative dryness of the climate from 800 cal yr BP to present at Lake Chamo.

The reversals to relatively wet conditions in the Lake Chamo and Lake Chew Bahir records (Foerster et al., 2012) at around 2400 to 1850 cal yr BP (Figure 3.10) as inferred from lower K value at about 1500 to 800 cal yr BP, are also clearly indicated in the lake level rise of Lake Turkana (Johnson et al., 1991). These wetter conditions of Lake Chamo also agree well with the lake level rise at around 1900 to 1400 cal yr BP in Lake Ziway - Shala (Gillespie et al., 1983). Therefore the detailed lake sediment record of Lake Chamo resolves the debates about the reversal of wetter climatic condition and fluctuations of moderate amplitude during late Holocene.

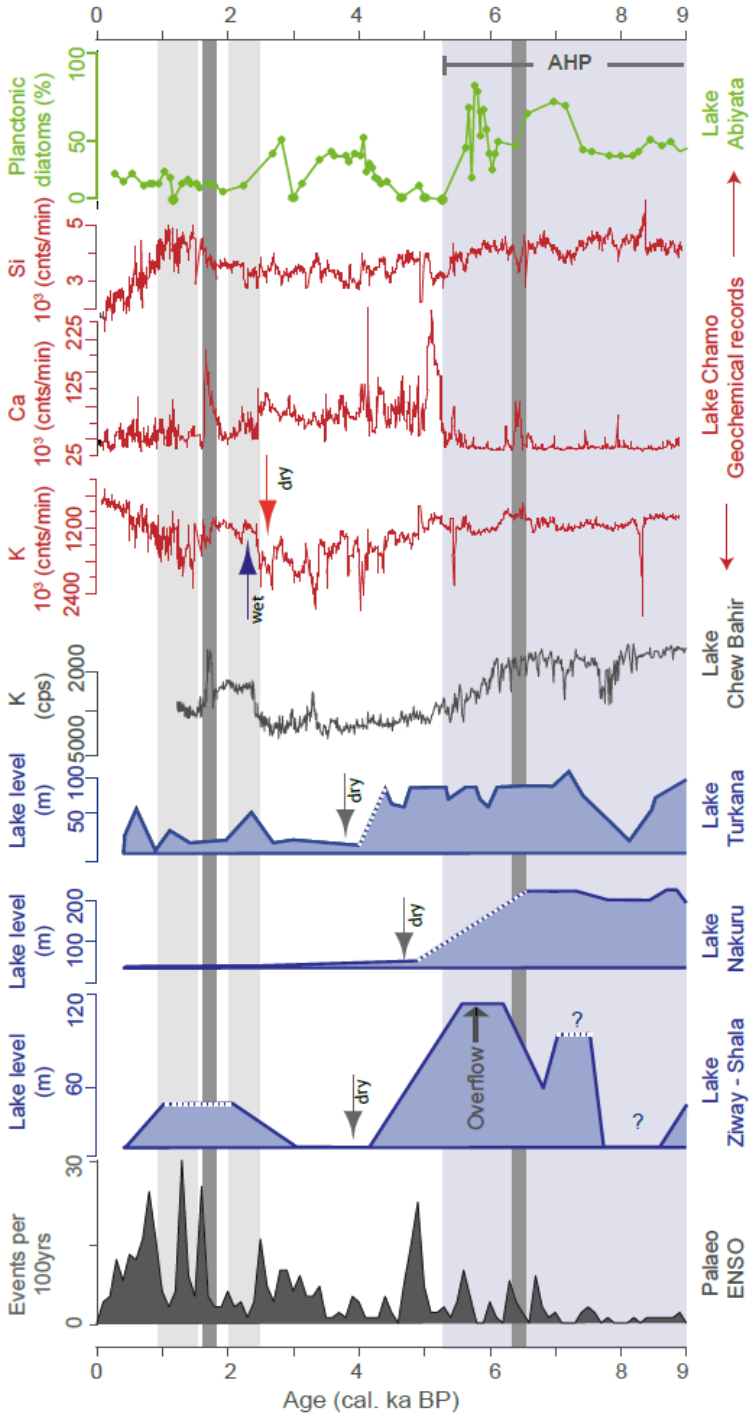

Figure 3.10. Comparison of transition towards arid condition of Lake Chamo data with other Ethiopian Rift Valley Lakes: Lake Ziway-Shala (Gillespie et al., 1983), Lake Abiyata (Chalié and Gasse, 2002), Lake Chew Bahir (note reverse scale for aridity proxy K) (Foerster et al., 2012) and with Kenyan Rift Valley lakes,

adapted from (Junginger, 2011): Lake Nakuru (Richardson and Dussinger, 1986) and Lake Turkana (Johnson et al., 1991) and the paleo-ENSO record from Laguna Pallcacocha, southern Ecuador (Moy et al., 2002). Light blue bar indicates the so called African Humid Period (AHP) during early to mid-Holocene and light gray bars indicative for relative wetter and intensive erosion phases during late Holocene. Dark grey bars show brief dry spells. K – Potassium (note reverse scale); Ca – Calcium; Si – Silicon.

3.5 Conclusions

The high-resolution lacustrine sedimentary records preserved in Lake Chamo provide opportunities to reconstruct high resolution palaeoenvironmental conditions of the region during the Holocene. These high resolution sedimentological, geochemical and geophysical data show gradual but large changes from relatively wetter conditions during the early Holocene, starting at 5100 - 4000 cal yr BP, to dry conditions during the mid Holocene. The relatively low lightness (L*) and lower calcium carbonate value also reflect the wetter conditions during the early Holocene. These records constrain the time period for the mid-Holocene change from humid to arid climate which is known to occur in most of East Africa. The record of Lake Chamo documents the termination of the African Humid period at about 5000 cal yr BP. The transition is thought to have persisted for at least 1100 years (from 5100 to 4000 cal yr BP), suggesting the end of the AHP may have been gradual, despite the lake being in a temporary endorhëic system during this period, but this may be due to its large size and having a big catchment area. Therefore Lake Chamo may have responded gradually to short-term climate fluctuations and environmental instability during the termination phase of AHP. A return of relative humid conditions occurred between 2400 and 800 cal yr BP with brief dry spells at about 1850 to 1500 cal yr Bp. The geochemical data along with higher value of "L*–a*–b*" color data from 800 cal yr BP to the present indicate generally dry conditions but is not as diverse as the dry period found to have occurred between 5100 to 2400 cal yr BP. In addition to climatic variability, anthropogenic impact might be a major reason for catchment area instability and for the presence of high sedimentation rate at the upper part of the record. Separating the effects of climate and human impact during this time is particularly difficult, hence high-resolution and well dated records are needed at shorter time-scales at least for the upper 2000 cal yr

BP. Generally, the high resolution and multi-proxy records of Lake Chamo show a strong similarity with other Ethiopian and East African Rift Valley lakes and provide a more detail record for the region.

Chapter 4

4. Holocene fires in Southern Ethiopia: towards interpreting relationships between climate, vegetation, and human activity at local scales

Abstract

Charcoal analysis provides key insight into understanding the natural range of variability in fire frequency, as well as the role of fire in ecosystems structure. To our knowledge, no research regarding the fire history of Lake Chamo, Ethiopia, has been published, even though fire use by humans is one of the main factors which can influence local ecosystem structure. Macroscopic charcoal counting and detection of benzene polycarboxylic acids (BPCA) from sedimentary charcoal of Lake Chamo provide key evidence to Holocene paleofire reconstruction in relation to vegetation, climatic and anthropogenic impact on the region. The abundant of charcoal particles and high black carbon input into Lake Chamo suggests more stable, woody savanna vegetation and wood fuelling fires during the early Holocene. A major change to arid conditions occurred at 5100 yrs cal BP, as indicated by a higher burning frequency of steppe vegetation. The dramatic decline of charcoal and black carbon concentration during the mid-Holocene also shows the vegetation response to increased aridity, which is a millennial scale arid period documented in most regions of East Africa. Although separating the effects of climate and human impact during the late Holocene is usually difficult, the BC quality pointing at higher burning temperatures of fires implies a rising anthropogenic activity in the surrounding. Our finding supports the notion that human activity was a primary driver of global fire occurrence for the past 2,000 years. Furthermore, the data from Lake Chamo show major environmental changes of the

Holocene, and ultimately provides an interesting input to infer about fire history and human activities.

4.1 Introduction

The equatorial East Africa vegetation is controlled by frequently changing Holocene climate and human activity. On the other hand, fire, which provides information about palaeoclimatic conditions, is not influenced by climate alone especially in regions like East Africa where human presence has a long history. Fire history research provides an important insight into understanding the range of variability in fire frequency, severity, extent, and spatial complexity, as well as the role of fire in ecosystem structure. Fire causes a major disturbance in the ecosystem and can also impact carbon cycles to the atmosphere. Charcoal residues of different fire regimes can assist in the understanding of interactions between climate, vegetation, and human populations. Humans have used fire for different purposes through time and understanding the relationship between fire and land use can help to gain an insight into past human dispersal and cultural development. Differentiating human-induced fires and natural fires reveal how humans have dispersed from their original location and have been affected by changing climatic condition, which contributes to one of the objectives of the CRC 806 project. For this purpose, charcoal counting and chemical variations in charcoal residues are used as a fingerprint for fire regime reconstruction in this region where human presence has had a long history.

Paleofire records of East Africa provide an important insight into understanding the roles of climate, fire, and human activity on African Woodland/Savanna ecosystems, all which are currently under vigorously debate. Typically, in Africa, some ecologists argue that savannah vegetation is a product of fire and human activity (Bond et al., 2003; Bond et al., 2008; Rucina, et al., 2009). In contrast Finch and Marchant (2011) argue for long term persistence of montane grassland with little expansion during the late Holocene. However, long-term fire history in East Africa is still poorly documented due to the lack of archives suitable for well-established paleoefire approaches. Specifically, there is almost no research

work on fire history in Ethiopia except the identifications of fossil charcoal from gully soil samples (Gebru et al., 2009; Terwilliger et al., 2011) to get an insight for reconstruction of palaeoclimate in the Tigray region (Northern Ethiopia) and few rudimentary lake studies (Darbyshire et al., 2003; Lamb et al. 2004). In this context, this chapter has contributed to fill this gap by investigating how the landscape of Lake Chamo region responded to prehistoric fires using sedimentary charcoal counting and black carbon analyses.

The response of Ethiopian Rift Valley savannah vegetation to climate variability has revealed vegetation change from forest to grass dominated savannah, inferred from pollen records, C/N ratios and $\delta^{13}C$ data from Lake Tilo (Lamb, 2001; Lamb et al., 2004). In addition, pollen records at Bale Mountains, southern Ethiopia, have also shown that in response to increased moisture and temperature during the early-mid Holocene, the altitudinal belts of vegetation began to establish themselves (Mohammed and Bonnefille, 1998; Umer et al., 2007). The climatic variability and its impact on vegetation composition may promote the occurrence of fire in the region. Like other ERVLs region, Lake Chamo is situated in a savannah ecosystem. The savanna ecosystems are the most extensive and frequently burnt ecosystems in the world (Dwyer et al., 2000; Bond et al., 2005). Additionally, the interannual and seasonal climate variability might be suitable for fire to spread in savanna ecosystems (Dwyer et al., 2000; Bond et al., 2005; Daniau et al., 2012). Therefore, fire is the dominant direct control of vegetation in this tropical environment. Over three quarters of savanna burning occurs in the African continent and more than 60% of the global total of biomass burning is from tropical grass savanna fire (Dwyer et al., 2000; Colombaroli and Verschuren, 2010). Power et al. (2008) suggested that a marked increase in frequency and aerial extent of fire results in more biomass burning during the Holocene on a global scale. Recently, fires in East Africa have been found to be associated with land use change to intensive agriculture (Thevenon et al., 2003; Colombaroli and Verschuren, 2010). In addition, the latitudinal movement of the ITCZ in East Africa has also been found to control fire regimes and intensity, by producing a climate wet enough to grow combustible vegetation and then dry enough for them to burn (Thevenon et al., 2003).

Despite the great fire activity in this tropical ecosystem, few paleofire records are documented so far in tropical Africa and in particular in the Lake Chamo region.

Paleofire intensity and frequency are estimated herein for the first time by two independent methods (charcoal counting and detection of benzene polycarboxylic acids (BPCA). In this context, the quantitative analyses of lake sediment enables the accumulation of charred particles in sediments during and following a fire event to be known, whilst chemical analysis of charcoal also plays an important role in reconstructing fire temperature and type of vegetation that was burning during different fire regimes. The use of benzene polycarboxylic acids (BPCAs), as geochemical markers for BC, is sensitive for detection of molecular admixtures of fire residues in sediments (Hammes et al., 2007; Roth et al., 2012). The molecular marker method employed identifies chemical oxidation of BC in BPCAs as markers for coalified and charred residues (Glaser et al., 1998; Brodowski et al., 2005).

This study is the first work to analysis fire history in the East and Horn of Africa which combines charcoal counts and organo-geochemical characterization of fire residues (BC quantity and quality by the BPCA method). The coupled methods, therefore, give an opportunity to understand the complex interaction between climate, vegetation, and human activity which drive fire activity over longer temporal scales. By applying these two methods, the following research questions will be addressed: 1) What does the past tell us about the respective roles of climate and human actions in determining long-term fire regimes in the Lake Chamo region? 2) Was fire an important landscape feature in the grassland ecosystem of that region? 3) Does it contribute information that can inform efforts to understand global fire history? Therefore, the aim of this chapter is to make palaeoclimate estimates for paleofire occurrence in relation to climatic and anthropogenic impact of the region. Thus, our charcoal data has contributed to an improved understanding of the relationship between climate, fire and vegetation. Our study presents details about prehistoric fire and its connection with vegetation, climate, and humans, particularly in southern Ethiopia, and could also contribute to a broader understanding of fire history characteristics of East Africa and globally.

4.2 Methods

4.2.1 Charcoal separation and counting

Charcoal occurrence was quantified to obtain an insight into changes in fire dynamics and their causes for determining long term climate, fire and vegetation interactions. Our preliminary charcoal analysis was carried out at 32 cm intervals. A high resolution charcoal analysis was done at each 1 cm interval from 11– 9.5 m, with emphasis on the transition period between early to mid Holocene, in order to get insight about the response of climate on the fire occurrence in the catchment. Specifically only at the transition period, the attempt was made to quantify and differentiate grass and wood charcoal in order to infer changes in vegetation related to Holocene changes in climate and fire. The identification of wood or grass charcoal was based on the morphology of the charcoal; wood charcoal has relatively shorter length and is thicker, whereas grass is longer in size and thinner. Separation and counting of sedimentary charcoal was done following the methods outlined by Whitlock and Anderson (2003), Long et al. (2007), Gebru (2007) and Gebru et al. (2009). Each sample (2 cm^3) was soaked in sodium hexametaphosphate for 24 hrs to deflocculate the sediment and separate charcoal particles from clays and other materials. The soaked samples were wet sieved and washed gently through 125 and 250 μm sieves. The sieving method reduces fracturing of charcoal as compared to the charcoal counting on pollen slides, which is a common method used by those few rudimentary lake studies from Ethiopian Lakes (Darbyshire et al., 2003; Lamb et al. 2004). A risk in the method used is that charcoal particle could break during pollen preparation and produce an artificially high abundance of microscopic charcoal. Macroscopic charcoal (>125 μm) in lake sediment profiles is a powerful proxy which provides a record of local or nearby fire events in the catchment (Whitlock and Millspaugh, 1996; Whitlock and Larsen, 2001; Whitlock and Anderson, 2003; Long et al., 2007). Some studies used different size ranges to determine local and regional fire, although this method is still under debate. In this chapter, >250 μm size class is used to identify local fires and indicates burning nearer to the shores, whereas the size class between 125 - 250 μm indicates a longer transport path but within the

catchment. Following the assumption of Whitlock and Anderson (2003), the smallest < 125 µm size fraction contains abundant charcoal and it was difficult and time consuming to count accurately for every sample and I only considered those which are >125 µm fraction. Whitlock and Millspaugh (1996) also pointed out that charcoal particles accumulation >125 µm diameter were abundant in sites < 7 km from the fire but declined sharply beyond that distance in a study carried out following the 1988 fires in Yellowstone National Park. In this contexts, Whitlock and Anderson (2003) tested the 125–250 µm and >250 µm fractions as the most practical size range and most often used for macroscopic charcoal analysis, hence this study implemented these sieves size for extracting the local fire signal. Under a stereomicroscope, the charcoal particles were counted on a gridded petri dish and charcoal counts were converted into charcoal concentrations (particles/cm^3) and charcoal accumulation rates (particles cm^{-2} yr^{-1}). Charcoal concentration was calculated by dividing the total count for each sample by volume of the sample (2 cm^3) and charcoal accumulation rates was calculated by dividing the charcoal concentration by deposition time (yr/cm) of the sample.

We hypothesize that the loss of vegetation and its relation with high runoff and accumulation of charcoal from the watersheds can be determined from high resolution physical (MS) and chemical (Ti and K) measurements from the MSCL and XRF core scanner, respectively. Magnetic susceptibility is associated with runoff from adjacent slopes and could be a good indicator of catchment soil erosion. The fluxes of K and Ti in mineral form were normally found to coincide with reductions in the presence of dense vegetation and soil stabilization (Cohen, 2003), but when vegetation cover was reduced due to the prevailing arid periods and whenever there is a short strong rainfall event, fluvial inwash from the upland of the catchment into the basin increased, both of which were also found to coincide with accumulation of charcoal in the sediment.

4.2.2 Black carbon (BC) assessment by benzene polycarboxylic acids (BPCA)

The analyses of black carbon (BC) for our samples were done in collaboration with the University of Bonn, Germany. In this study, in addition to the charred material count, chemical determination analysis is found to explain charcoal representation in Lake Chamo sediments as markers for coalified and charred residues. In previous studies, various methods have been implemented to quantify BC in sediments, each method covering a different part of the BC continuum (Schmidt et al., 2001; Hammes et al., 2007; Roth et al., 2012). The chemical oxidation of BC in to BPCAs as markers for coalified and charred residues (Glaser et al., 1998; Brodowski et al., 2005) was employed to determine the different fuel types during burning. The sums of carboxylic acids (B3CA, B4CA, B5CA, and B6CA) after the oxidation process were found to correspond to a marker for the total amount of polyaromatic carbon and stand for the BC quantity (Brodowski et al., 2005; Wolf et al., 2013). The ratio of five- to six-times carboxylated benzenes (B5CA/B6CA) serves as a measure for the original degree of aromatic condensation in the charcoal and as a marker for BC quality (Wolf et al., 2013). The oxidation of BC to benzene polycarboxylic acids was carried out according to Brodowski et al. (2005). In brief, samples (ca. 5 mg carbon) were hydrolyzed with trifluoro-acetic acid for metal elimination (105 °C, 4 h). The residue was oxidized with 65% HNO_3 (170 °C, 8 h), and BPCAs subsequently purified using a cation exchange column (Dowex 50 W X 8, 200–400 mesh, Fluka, Steinheim, Germany). The individual BPCAs were then converted to trimethylsilyl derivatives, separated by gas-chromatography using an Equity-5 column (30 m x 0.25 mm i.d., 0.25 µm film thickness; Supelco, Steinheim, Germany), and detected via flame ionization (Agilent 6890 gas-chromatograph). Citric acid was used as a first internal standard for BPCA quantification and added immediately before the cation exchange step. Biphenylene-dicarboxylic acid was used as a second internal standard to quantify the recovery of citric acid (recovery 70–95%). The BPCA yields were corrected for CO_2 loss and insufficient conversion of BC to BPCAs by a factor of 2.27 (Glaser et al., 1998), representing a conservative minimum of BC estimation (Brodowski et al., 2005).

4.3 Results

4.3.1 Charcoal concentration, physical, and non-BC chemical parameters

Charcoal concentration (particle (cm^{-3}) is generally high at the deepest part of the core (Unit 1) particularly during the transitional mid Holocene period (until around 5100 cal yr BP) (Figure 4.1). In order to examine the relationships between the impact of vegetation loss, high runoff and the accumulation of charcoal from the watersheds, MS (SI 10-5), Ti (10^3cnts/min) and K (10^3cnts/min) are plotted against charcoal concentrations (Figure 4.1). In Unit 1, MS, Ti, and K are at lower levels. Although charcoal concentration is low in Unit 2, charcoal peaks are observed at 10.50 m and 10.20 m of its base. High fire frequency periods (at 5100 and at 4800 cal yr BP) were distinguished (Figure 4.1) at the base of this unit. In the upper part of this unit, where charcoal concentration is almost negligible, the K value shows a general increase but MS and Ti values show similar patterns of fluctuation in both Unit 1 and 2 (Figure 4.1).

Charcoal concentration, MS, and Ti in Sub-unit 3a show a slight increment while K values are lower at this Sub-unit. In Sub-unit 3b, MS, Ti, and K show a slight increase whilst the charcoal concentration declines. In Sub-unit 3c charcoal concentration is lower, and negligible between 1500 – 1000 cal yr BP despite evidence of significant input of terrigenous material during this period (Figure 4.1). Charcoal concentration is inversely proportional to MS, K and Ti, particularly around 1500 to 1000 cal yr BP. In Unit 4, MS, Ti, and K value show a declining trend but the charcoal concentration is slightly higher than in Unit 3, although it is not significantly high in comparison to Unit 1 and at the base of Unit 2. The charcoal concentration of the coarser fraction (>250 μm) show higher values compared to the finer fraction (125 μm) in this unit.

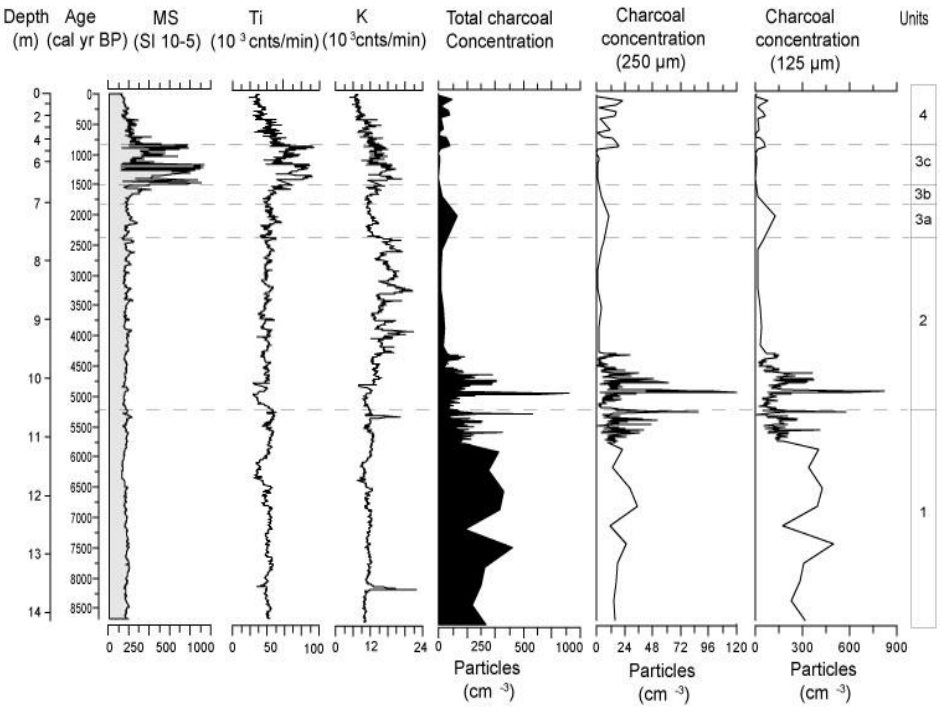

Figure 4.1. Charcoal data along with MS and geochemical data from Lake Chamo. From left to right are, magnetic susceptibility (MS), Ti–Titanium, K–Potassium; total charcoal concentrations, charcoal concentrations (250 µm), charcoal concentrations (250 -125 µm) and the different unit versus age. Dashed lines in the figure mark the different units described and discussed on pages 24-28.

4.3.2 Charcoal accumulation rate and Black carbon (BC) analysis

Charcoal concentrations vary when presented as charcoal accumulation rate (CHAR) values, due to variations in sedimentation rates (SR), particularly towards the upper part of the core (Figure 4.2). Sedimentation rates were observed to increase from 1170 cal yr BP onwards (from 1.04 mm/ka to 5.19 mm/ka; Figure 3.4), thereby diluting absolute concentrations of the charcoal. Input rates of charcoal (concentration per year (cm^{-2} yr^{-1})) were calculated to estimate changes in fire intensity in this lake catchment (Figure 4.2).

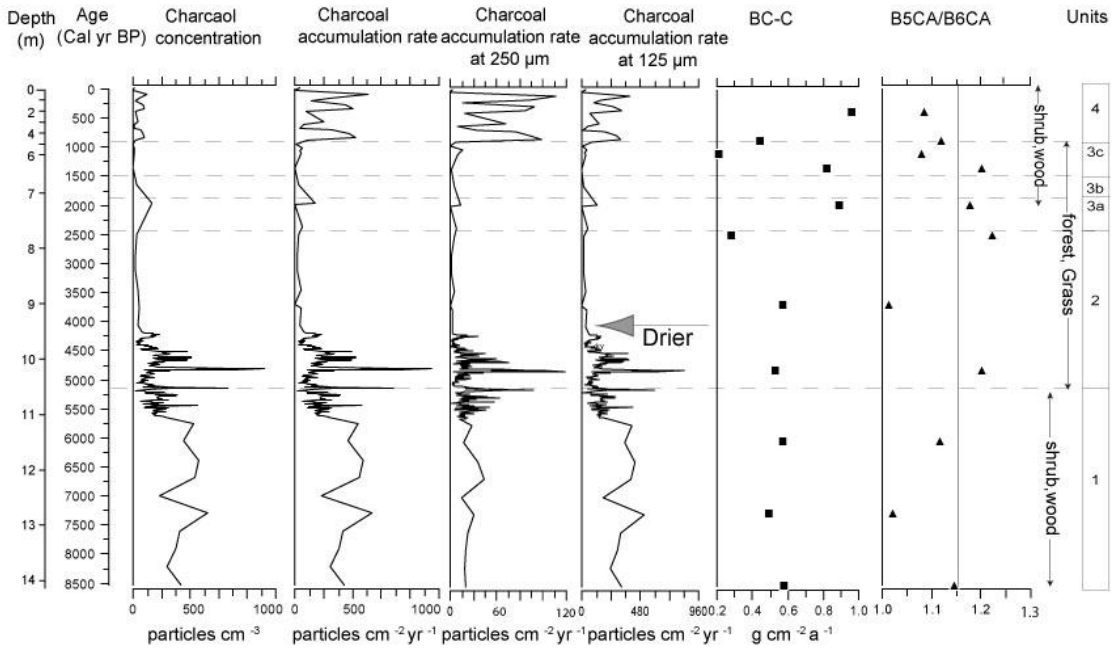

Figure 4.2. Charcoal data from Lake Chamo, from left to right total charcoal concentrations (particles cm $^{-3}$), total charcoal accumulation rates (particles cm $^{-2}$ yr $^{-1}$), charcoal accumulation rates at 250 µm and 125 µm (particles cm $^{-2}$ yr $^{-1}$), black carbon (BC) (g cm $^{-2}$ a^{-1}), B5CA/B6CA ratio (BC quality) and units plotted against age. Dashed lines in the figure mark the different units and the grey line is the average value of the fire temperature sensitive ratio of B5CA/B6CA. The arrow indicates the drier period in the record.

Both the charcoal accumulation rate and the molecular BC consistently show the occurrence of higher fire intensity in Unit 1 (Figure 4.2). The lower values of fire temperature sensitive ratio of the B5CA/B6CA are recorded in this part of the core (Figure 4.2). At around 4800 cal yr BP maximum fire intensity was shown in both charcoal accumulation rate and molecular BC. The highest B5CA/B6CA ratio around 4800 cal yr BP was also observed.

As with charcoal concentration, both charcoal accumulation rate and the molecular BC concentration are lower in the uppermost section of Unit 2, but higher amounts are recorded at the base of Unit 2. Decline of both charcoal accumulation rate and the concentration of the molecular charcoal residues from 4200 to 2400 cal yr BP are recorded (Figure 4. 2). Generally, B5CA/B6CA ratio is high in Unit 2, but at around 3725 cal yr BP this ratio is low.

In Sub-units 3a and 3b both charcoal concentration and accumulation rate remain low. The high value of BC concentration and a slight increase of charcoal concentration are recorded at these subunits especially since around 2000 cal yr BP. Similarly, charcoal concentration and accumulation rate remain lower in Sub-unit 3c. BC concentration and the B5CA/B6CA ratio values are also found to decline at this subunit.

In Unit 4, starting following Sub-unit 3c (at around 1000 cal yr BP) to the present, both the molecular BC and charcoal accumulation rate are found to consistently increase. The B5CA/B6CA ratio has a lower value in this part of the core. In this unit, the CHAR and the charcoal concentration curve vary due to a difference in SR. The CHAR indicated the total influx of charcoal and generally high charcoal input is recorded in this unit than in units 2 and 3.

4.4 Discussion

4.4.1 Fire and its relation with palaeoclimate and vegetation

The characteristics of fire residues preserved in sediments are influenced by fire events and the type of vegetation in the lake catchment as well as in the region. The results indicate that the fires event during the last 9,000 years in the Lake Chamo region is not only the result of one large burning rather a number of fires varying in size throughout the record. In this context, it is likely that more information about burning conditions could be obtained from the combination of macro-charcoal and that of molecular BC analysis. Therefore, charcoal data of Lake Chamo from both methods imply that, for most of the Holocene, wet-dry oscillations in climate determine the type of vegetation and biomass burning. These charcoal data imply that, for the early Holocene, increased productivity of the vegetation led to increased fuel availability, which subsequently promoted fires to occur. An increase in wood charcoal was observed towards the end of the early Holocene, identified through macroscopic charcoal characterization. This evidence is complemented by the fire temperature sensitive ratio of benzene polycarboxylated acids produced from BC (B5CA/B6CA ratio; Figure 4.2), which indicates below average fire temperatures

suggesting fires occurred in woody or shrub vegetation (Wolf et al., 2013). Grass and wood have varying proportions of lignin and cellulose and therefore combust at different temperatures, and exhibit different chemical properties. In this context, grasses burn at lower fire temperature while woods/shrubs burn at higher temperature. In most cases soft wood forest, including grass is prone to burn naturally, while hardwood forests rarely burn and a fire containing this material is predominantly human induced (Pyne et al., 1996), hence the BPCAs method can determine natural and human-induced fire activity.

The degree of condensation of aromatic structures in BC is affected by burning temperature and reflected by the BPCA pattern after oxidative treatment of BC (Wolf et al., 2013). Wolf et al. (2013) found the proportion of 6-times carboxylated benzene emitted during a grass burn at lower temperature is significantly lower than the one emitted during domestic wood burning at higher fire temperature. Therefore, the ratio of B5CA/B6CA lower when the source of fire is woody/shrub but it records higher value during burning of grass as a fuel source (Wolf et al., 2013). In this perspective, the use of BPCAs method could discriminate the fuel types along with specific combustion temperature and complement the charcoal counting method to fully understand the fire history of the region.

Pollen data (Lamb, 2001), C/N ratios, and $\delta^{13}C$ data (Lamb et al., 2004) from Lake Tilo (south-central Rift Valley) indicates the presence of woody savanna vegetation during the early Holocene. Pollen analysis offers information on changes in vegetation type in response to the changing palaeoclimatic and anthropogenic condition and identified fire-tolerant taxa during the fire event (Lamb, 2001; Rucina et al., 2009). C/N ratios and $\delta^{13}C$ analysis from bulk organic material can help to differentiate the source of organic carbon either from aquatic or terrestrial plants and to determine whether the land plants were C_3 or C_4. In this context, Lamb et al. (2004) found that high C/N ratio and relatively low $\delta^{13}C$ value in Lake Tilo suggest that the predominant input of the lake was from terrestrial plants, and C_3 vegetation (wood) was the dominant plant type. In contrast, low C/N ratios and higher $\delta^{13}C$ values reflect the aquatic plant input and correspond to increase in C_4 vegetation (grasses). Most C_4 plants in tropical Africa are able to withstand hotter, drier

conditions better than C_3 plants, and could severe as indicator of drier conditions (Wooller et al., 2003 ; Lamb et al., 2004).

In southern Ethiopia, abundant and evenly distributed rains during the early to mid Holocene resulted in the increase of arboreal pollen content in bog and lake sediments (Mohammed and Bonnefille, 1998; Umer et al., 2007) and may also be further evidence for the presence of woody vegetation at this time. Particularly the abundance of a higher proportion of moisture indicator trees and shrubs pollen like ferns and Urticaceae supported the prevailing of wet early to mid-Holocene climate at Lake Tilo region (Lamb, 2001). However, the rare presence of ferns along with the decline of the diversity of woody species and increased grasses may respond for the start of aridity in regional scale including Lake Chamo area. Lake Chamo is found in a savannah ecosystem and, according to Jeltsch et al. (1998), savanna ecosystems show occurrence of trees and grasses in a natural state. On the other hand, climatic variability and anthropogenic activities may alter the coexistence of the trees and grasses in the savannah ecosystem, which may be a consequence of the interplay between fire, grazing, rainfall, and seasonality which could all affect the spatial and temporal pattern of trees and grasses in savannahs (Jeltsch et al., 1998; Yusuf et al., 2011). Fire has resulted in the reduction of trees and in the evolution of some of the most biodiverse ecosystems in the world, and is thought to have facilitated the rise of C_4 grass-dominated floras (Wooller et al., 2003; Bond et al., 2005).

The relatively rapid oscillations in fire regime during the period from 5200 – 4500 cal yr BP in Lake Chamo may have responded to a millennia scale regional aridity as inferred from speleothem records of south west of Ethiopia and other ERVL studies (Gillespie et al., 1983; Telford and Lamb, 1999; Lamb et al., 2000; Chalié and Gasse, 2002; Lamb et al., 2002; Lamb et al., 2004; Asrat et al., 2007; Baker et al., 2010; Foerster et al., 2012). The variation in regional levels might influence fire and vegetation patterns, which suggest that climate-driven changes determine vegetation and biomass productivity. Specifically, at around 5100 and 4800 cal yr BP, maximum fire intensity was observed from both charcoal concentration and molecular BC as a result of drier climatic conditions which promoted ignition.

It is also imperative to note that the high peak of charcoal during these periods especially in East Africa where human presence has long history may not be due to changes of the mid-Holocene climatic conditions only. In this regard, although the archaeological assemblages and dating along with oral history on the highland, at around 30 km from Lake Chamo, prove that the area has been settled since about 6400 years cal BP (Arthur et al., 2010); there is no indication about the human impact on the lowland particularly in the Chamo basin. The other line of evidence within the Turkana Basin of northern Kenya, archaeological excavations show a marked maximum human occupation between ~5000 and ~4000 cal yr BP (Garcin et al., 2012) which is coeval with a millennia scale regional aridity in East Africa including Lake Chamo. Garcin et al. (2012) explained that pastoralism was expanded as a result of lake regression due to aridity and the opening up of new browsing land in the region. Especially, after ~5300 cal yr BP in northeast Africa, local herders and their domesticated livestock were forced to concentrate around Lake Turkana for securing sufficient water and pasture to encourage the settlement of pastoralists and to combat the arid climate (Garcin et al., 2012). This arid climate is also seen in Lake Chamo records and if the same scenario works during this period and pastoralists were settled in the basin that might have impacted the surrounding vegetation and would result in maximum fire intensity particularly around 5100 and 4800 cal yr BP. Putting the foregoing connections in mind, it seems logical that high peak of charcoal during these periods might be due to the changes of the mid-Holocene climatic conditions along with the expansion of pastoralists.

In response to the onset of arid conditions starting at around 5100 cal yr BP, vegetation changed from a woody to a grass savanna with lower biomass for fires. This was observed by an increase in grass-derived macro-charcoals and by a high B5CA/B6CA ratio value indicating that the fire was colder and derived from grass or steppe fires (Wolf et al., 2013). This also supported by a pollen record done in other parts of Ethiopia which is carried out both at high and low altitude. Pollen record at high altitude, above 3000 m at Bale Mountains of south-central Ethiopia (Umer et al., 2007) indicated that after 4500 cal BP, mid-altitude dry Afromontane Juniper–Podocarpus forests developed in response to

reduced rainfall. This interpretation broadly fits with decline of both charcoal counts and black carbon of Lake Chamo in response to a prevailing arid period. However, at lower elevation in south-central Rift Valley (Lake Tilo), the pollen record did not show a clear vegetation response to this Holocene arid events particularly at c. 5100 cal yr BP (Lamb, 2001), when a high peck of charcoal is recorded at Lake Chamo.

The response of the East Africa savannah vegetation to this climate variability reveals that vegetation changed from forest dominated to grass dominated savannah, as is apparent from pollen, C/N ratios and $\delta^{13}C$ data from Lake Tilo during the early-mid Holocene transition (Lamb, 2001; Lamb et al., 2004). An abrupt decline in arboreal pollen percentages seen in other East Africa regions (Burundi and on Mount Kenya) also reflect the presence of arid conditions during the transition to the mid-Holocene (Jolly et al., 1994; Wooller et al., 2000). This is in accordance with the fire residue record of Lake Chamo, which shows a dramatic decline in charcoal counts and can be related to the production of small charcoal fragments from burnings in grass savannahs. A devoid of vegetation cover following this long term aridity is also shown by a generally high flux of K since 4500 to around 2400 cal yr BP (Figure 4.1). BC quality during transition between wood and grass savannah (Unit 1/ Unit 2) reveals a trend towards lower fire temperatures, which have been related to grass or forest ground fires in a previous study (Wolf et al., 2013). However, particularly at 3750 cal yr BP, the lower value of B5CA/B6CA indicates hotter fire events, e.g. by human activity or by lighting processes, however, further evaluation of the BC quality at higher resolution would be needed in order to prove this conclusively. A slight increase in charcoal count paralleled with a notable decrease of BC at around 2400 cal yr BP, whilst at the same time the BC quality still points to elevated fire temperatures which might also be typical for forest burnings (Figure 4.2; Wolf et al., 2013). According to Pyne et al. (1996), forests burn rarely and leave low total BC. The regional pollen data suggested that the onset of a wet period around 2500 year BP at Bale Mountains as recorded by the rise of Juniperus and Hagenia forest taxa (Mohammed and Bonnefille, 1998) and at around 2430 cal yr BP, Podocarpus, Juniperus and Hagenia increased in Lake Tilo region which

indicating the presence of both wet and arid period (Lamb, 2001) might be supporting the above notion of Lake Chamo charcoal data.

4.4.2 Late Holocene Fire implication for Human impact

Although separating the effects of climate and human impact during the late Holocene is difficult, the BC quality pointing at higher burning temperatures of fires might be due to rising anthropogenic activity in the surrounding area. This finding seems to follow previous research which states that human activity was a primary driver of global fire occurrence for at least the past 2000 years (Power et al., 2008). Lake Chamo charcoal data indicate that from about 2000 cal yr BP inputs of fire residues increased notably. Increases of BC, lower charcoal counts with elevated fire temperature indicate the burning of grass vegetation (Wolf et al., 2013). In particular, this increase in fire residues inputs suggests that the fires may be a result of intensive agricultural land use (e.g. stubble burnings (Clark et al., 1989)). Soil erosion due to clearing vegetation in Northern Ethiopia was significantly populated from the mid Holocene and agricultural activity was intensified in the Late Holocene, as a consequence of the rise of state like, Aksum, the capital of a powerful African state (Bard et al., 2000). The initiation of agricultural activity, and its impact, in southern Ethiopia is currently not well understood. The indirect evidence about the start of agricultural activity in the region may be inferred from indigenous terraces which were practiced by the local people. The radiocarbons from stonewalled indigenous terraces at Chencha–Dorze Belle, prove that the terraces have been long-lived agricultural activities in the region and they were built and used over the last 800 years (Assefa and Bork, 2014) which indicate that the stepland was cultivated at least during this time (see section 2.4 for detail). The settlers on a mountain top above Lake Abaya on the western edge of the Rift Valley, which dated from the thirteenth to the nineteenth centuries, also practiced symbols of fire as a tradition (Arthur et al., 2010) which suggesting anthropogenic fires had a long history in that region. Therefore, this result suggests that a human regulated fire regime may have taken place during the last 2 millennia. Rucina et al. (2009) mentioned the expansion of grasslands during the late Holocene as a result of elevated human presence

within the Rumuiku Swamp and suggested that fire is the key driver of grassland dynamics in East Africa at this time.

A drop in fire residue input in Sub-unit 3c after 1600 cal yr BP might be a result of high population density, which suppresses natural fires (Marlon et al., 2013). A strong influence of anthropogenic fires to the inputs in Lake Chamo is also reflected in the increase in fire temperature, which is typical for cooking fires (Wolf et al., 2013). The increased charcoal and black carbon input and the black carbon quality point to higher burning temperatures of fires, implying rising anthropogenic activity in the region, specifically since 1200 cal yr BP.

The occurrence of both high BC input and charcoal amounts in Unit 4 indicate a general tendency to increasing fire frequency. Natural fire is a common phenomenon in the savanna environment and, more recently, fires in East Africa have been found to be associated with land use change to intensive agriculture (Colombaroli and Verschuren, 2010). Increased charcoal concentration (Figure 4.2) and high sedimentary charcoal influx, especially in large size classes (> 250µm), of the most upper part of the core reflect local fires to the catchment which may be associated with forest clearance and an increase of wildfire frequency closer to the shore. The microscopic and macroscopic charcoal record in Lake Hayk and Hardibo, northern Ethiopia, also show a conversion of secondary bush land vegetation to grassland at around 1200 to 1400 AD was intensified by human induced burning and forest clearance (Darbyshire et al., 2003). The charcoal data has provided information on the vegetation response to aridity, as documented by geochemical and biological proxies of Lake Chamo and similar findings of other nearby studies. Specifically, the onset of a millennia scale regional aridity during the mid Holocene, as evident from high peaks of Ca and Sr counts from the XRF measurement, diverse and high abundance of ostracods, and also reflected by lower biomass for fires, resulted in lower charcoal and BC concentration in Lake Chamo records.

On the other hand, Conedera et al. (2009) stated that magnetic susceptibility can also be used to identify past forest fires and allows differentiating between fire burning within the catchment or outside. Local fire preferentially recorded due to the deposition of

magnetically enhanced secondary ferrimagnetic oxides during burning. The amount of magnetic minerals in Lake Chamo is not related to burning since the magnetic susceptibility peak did not match the charcoal peak (Figure 4.1), but after burning erosion of fire-induced magnetic regolith from a catchment area may produce an important inflow of ferrimagnetic particles, creating magnetically distinct layers in lake sediments (Whitlock and Anderson, 2003; Conedera et al., 2009). In contrast, magnetic susceptibility and Fe were high in Subunit 3c, due to erosion of volcanic clasts (Figures 3.8, 4.1) whilst total charcoal abundance was dramatically low.

4.5 Conclusion

The charcoal record from Lake Chamo reveals that fire has been a part of the seasonally dry savanna ecosystem in southern Ethiopia for the past 9000 cal yr BP, and fire frequency varied significantly throughout the Holocene. The charcoal influx and fire frequency indicate the presence of greater fire during the early (8600 - 5100 cal yr BP) and late Holocene (2500 cal yr BP to present) and were lower during mid-Holocene (5000 - 2500 cal yr BP). The two independent methods for fire reconstruction; charcoal counting and detection of benzene polycarboxylic acids (BPCA), show that fire intensity was consistently higher and woody or that shrub vegetation was increased source of BC during the Early Holocene than after the period. The particularly low B5CA/B6CA ratios of this time interval suggest that the temperatures of these burns were high. During the transition period at 5100 and 4800 cal yr BP, the combination of high BC input and high charcoal counts suggest high fire frequency. The change in fire characteristics from hotter (lower value of B5CA/B6CA) prior to 5100 cal yr BP, to more frequent, cooler temperature (higher value of B5CA/B6CA) burns during this transition interval could have been the result of a shift in vegetation from woody savanna vegetation to grassland savannah. The decline of fire residue input (visible in both independent fire parameters) during the later mid-Holocene (after 3800 cal yr BP) indicates the vegetation's response to aridity, which is attributed to burnings of grass savannah with reduced biomass. These findings suggest a general dryland climate with very limited fuel production and low availability for bushfires during the mid-

Holocene. The increased input of BC after 2000 cal yr BP might be related to the occurrence of anthropogenic fires, which indicate that human activities became one of the main drivers of fire in the region. The fire temperature proxy indicates that burning of grasses, likely to be cereal stubbles, was dominating until around 1500 cal yr BP, due to the intensification of agricultural and pastoralist land. From 1200 cal yr BP hotter fire, likely domestic fires, were dominant. Additional paleofire records are still needed to derive a regional scale fire history of the East and Horn of Africa and to better examine fire, climate and human interactions. Particularly, the application of these two independent methods, macroscopic charcoal counting together with an organo-geochemical characterization of fire residues (BC quantity and quality by the BPCA method), in a more widely region would be a powerful means for understanding the impacts of fire and its interactions with human activity and climate.

Chapter 5

5. Climatic and hydrological instability in East Africa during the Holocene: Ostracod evidence in South Ethiopia, Lake Chamo

Abstract

Ostracod assemblages data recovered from Lake Chamo, southern Ethiopia, together with XRF geochemical data, provide evidence for climatic and hydrological instability in southern Ethiopia during the Holocene. Changes in ostracod assemblages are interpreted in terms of changing lake water salinity, as a result of fluctuations in the evaporation-precipitation rate due to climate variability. During the wettest phase of the reconstructed palaeoenvironment, the period between 8600 - 5400 cal yr BP, the lack of ostracod is probably caused by low calcite concentration availability in the lake water. During more arid periods, specifically from 5100 - 4200 cal yr BP, where the lake was shallow, more open, and a more alkaline habitat dominated by a diverse ostracod fauna. *Gomphocythere angulata, Oncocypris omercooperi, Ilyocypris gibba, Humphcypris* cf. *brevisetosa*, *Sclerocypris clavularis* Sars and *Pseudocypris bouvieri* are restricted to this time interval. The ostracod assemblages represent a wide range of saline-tolerant species when the level of the lake is low. The dominance of *Heterocypris giesbrechtii* following these assemblages is a good indication for the point at which the lake level fell to a minimum. This shallower, alkaline-saline environment persisted until 2400 cal yr BP where members of *Limnocythere* are found together with other associated genera. The climate shifted from warm-dry to warm-wet between 2400 and 1850 and from 1500 to 800 cal yr BP, and from relatively fresh water to shallow saline conditions, as shown by the dominance of only a few taxa. Finally, from 800 cal yr BP to the present, the climate was drier, as indicated by the

predominance of *Limnocythere*. *Darwinula stevensoni* dominated again towards the upper most part of the core, possibly due to an increase in littoral vegetation. The geochemical sediment data correlate well with the changes in ostracod communities during the past 8600 cal yr BP. The results of this study are compatible with other regional studies of Holocene lake level and palaeoclimate in East Africa.

5.1 Introduction

Ostracods are defined as small, bivalve aquatic crustaceans that secrete shells of low magnesium calcite. They are common in all types of aquatic environments and can be taxonomically distinguished according to the ecology of their niches, since their ecology is often reflected in the shape and structure of their carapaces, making them useful for palaeoenvironmental indicators. Their remains are commonly preserved in lake sediments and are increasingly being used to reconstruct Quaternary palaeoenvironments (Holmes and Chivas, 2002). In addition to providing a complementary line of evidence in multi-proxy investigations (Richardson and Dussinger, 1986), ostracods have a number of specific advantages as biological proxies because of their sensitivity to a range of ecological variables (Holmes and Chivas, 2002). They also respond to the climatic impacts on their aquatic environment. Hence, the species composition of palaeoecological ostracod assemblages is used in this work to reconstruct the climatic variability of the hydrological sensitive lakes of East Africa.

The Rift Valley Lakes of Ethiopia have been the focus of many palaeonvironmental studies for the last few decades; however, the reconstruction of palaeonvironment by using ostracod assemblages has only been done for the Ziway-Shala basin (Atnafu and Russo, 2004). The attempt was made by Lindroth (1952) but he did not find ostracods in Lake Chamo while he did investigation from many ERVLs. Different recent genera and species of ostracod from different ERVLs were reported by (Lowndes, 1932; Lindroth, 1952; Kibret and Harrison, 1989; Martens, 1990 b; Martens and Tudorancea, 1991). Too little is known about the ecology of East Africa species to allow detailed palaeoecological research

using ostracods in the Ethiopian rift valley lakes. Atnafu and Russo (2004) provided an enlightening basis to use this potential proxy to reconstruct palaeoenvironmental changes of Ziway - Shala Basin by using ostracod assemblages during late Pleistocene and Holocene.

In other parts of the East African region, climate reconstructions using ostracods from sediment records of Kenyan rift lakes were used (Cohen et al., 1983; Richardson and Dussinger, 1986). Cohen (1986) described the substrate preference of individual ostracod taxa in Lake Turkana and Verschuren et al. (2000) determined the response of ostracod taxa to changes in salinity, depth, and macrophyte cover in the hydrologically-closed Lake Oloidien (Eastern Rift Valley, Kenya). Lake-level history reconstruction using ostracods fossil assemblages and typology (Alin and Cohen, 2003; Park and Cohen, 2011) provide an important insight on the extent and influence of environmental changes in Lake Tanganyika and Lake Malawi. The palaeohydroclimatic condition of Lake Mobutu during the Late Quaternary (Cohen, 1987) and the influnce of anthropogenic disturbance of Lake Tanganyika during Late Holocene (Wells et al., 1999) were also determined by fossil ostracod assemblages.

In this study, ostracod assemblage analysis from Lake Chamo provides valuable biological insights in the extent and influence of environmental changes in this previously unstudied site. Lake Chamo is found in a semi-arid region representing a hydrologically-closed basin as it is located in a temporary endorheic system (Schutt and Thiemann, 2006). Therefore, the volume and chemistry of the lake are sensitive to the ratio of precipitation to evaporation and could give clue to the lake-level fluctuations and palaeohydrological changes as a result of climate variability in this lacustrine ecosystem. Accurate information on the ecology of individual recent ostracod species is lacking, thereby limiting their use in palaeoecological applications. Hence in this study, their ecological preference is obtained indirectly from the geochemical data obtained from the XRF measurements. In this context, the present work focuses on the taxonomy, stratigraphy and the use of ostracod assemblages to interpret the palaeoenvironments established during the Holocene period. Therefore, the main objective of this study is to identify significant autecological changes of ostracod fauna for providing initial bases to reconstruct the palaeoenvironmental

conditions of the lake Chamo and its region. It aims further to provide a quantitative, high-resolution analysis of shifts in ostracod fauna to investigate further the climate variability of Holocene period.

5.2 Material and methods

5.2.1 Ostracod extraction and identification

Ostracod samples (10 ml) at 32 cm at lower resolution and every 8 cm at high resolution were soaked in Calgon ® (sodium hexametaphosphate) and distilled water. Freeze-thaw physical treatment was applied to disaggregate fine-grained and compacted sediment (Forester, 1988). The soaked samples were frozen overnight, and then thawed for 2-4 hrs. The Freeze-thaw process was repeated before the samples being gently wet-sieved to separate ostracod valves and other coarse materials using 125 and 250 µm sieves. The residue containing the fossil ostracod valves was thoroughly rinsed with distilled water and frozen for at least 72 hrs. The frozen samples were freeze-dried. Ostracod specimens were sorted, identified and numbered under a stereo-microscope at high magnification. Identification was only carried out for fully matured adult ostracods. From each sample 300 - 500 valve was examined, if ostracods were abundant enough, but if the sample contained less than 300 valves all valves were used.

The valves were mounted on metal stubs and imaged using Scanning Electron Microscopy (SEM). SEM is useful for detailed work on sculpturing, muscle scar patterns and internal structures of the valves. The fossil identification was determined using scanning electron microscope images and compared with the published literatures in tropical Africa and a European region (Vavra, 1891; Vavra, 1897; Sars, 1928; Lowndes, 1932; Klie, 1933; Klie, 1939; Lindroth, 1952; Rome, 1962; Martens, 1984 a; Martens, 1990 a; Martens, 1990 b; Martens et al., 1997; Meisch, 2000; Atnafu and Russo, 2004; Cabral et al., 2005; Rumes, 2010). Additional information on their distribution of the fauna was checked on the checklist of African inland waters (Martens, 1984 a) and a subjective checklist of the recent, free- living non-marine ostracod (Crustecea) (Martens and Savatenalinton, 2011).

In order to reconstruct the palaeosalinity and palaeohydrology of a lake, and to gain evidence for climatic change, the ostracod shells underwent (elemental and isotopic) analysis. For this purpose 6-10 fully calcified adult specimens were picked from the identified species and manually washed under a stereomicroscope with a fine paintbrush. The valves were thoroughly cleaned at each stage with distilled water, 30% H_2O_2 and pure ethanol. They were then permitted to dry at room temperature and were placed in vials. The isotopic and elemental analyses are under investigation.

Eleven samples were analyzed for $CaCO_3$ and TOC in order to verify the high resolution XRF and geophysical measurement by Eva Lehndorff (collaboration with University of Bonn). Calcium carbonate and TOC measurements were conducted by an elemental analyzer EuroEA 3000, Series, EuroVector, Italy. 100 mg from each sample were treated with 25 µl of hydrochloric acid (20%), dried at 70°C for 30 min and then the milled sample were combusted and analyzed in the elemental analyzer (EA). Smear slide analyses were conducted on the fine fraction (residue) of samples sieved for charcoal at every 32 cm intervals in order to check the absence and presence of diatoms. Semi-quantitative analyses were done at x400 magnification under light microscopy.

5.2.2 Geometric morphometrics analysis for *Limnocythere* species

The taxonomy of the fossil ostracods retrieved from Lake Chamo was determined from valve morphology using the literatures on tropical Africa. For the Limnocythere species, geometric morphometrics were also performed. This study uses the geometric morphometrics following (Baltanas and Danielopol, 2011) and multivariate statistical analysis along with classical morphological observations to identify the *Limnocythere* species of Lake Chamo in comparison with the *Limnocythere* species found in the other ERVLs. Geometric morphometry deals with the quantitative analysis of outline shape to study how specimens are similar or different in shape and to perform statistical analyses of shape (Baltanas et al., 2003). The geometric morphometry analysis of the genus *Limnocythere* of Lake Chamo is compared to different *Limnocythere* species of Ethiopian and other East African rift lakes which were identified and revised based on their soft part

by Martens (1990 a). The SEM of genus *Limnocythere* from Lake Chamo samples and scanned images of the genus *Limnocythere* from different Ethiopian and other East African Rift Lakes (Martens, 1990 a) were used for this outline analysis (Table 5.1). For digitizing the valve, the SEM and the scanned pictures were inserted in the computer program called Adobe Photoshop. Outline modifications and cleaning of the background were performed using Adobe Photoshop following the principle of Stracke (2008).

Table 5.1. The list of the *Limnocythere* species studied for outline analysis along with their locality in Ethiopian Rift Valley Lake and other East African lakes. Abbreviation used are : Lbb – *Limnocythere borisi borisi*; Lbs – *Limnocythere borisi shalaensis*; Lba – *Limnocythere borisi awassaensis*; Ltt – *Limnocythere thomasi thomasi*; Ltl – *Limnocythere thomasi langanoensis*; Lt – *Limnocythere tudoranceai*; La – *Limnocythere africana* Klie; Lm &Ld – *Limnocythere michaelseni* Daday and *Limnocythere dadayi*; Lm – *Limnocythere minor*. M – male; F– female; RV– right valve; LV– left valve; Ext – external view. The numbers and the letters are corresponding to the figure captions in Martens, 1990 a. The abbreviations used from Lake Chamo in this study correspond to the levels from the SEM pictures.

Species	Abbreviations used	Location
Limnocythere borisi borisi Martens, 1990	Lbb_M_17_A_RV_Ext, Lbb_M_17_B_LV_Ext Lbb_F_17_E_RV_Ext, Lbb_F_17_F_LV_Ext	Lake Abiyata
Limnocythere borisi shalaensis Martens, 1990	Lbs_M_18_P_RV_Ext, Lbs_M_18_Q_LV_Ext Lbs_F_18_M_RV_Ext, Lbs_F_18_L_LV_Ext	Lake Shala
Limnocythere borisi awassaensis Martens, 1990	Lba_M_19_D_RV_Ext, Lba_M_19_F_RV_Ext Lba_F_19_E_LV_Ext, Lba_F_19_G_LV_Ext	Lake Awassa
Limnocythere thomasi thomasi Martens, 1990	Ltt_M_16_F_RV_Ext, Ltt_M_16_G_LV_Ext Ltt_F_16_K_RV_Ext, Ltt_F_16_J_LV_Ext	Lake Ziway
Limnocythere thomasi langanoensis Martens, 1990	Ltl_M_18_H_RV_Ext, Ltl_M_18_G_LV_Ext Ltl_F_18_A_RV_Ext, Ltl_F_18_B_LV_Ext	Lake Langano
Limnocythere tudoranceai Martens, 1990	Lt_M_20_A_RV_Ext, Lt_M_20_B_LV_Ext Lt_F_20_E_RV_Ext, Lt_F_20_F_LV_Ext	Ovamboland (Namibia)
Limnocythere africana Klie, 1939	La_M_17_Q _RV_Ext, La_F_17_P_LV_Ext	Lake Turkana (Kenya)
Limnocythere borisi shalaensis Martens, 1990	Lbs_M_17_M_RV_Ext, Lbs_M_17_L_LV_Ext, Lbs_F_17_N_RV_Ext	Lake Langano
Limnocythere michaelseni Daday and *Limnocythere dadayi* Marthens, 1990	Lm &Ld_M_19_N_RV_Ext, Lm &Ld_M_19_O_LV_Ext , Lm &Ld_F_19_S_RV_Ext, Lm &Ld_F_19_T_LV_Ext	Lake Rukwa(Tanzania)
Limnocythere minor Lindroth, 1953	Lm_M_17_O_RV_Ext	Lake Turkana (Kenya)
Limnocythere in Lake Chamo	L1_M_ TG2_40_RV_Ext, L1_M_TG2_41_RV_Ext L1_M_TG2_43_RV_Ext, L1_M_TG4_1_LV_Ext L3_M_TG4_15_LV_Ext, L3_M_TG4_21_LV_Ext L3_M_TG4_23_LV_Ext, L2_F_TG4_7_RV_Ext L2_F_TG4_9_RV_Ext, L2_F_TG4_10_LV_Ext	Lake Chamo

Outlines of the different SEM and scanned images of *Limnocythere* species from both male and female with their corresponding right and left valves were digitized using the tps software program (Rohlf, 2001). In order to describe shape in terms of a series of numerical descriptors a mathematical function was fitted to the outlines in a list of x-y coordinates. Shape functions were normalized for size mathematically, adjust to be independant to size of the outline trace (Danielopol et al., 2008 a). Normalizing for area allows comparison of shapes which differ in size and to compute mean-shapes whilst avoiding bias in the analysis due to unbalanced sample size. The outline analysis was performed and outlines were approximated using the B-splines method (Baltanas et al., 2003) with Morphomatica computer programs (Linhart et al., 2006). Approximation by B-splines allows description of practically any curve by a few "control points" up to a certain tolerance by a relatively small number of coordinates of the control points (Figure 5.1) (Baltanas et al., 2003). Normalized shape functions data can be used by multivariate analysis to map similarities and this shape similarity can be measured as the quadratic mean of the (Euclidean) distances between corresponding sets of control points (Baltanas et al., 2003; Danielopol et al., 2008 a). Finally, geometric morphometry results were processed using multivariate numerical techniques using the free software PAST (Paleontological Statistics) (Hammer et al., 2001) in order to obtain cluster analyses based on their Euclidean distances.

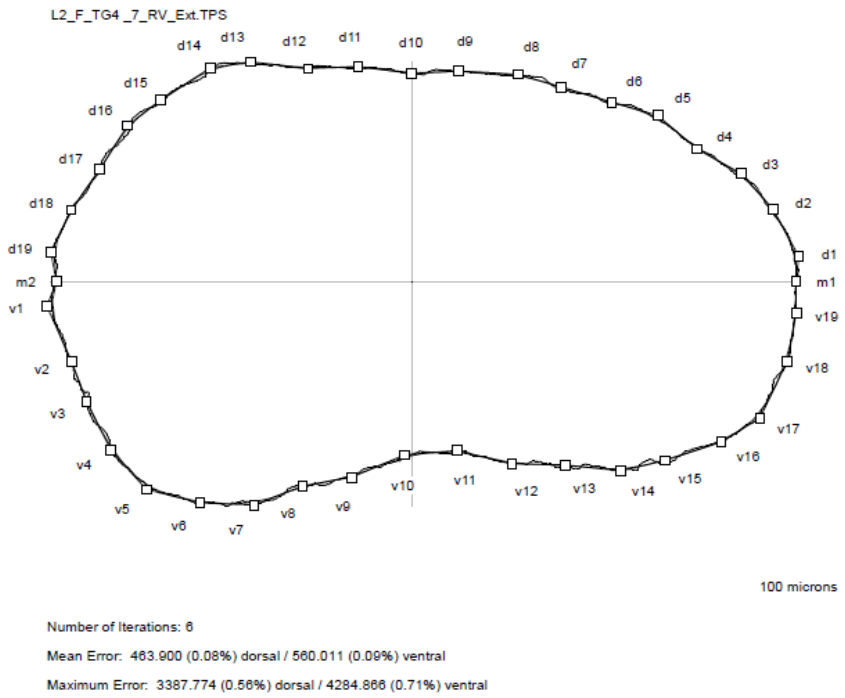

Figure 5.1. The positions of the B-spline control points which are very intuitively related to the shape of the curve.

5.3 Results

5.3.1 The geometric morphometrics analysis – *Limnocythere* species

Comparison of the valve outline of *Limnocythere* sp. from the different Ethiopian and East African Rift valley lakes were performed in order to obtain the most similar species to *Limnocythere* sp. found in Lake Chamo. According to the individual valve outline analysis coupled with the classical morphological observation, *L. tudoranceai* is the most nearest similar species with *Limnocythere* found in Lake Chamo (see Figures 5.2 - 5.5). Similarly, comparing the SEM pictures of *Limnocythere* in Lake Chamo with the valve outline with other species, *L. Africana, L. minor, and L. borisi shalaensis* (Lake Langano population) also confirm the similarity of these groups of *Limnocythere* (See in Appendix B for detail). All the other outline analyses performed in this study are presented in Appendix B.

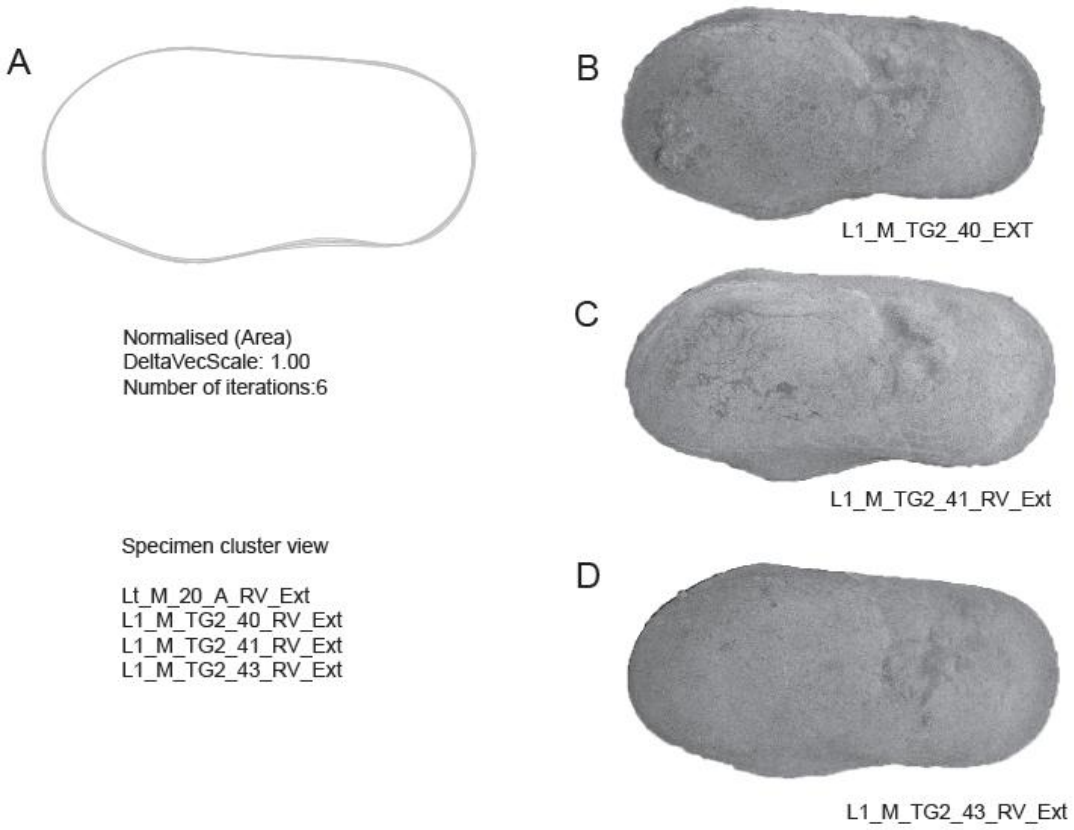

Figure 5.2. A- Outline analysis performed on right valves of male *L. tudoranceai* and *Limnocythere* in Lake Chamo using a Geometric Morphometric approach. Comparison of mean outlines calculated for the species in "normalised for area" mode. B – D, SEM images of the male *Limnocythere* in Lake Chamo that used for the outline analysis.

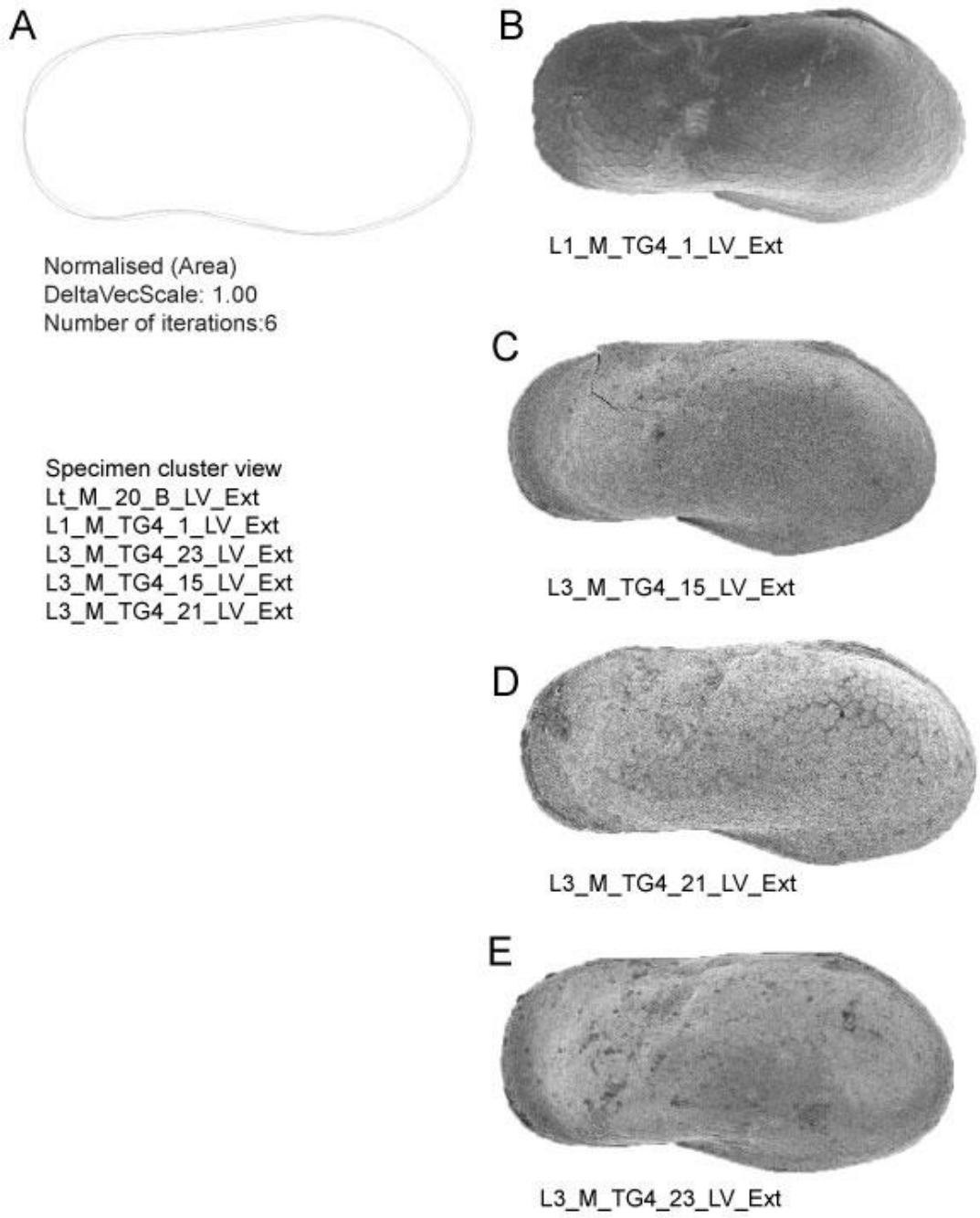

Figure 5.3. A - Outline analysis carrid out on left valves of male *L. tudoranceai* and *Limnocythere* in Lake Chamo using a Geometric Morphometric approach. Comparison of mean outlines calculated for the species in "normalised for area" mode. B-E, SEM images of the male *Limnocythere* in Lake Chamo that used for the outline analysis.

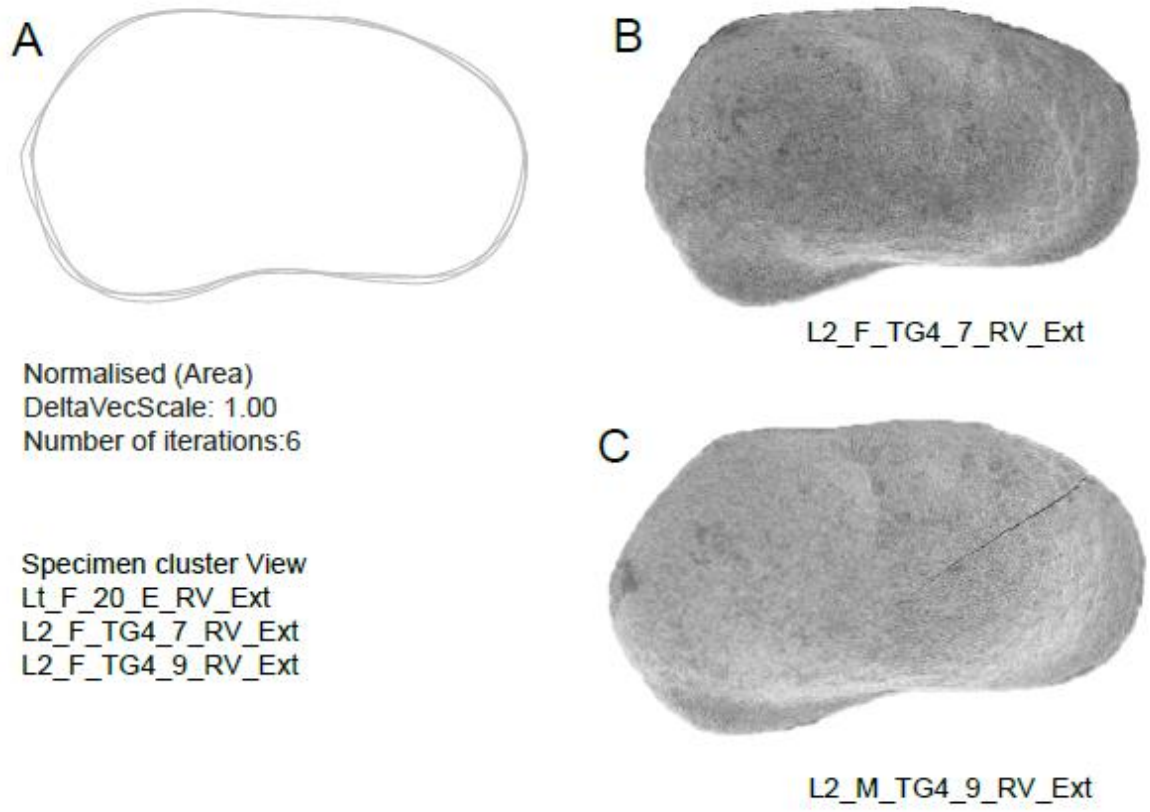

Figure 5.4. A - Outline analysis presented right valves of female *L. tudoranceai* and *Limnocythere* in Lake Chamo using a Geometric Morphometric approach. Comparison of mean outlines calculated for the species in "normalised for area" mode. B-C, SEM images of the female *Limnocythere* in Lake Chamo that used for the outline analysis.

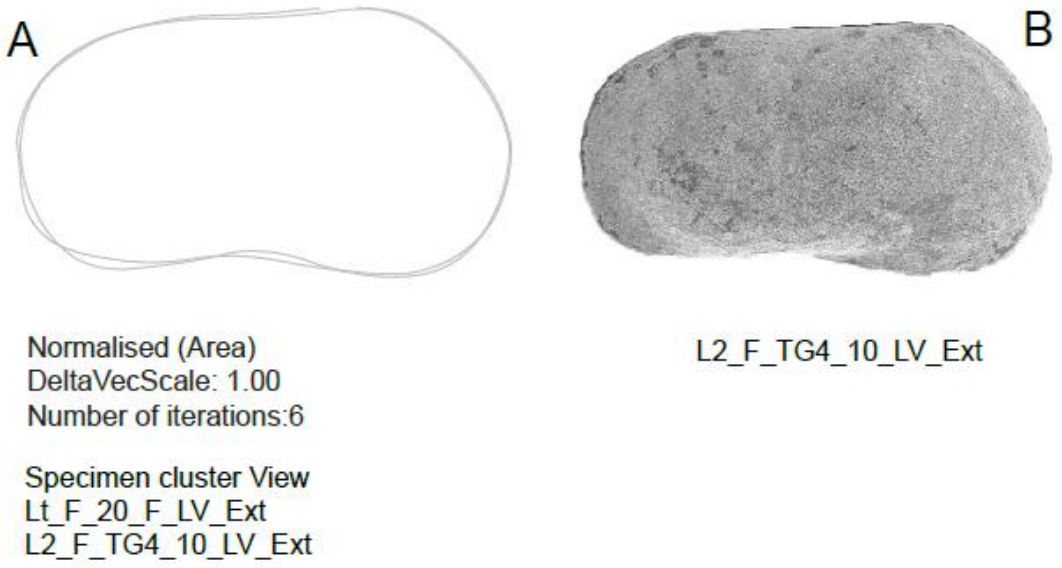

Figure 5.5. A - Outline analysis performed on left valves of female *L. tudoranceai* and *Limnocythere* in Lake Chamo using a Geometric Morphometric approach. Comparison of mean outlines calculated for the species in "normalised for area" mode. B - SEM image of the female *Limnocythere* in Lake Chamo that used for the outline analysis.

The individual outline analysis was combined with the clustering analysis using the PAST (Paleontological Statistics software), in order to determine their similarity using their distance differences among the successive species (Figure 5.6). This morphometric analysis compared the outlines of all the analyzed *Limnocythere* species and shows the similarity and difference among the different group.

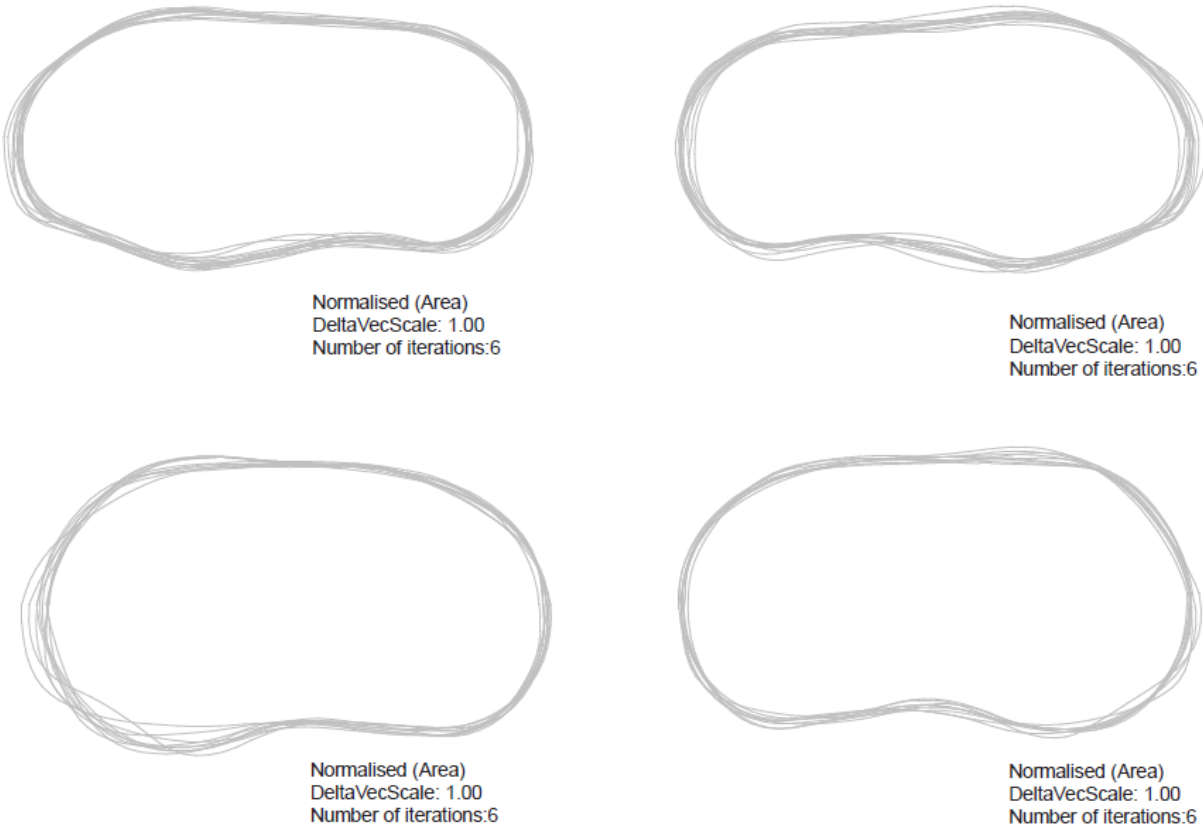

Figure 5.6. Outline analysis carried out on different *Limnocythere* species found in Lake Chamo and other Ethiopian Rift Valley lakes using a Geometric Morphometric approach. Comparison of mean outlines calculated for the species in "normalised for area" mode.

The results of the geometric morphometrics analysis on the valves of the different population of *Limnocythere* were processed using multivariate numerical techniques by using the free software PAST, reported in Figures 5.7 - 5.10. The hierarchical cluster analysis applied on the distance for "normalized for area" outline matrix from both male and female right valves show the *Limnocythere* found in Lake Chamo and *L. tudoranceai* show morphological convergence from their distance similarity. The cluster analysis based on the male right valves show two clusters (Figure 5.7); Cluster A includes the *L.thomasi* group and *L.borisi shalaensis* (Lake Shala population) and Cluster B with all the other *Limnocythere* species including the Lake Chamo once. In cluster B, three Limnocythere

from Lake Chamo (L1_M_TG2_40_RV_Ext, L1_M_TG2_41_RV_Ext, and L1_M_TG2_43_RV_Ext) and L. tudoranceai clustered together.

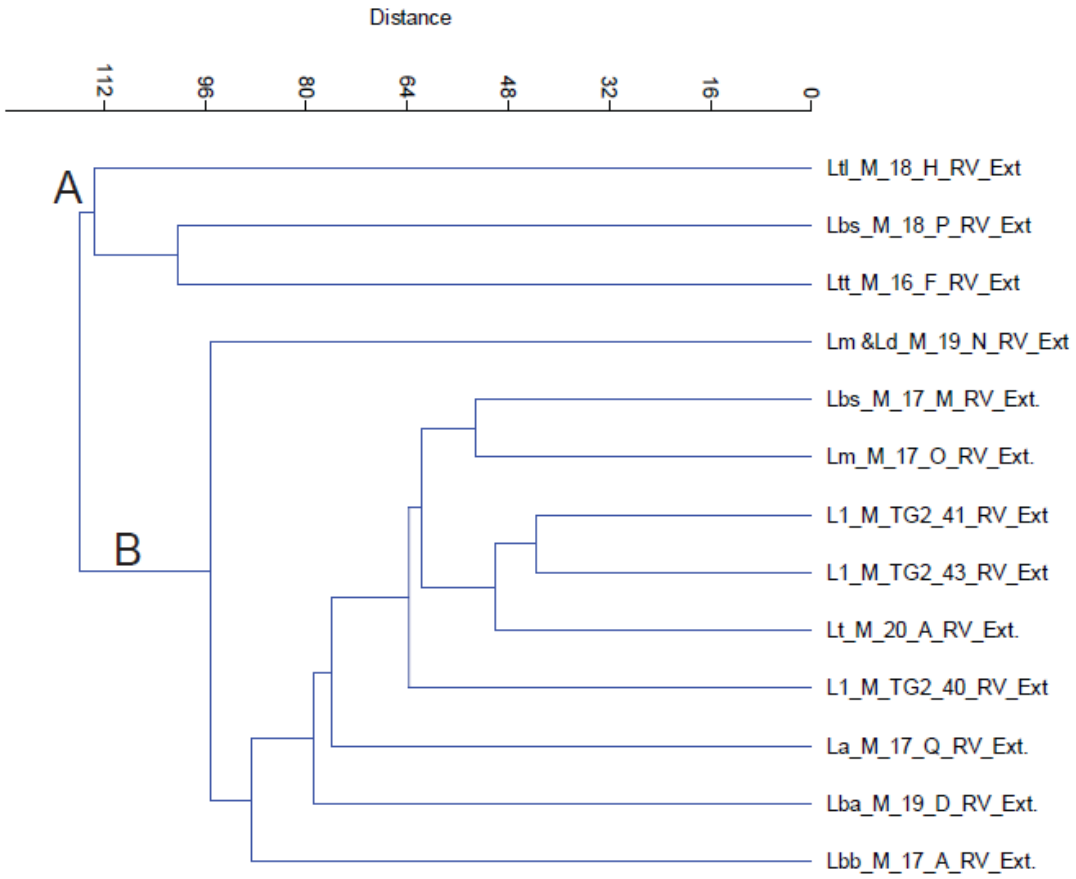

Figure 5.7. Outline analysis presented on different male right valves of *Limnocythere* species found in Lake Chamo and other Ethiopian Rift Valley lakes using a Geometric Morphometric approach. Dendrogram derived from the cluster analysis of (euclideans's distance) on the matrix obtained from the analysis of the outlines in "normalized for area" mode.

The cluster analysis based on the female right valves show great disparity between the seven different groups (Figure 5.8). Cluster A includes the *Limnocythere* in Lake Chamo (L2_F_TG4_9_RV_Ext) as individual group and Cluster B has *L.borisi shalaensis* (Lake Shala population) while Cluster C has *L.thomasi thomasi* of Lake Ziway group. The other groups include two species; Cluster D contains *L. borisi awassaensis* and *L. michaelseni* and *L. dadayi*, Cluster E has *L. borisi borisi* and *L. thomasi langanoensis*, Cluster F contain *Limnocythere* in Lake Chamo (L2_F_TG4_7_RV_Ext) and *L. tudoranceai*. The last

Cluster, G, includes *L. borisi shalaensis* of Lake Langano population as an individual group.

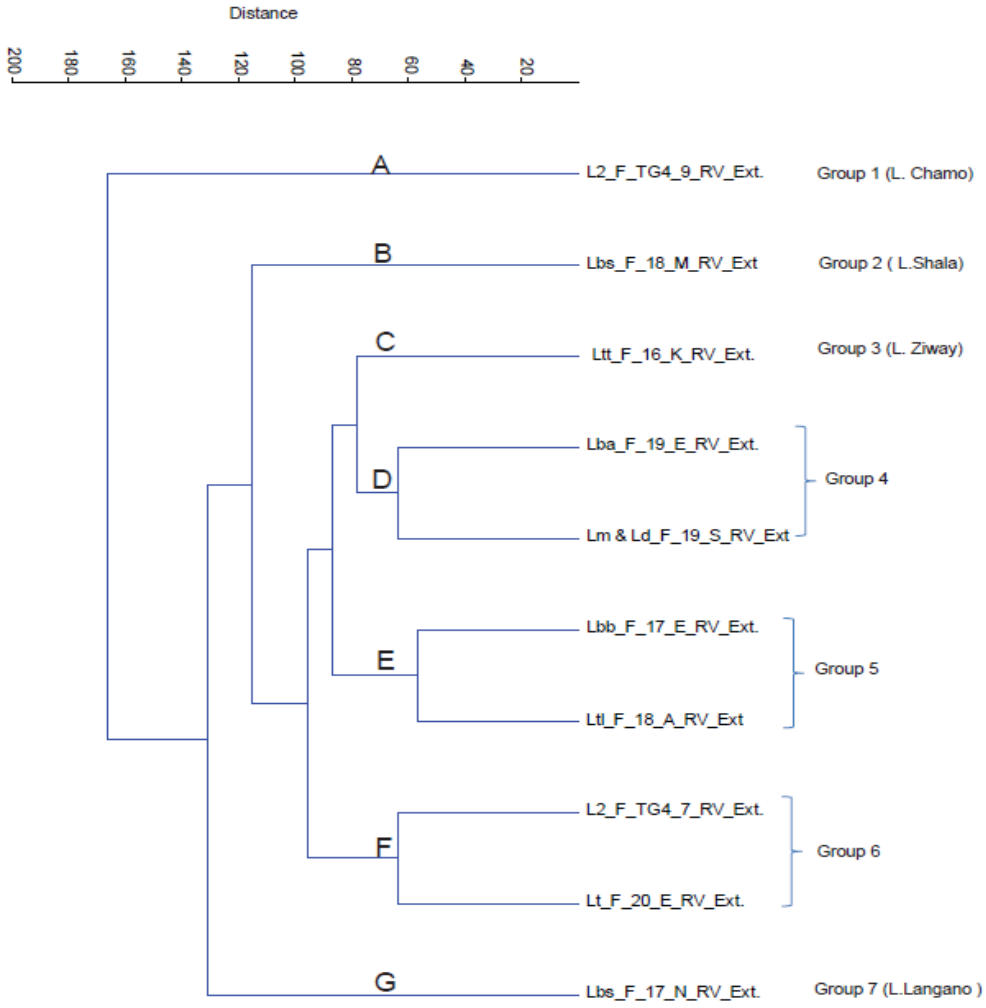

Figure 5.8. Outline analysis performed on different female right valves of *Limnocythere* species found in Lake Chamo and other Ethiopian Rift Valley lakes using a Geometric Morphometric approach. Dendrogram derived from the cluster analysis of (euclideans's distance) on the matrix obtained from the analysis of the outlines in "normalized for area" mode.

The cluster analysis based on the male left valves show 4 groups (Figure 5.9); Cluster A includes the *Limnocythere* in Lake Chamo (L3_M_TG4_21_LV_Ext) as individual group

while Cluster B has *L. borisi borisi*, *L. michaelseni* and *L. dadayi*, and *L. thomasi langanoensis*. Cluster C contains *L. borisi awassaensis* and *L.thomasi thomasi*. The last cluster, D, includes three *Limnocythere* from Lake Chamo (L3_M_TG4_15_LV_Ext, L3_TG4_23_LV_Ext and L1_M_TG4_1_LV_Ext), both *L.borisi shalaensis* from Lake Shala and Lake Langano and *L. tudoranceai.*

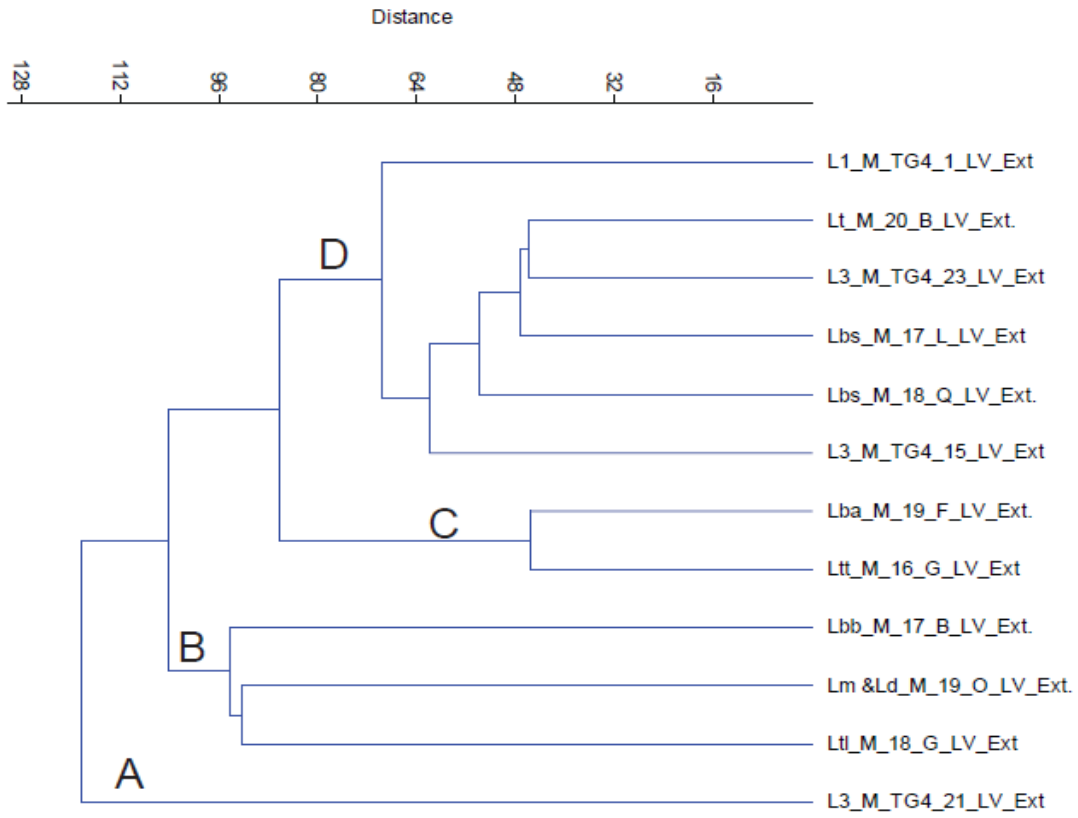

Figure 5.9. Outline carried out on different male left valves of *Limnocythere* species found in Lake Chamo and other Ethiopian Rift Valley lakes using a Geometric Morphometric approach. Dendrogram derived from the cluster analysis of (euclideans's distance) on the matrix obtained from the analysis of the outlines in "normalized for area" mode.

The cluster analysis based on the female left valves show two clusters (Figure 5.10); Cluster A includes one *Limnocythere* species of Lake Chamo (L2_F_TG4_10_LV_Ext) and Cluster B contains all the other groups.

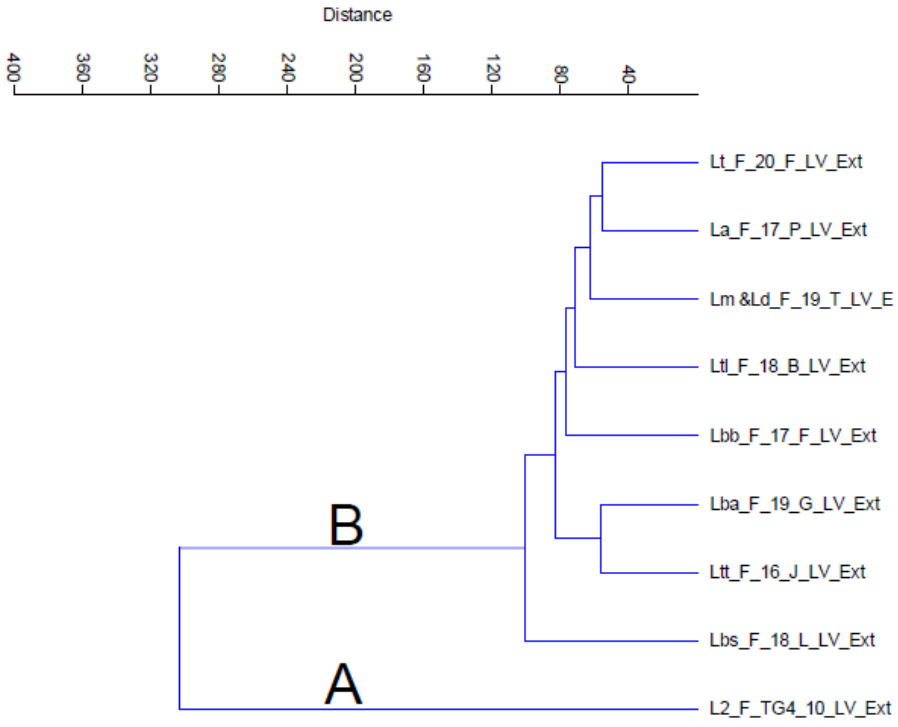

Figure 5.10. Outline analysis presented on different female left valves of *Limnocythere* species found in Lake Chamo and other Ethiopian Rift Valley lakes using Geometric Morphometric approach. Dendrogram derived from the cluster analysis of (euclideans's distance) on the matrix obtained from the analysis of the outlines in "normalized for area" mode.

As a summary, the hierarchical cluster analysis applied on the similarity "normalized for area" outline matrix indicated the presence of different group of *Limnocythere* that vary in form. On this basis, outline and cluster analysis of 10 *Limnocythere* valves from Lake Chamo were analyzed and three different *Limnocythere* groups are expected. The first group includes six out of the ten analyzed valves. Among these (L1_M_TG2_40_RV_Ext, L1_M_TG2_41_RV_Ext, L1_M_TG2_43_RV_Ext) of the male right valves, (L1_M_TG4_1_LV_Ext, L3_M_TG4_23_LV_Ext) of male left valve, and (L2_F_TG4_7_RV_Ext) of female right valve are grouped together and this group is clustered together with *L. tudoranceai.* The second group is male left valve (L3_M_TG4_21_LV_Ext) (Figure 5.9), female right valves (L2_F_TG4_9_ RV_Ext) (Figure 5.8), and female left valves (L2_F_TG4_10_LV_Ext) (Figure 5.10) which show

individual groups, which do not belong to any of the analyzed *Limnocythere* group. The third group is (L3_M_TG4_15_LV_Ext) (Figure 5.9) and this group seems to belonging to *L.borisi shalaensis* population.

5.3.2 Presence and/or absence of ostracod and diatoms and their relation with the geochemical data

As indicated in Chapter 3, the core shows four main lithostratigraphic units; based on geochemical and lithological data and the Q7/4 diagram. The presence and/or absence of ostracod and diatoms and their interpretation follow these units division. The ostracod concentration data is only based on 32 cm resolution. The abundance of ostracods follows more or less the same pattern like Ca counts and Ca/Ti ratio of the XRF measurement and $CaCO_3$ (g kg^{-1}) from elemental analyzer. Ostracods are generally restricted to below 10.76 m depth, with only few present at the upper part of Unit 1 (Figure 5.19) when carbonate values are generally low. Relatively high Si/Ti ratio also corresponds to the highest diatoms presence in this unit. Generally, high value of TOC is also recorded from elemental analyzer in this unit. The high values of Ca, Ca/Ti ratio and $CaCO_3$ correspond with highest abundance of ostracod shells in Unit 2 (Figure 5.19.). The highest abundance of ostracods is observed at around 9-10.5 m. In contrast, the low value of Si/Ti ratio coincides with the rare presence of diatom in this unit. In this unit a slight decline of TOC is observed.

In Unit 3, Ca concentration from XRF measurements and carbonate from EA measurements shows a declining trend. Parallel with the ostracod concentration pattern, it is also lower than in Units 2 and 4. Diatoms have lower value at this unit. TOC also show lower value in this unit. In Unit 4, where most of the geochemical values show a slight increase, ostracods concentration also has a higher value in this unit. Diatoms appear in lower values at this unit. TOC value increased upward to the upper part of the core.

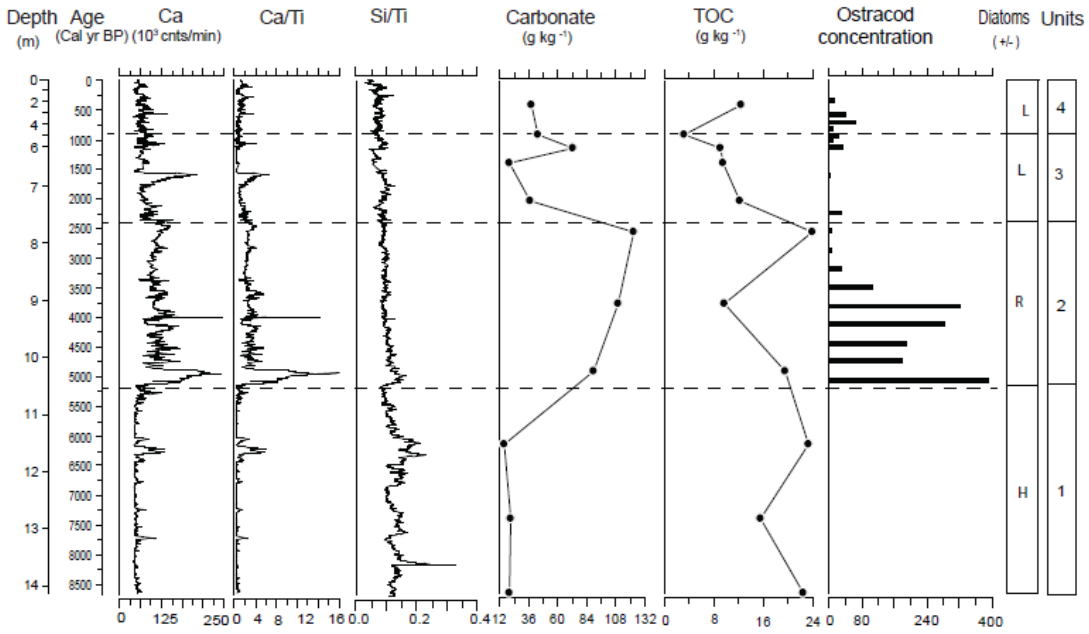

Figure 5.11. The relationship between the geochemical data and the presence and absence of ostracods and diatoms. From right to left are XRF Calcium counts (Ca) (10^3 counts/ min), Ca/Ti ratio, Si/Ti ratio, $CaCO_3$ (g kg^{-1}) from elemental analyzer, TOC (g kg^{-1}), total ostracod concentration (Number of valves per 10 ml), presence/ absence of diatoms (+/-) (H– high; L– low; and R– rare) and units. Y-axis is depth (m) and age (cal yr BP). Dashed lines in the figure mark the different units described and discussed on pages 24-28.

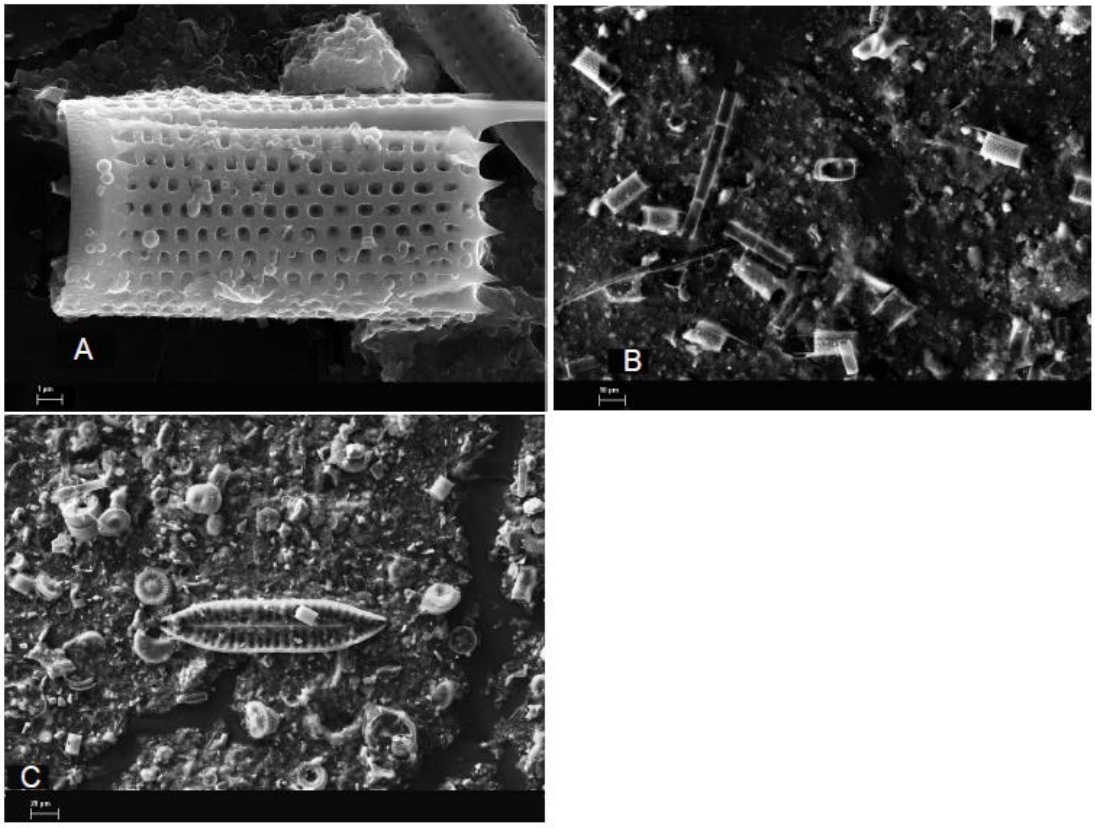

Figure 5.12. Unidentified SEM images of diatoms A) CHA-01-2010-1 B) CHA-01-2010-10 and C) CHA-01-2010-12. Photos by Ute Frank, 2011. Scale A = 1 µm; B = 10µm and C = 20 µm.

5.3.3. Species abundance distribution

At intervals of 32 cm the abundance and distribution of ostracods were determined (Figure 5.11), followed by identification of different ostracod species and detail palaeoecological analysis at a higher interval resolution of 8 cm (Figure 5.13).

There is a high diversity of ostracod species in Lake Chamo core; fourteen different taxa were identified (Table 5.2 and Figure 5.13). For the purpose of palaeolimnological applications, the identification of species is vital. SEM images of the valve morphology of all identified taxa are illustrated in Figures 5.14 - 5.16. Taxonomic comments are needed in order to avoid taxonomic uncertainties from this unstudied lake. The most widely distributed ostracod species in Lake Chamo are *Limnocythere* sp., *Darwinula stevensoni* and *Candonopsis africana* throughout the entire core above 10.76 m (Figure 5.13).

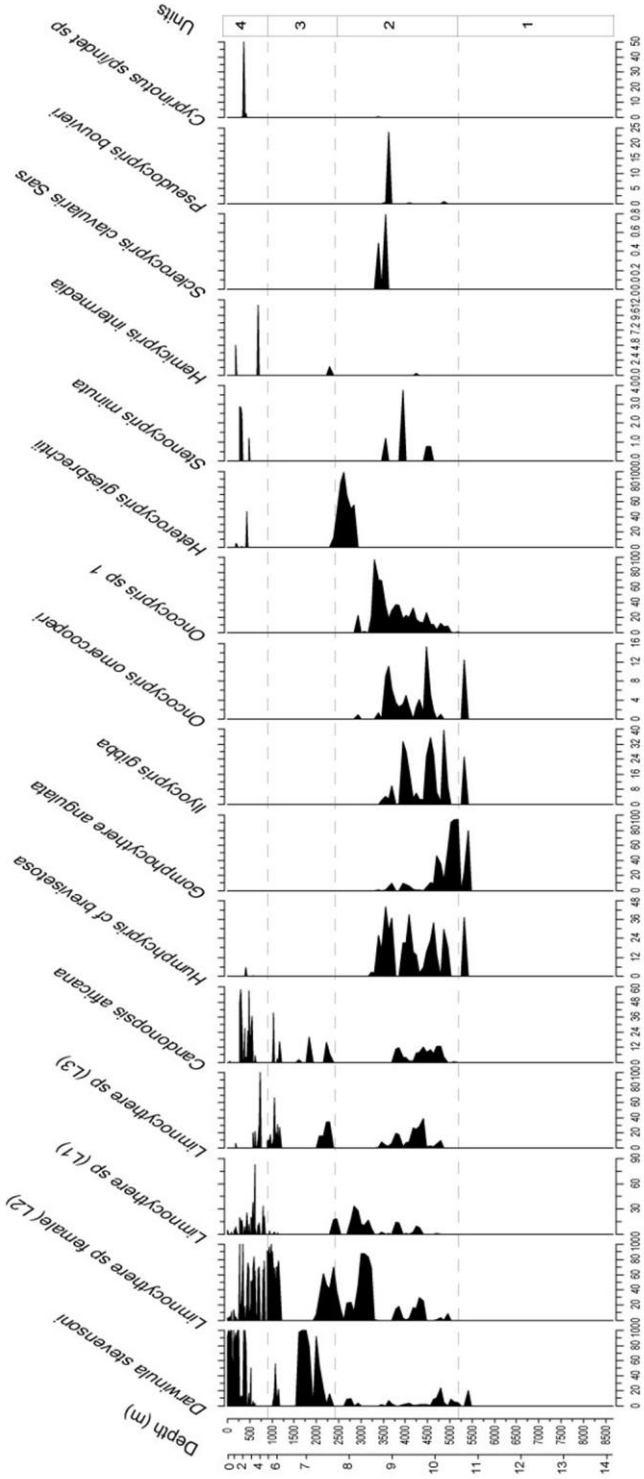

Figure 5.13. Ostracod stratigraphy showing valve abundance of the identified taxa presented in Lake Chamo, percentages refer to total counted valves for that core interval.

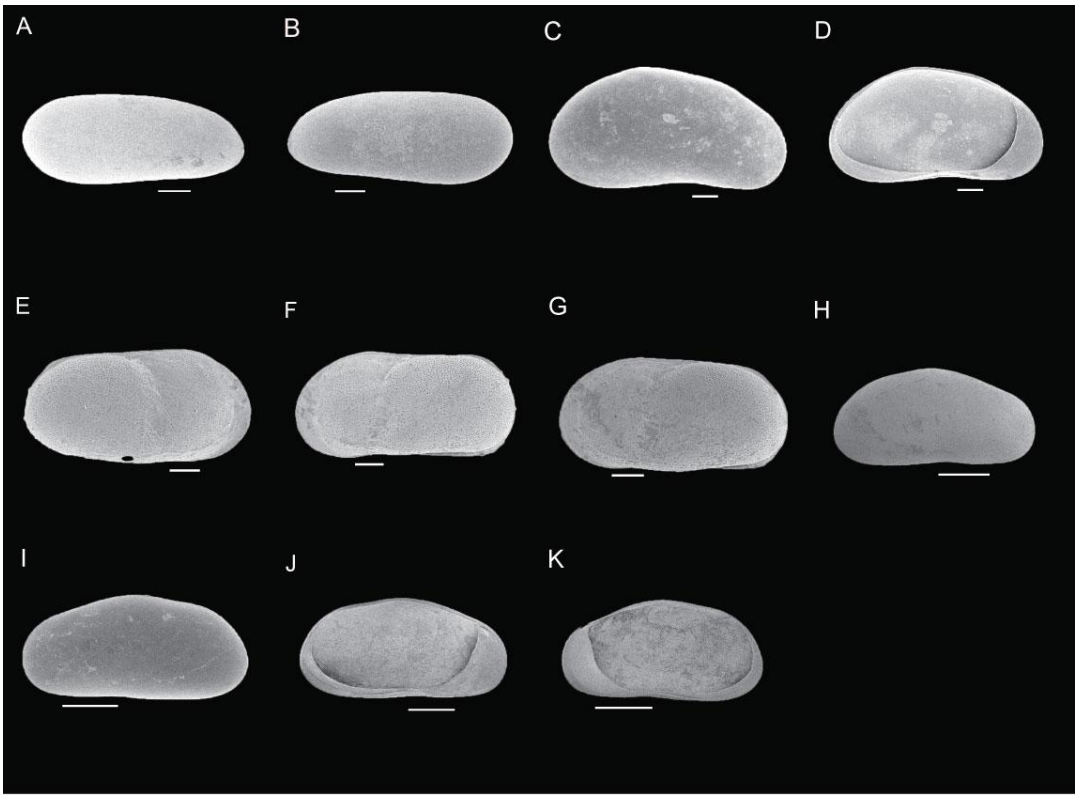

Figure 5.14. *Darwinula stevensoni* (A-B); *Candonopsis africana* (C-D); *Gomphocythere angulata* (E-G); *Humphcypris* cf. *brevisetosa (*H-K); D***. stevensoni***: A. right valve, external view; B. left valve, external view; ***C. africana*****:** C. right valve, external view; D. right valve, internal view. ***G. angulata***: E. right valve, external view; F. left valve, external view; G. left valve, external view. ***H.*** **cf.** ***brevisetosa*** : H. right valve, external view; I. left valve, external view; J. right valve , internal view; K. left valve, internal view. Scale A-G = 100 µm; H-K = 300µm.

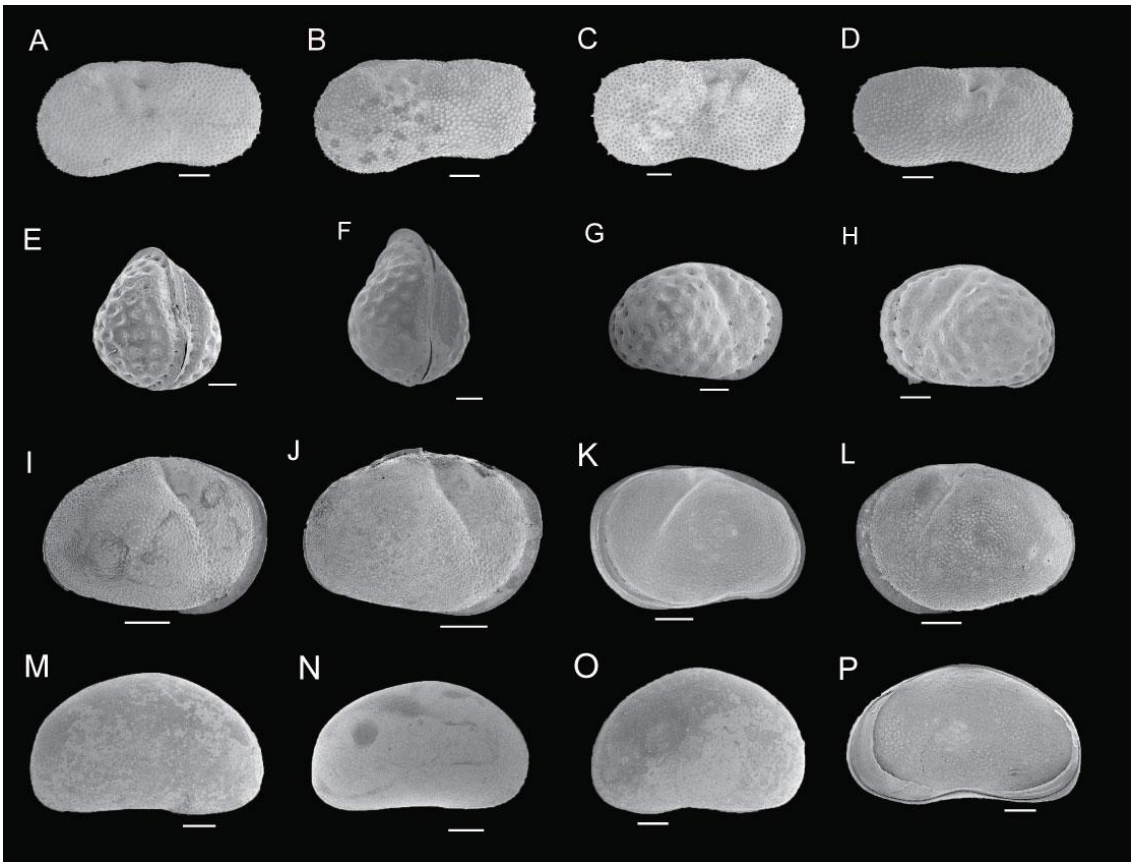

Figure 5.15. *Ilyocypris gibba* (A-D); *Oncocypris omercooperi* (E-H); *Oncocypris* sp. type Chamo (I-L); *Heterocypris giesbrechtii* (M-P); ***I. gibba***: A. right valve, external view; B. right valve, external view; C. left valve, external view; D. left valve, external view. ***O. omercooperi***: E. carapax, dorsal view; F. carapax, dorsal view; G. right valve, external view; H. left valve, external view. ***O.* sp. type Chamo** : I. right valve, external view; J. right valve, external view; K. left valve, external view; L. left valve, external view. ***H. giesbrechtii***: M. right valve, external view; N. right valve, external view; O. left valve, external view; P. left valve, internal view. Scale A-P = 100 µm.

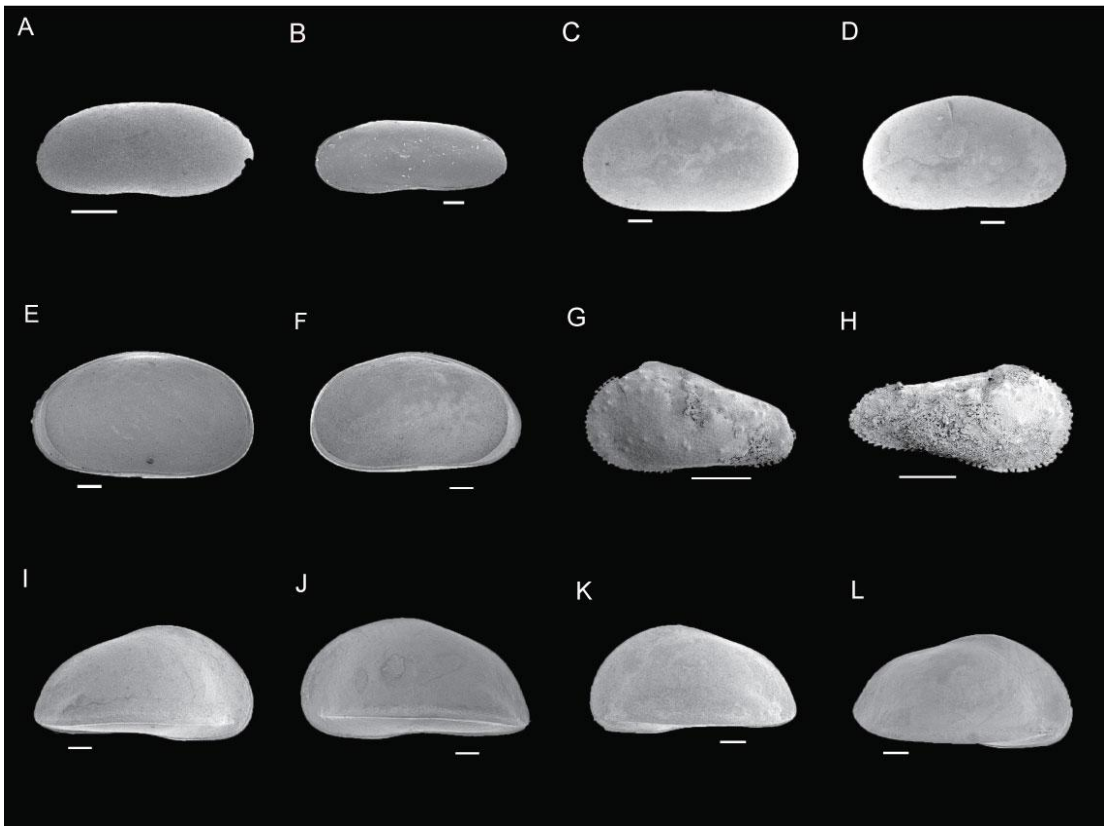

Figure 5.16. *Stenocypris minuta* (A-B); *Hemicypris intermedia* (C-F); *Sclerocypris Clavularis* Sars (G-H); *Psedocypris bouvieri* (I-L); ***S. minuta***: A. left valve, external view; B. right valve, internal view. ***H. intermedia***: C. left valve, external view; D. right valve, external view; E. left valve, internal view; F. right valve , internal view. ***S. Clavularis* Sars**: G. juvenile, right valve, external view; H. juvenile, left valve, external view. ***P.bouvieri***: I. right valve, external view; J. left valve, external view; K. left valve, external view; L. right valve, external view. Scale A-F = 100 µm; G-H = 300µm; I-J=100 µm.

Unit 1 (14.13–10.50 m, 8646 – 5130 cal yr BP)

In the geochemical and lithological analysis of Unit 1 below 10.50 m the ostracod count at 32 cm intervals did not show the presence of ostracod below this depth, but the high resolution ostracods analysis indicated the presence of ostracod up to 10.76 m. Overall ostracods are almost entirely restricted below 10.76 m (corresponding to an age of 5375 cal yr BP) of the core; only five out of the fourteen different taxa are found at the top of this unit. In this unit, *D. stevensoni* constitutes up to 20 %, *H.*cf. *brevisetosa* constitutes up to

36%, *G. angulata* reaches up to 80%, and *O. omercooperi*, up to 12 % of the total ostracod abundance (Figure 5.13).

Unit 2 (10.50 – 7.66 m, 5130 – 2405 cal yr BP): A highly diverse assemblage of ostracods taxa are found in this unit. *Limnocythere* sp. occurs in great abundance in almost all parts of the core and specifically at a depth of 8.52 to 8.20 m. *D. stevensoni* is found frequently in this unit but in small abundance. *C. africana* occurs in relatively low amount at depth of 10.40 to 9.00 m in this unit. Particularly *H.*cf. *brevisetosa, I. gibba, G. angulata, Oncocypris* sp. type Chamo, *O. omercooperi, H. giesbrechtii, S. minuta, S. Clavularis Sars* and *P. bouvieri* are found to occur frequently but are mostly restricted at this interval within the core (Figure 5.13). *Humphcypris* cf. *brevisetosa* constitutes 44% of the ostracod fauna at 8.84 m and is quite common throughout the interval 10.68 to 8.52 m, whilst in other parts of the core it is rare or absent. *I. gibba* sp. was found at a core interval between 10.68 to 8.6 m and constitutes only 40% of the ostracod fauna at 10.2 m. *G. angulata* sp. constitutes as much as 95% of the ostracod fauna at 10.52 m and is quite common throughout the interval from 10.76 to 8.68 m. It is absent in the upper part of the core (Figure 5.13). *Oncocypris* sp. type Chamo occurs abundantly but more restricted on the interval from 10.52 to 8.12 m and it reaches its maximum of 97% of the total ostracods at depth of 8.6 m. Even if *O. omercooperi* occurs in association with *Oncocypris* sp. type Chamo on the same depth range (10.76 to 8.2 m), its amount is less than 16% of the total fauna. *H. giesbrechtii* reach 99% of the ostracods fauna at a depth of 7.88 m and very abundant between 8.12 to 7.64 m. *S. minuta* which comprise up to 4% of the total ostracod fauna and only few *H. intermedia* are found in Unit 2. *S. Clavularis* Sars is rare (only 4 juveniles valves) at 8.84 m and 8.68 m, making up 0.8% of the total ostracod fauna. *P. bouvieri* abundance is relatively low at 24% of the ostracod fauna at depth of 8.92 m but at depth of 8.84, 9.4 and 10.2 m a small amount of this species is found and entirely absent in the rest of the core (Figure 5.13).

Unit 3 (7.66 – 4.50 m, 2405 – 790 cal yr BP): In this unit there is a less diverse assemblage of ostracods. *D. stevensoni* is the most dominant one and reaches its maximum abundance at a depth between 7.4 and 6.84 m. *Limnocythere* sp. occurs in great abundance, particularly at depths between 7.72 to 7.32 m and 6.36 to 5.0 m, which constitutes up to

100%. *C. africana*, *H. giesbrechtii* and *H. intermedia* are also found in small amounts in this unit. At depth of 6.70 m to 6.20 m (1600-1200 cal yr BP), ostracod is absent (Figure 5.13).

Unit 4 (4.50 – 0.12 m, < 790 cal yr BP): A more diverse assemblage of ostracods are found in this unit in comparison to Unit 3. Generally, the three most widely distributed ostracod species are found in higher abundance in this unit. *Limnocythere* sp. shows a big fluctuation and higher abundance, especially at depths between 4.5 m to 1.8 m, where the species constitutes up to 100%. *D. stevensoni* is the most dominant species at this unit and reaches its maximum abundance from 1.8 m to the most upper part of the core. The highest abundance of *C. africana* is also observed at this unit, specifically at depth between 3.16 to 1.8 m, which constitute up to 56% of the total ostracod abundance but from 1.8 to 0.12 m the species is absent. *H.*cf. *brevisetosa* are rare at this unit. *H. giesbrechtii, S. minuta* are also found in relatively small abundance in this unit. *H. intermedia* attend its maximum value at this unit which constitutes only 12% of the total amount of the ostracod fauna. There are 6 valves which are still taxa indet (cf. *Cyprinotus kliei*) at the most upper part of the core (Figure 5.13).

5.4 Discussion

5.4.1 Genus *Limnocythere* identification using a geometric morphometric approach

The geometric morphometric approach used, together with the morphological observations of the carapaces shape, muscle scars, and selvages character suggest that the *Limnocythere* found in Lake Chamo can be grouped in to three types. Out of the ten valves analyzed for outline and cluster analyses, six of them are grouped as one and this group has very close shape similarity with *L. tudoranceai*. which suggests these two groups are of the same species, although they differ in their distribution. *L. tudoranceai* is found in Namibia (south West Africa) and their occurrence at different localities needs further investigation. In the second group, three out of ten valves might be grouped as one. All of them are individual

groups which are placed in Cluster A (Figures 5.8, 5.9 and 5.10) and do not belong to any one of the *Limnocythere* found in ERVLs and other East African lakes. This group needs taxonomic revision since this approach does not relate to other groups. In the third group only one out of the ten valves is found which indicates that this group might belong to *L.borisi shalaensis*. Specifically, the morphological observations verify that this group resembles the one found in Lake Langano rather than Lake Shala population.

Although their occurrence in different regions is still in question, Martens (1990 a) observed the close relation of *L. tudoranceai* and *L. africana.* In this context, the *L. africana* male right valve and female left valve used for outline and cluster analyses confirm this relationship with *L. tudoranceai* (Figures 5.7 and 5.10). Therefore, the geometric morphometric analyses in this study also indicates that the *Limnocythere* of Lake Chamo (Group 1) is similar to *L. tudoranceai* and *L. africana* and follow Martens (1990 a) observations. Here one can deduce that both phylogenetic analysis (Martens, 1990 a) and geometric morphometric analysis can complement each other and applying both approaches for further analysis of ostracod taxonomic work is recommended. The shortcoming of using only a geometric morphometric approach for the identification of this genus should be considered, as it does not show the detailed heterogeneous structures observed during the visual identification of the different *Limnocythere*. Geometric morphometric and morphological observations approaches do not show the close similarity between Lake Chamo *Limnocythere* species with *L.thomasi* group, although Martens (1990 a) anticipated the occurrence of this group in lakes other than Lake Langano and Ziway.

The genus *Limnocythere* is the most popular and widespread in ERVLs (Martens, 1990 a; Atnafu and Russo, 2004). Like other ERVLs, *Limnocythere* sp. is the most widely distributed ostracod genus in Lake Chamo. According to Martens (1990 b), during the Holocene, the genus *Limnocythere* underwent speciation in these Rift Lakes and mentioned the evolutionary potential of this genus in East Africa. The polymorphism of this genus has been studied on the living species (Martens, 1990 a), which displays a great variability in the soft parts particularly on hemipenis morphology. Martens (1990 a) did a taxonomic revision of this genus based on their hemipenis structure and suggested its endemism for

every particular lake and proposed further phenological work to understand the adaptive radiations of this genus. More recently, Atnafu and Russo (2004) focused on this particular genus for palaeoenvironmental reconstruction in the Ziway - Shala basin, to link regional climatic variations of the Late Pleistocene to Holocene period. Due to its wide tolerance ranges for conductivity and alkalinity, Martens (1990 a) strongly recommend not to use this genus as a palaeoenvironmental indicator group. According to Martens (1990 a) every ERVLs have their own endemic species, which can be determined from morphological observations and use of a geometric morphometric approach, and which shows that most of the *Limnocythere* species look similar. It is uncertain whether the unidentified species of the *Limnocythere* in Group 2 in Lake Chamo are endemic to the basin and if this group is indeed a different species. This shape resemblance between *Limnocythere* species may reflect the degree of genetic similarity or the existence of similar evolutionary responses to analogous environmental condition between the different lakes due to their underground interconnection by NE-SW united regional faults (Alemayehu et al., 2006). Although further investigation needs to be undertaken, this study has contributed to the identification and understanding of *Limnocythere* ecological and evolutionary processes for palaeoenvironmental reconstruction using both geometric morophmerics and morphological approaches.

5.4.2 Abundance of ostracod and diatoms as palaeoenvironmental indicators

This study provides qualitative information in relation to the response of ostracods to environmental variability in order to reconstruct past environments. Accurate information on the ecology of modern individual species has been lacking, thereby limiting their use in palaeoecological applications. Hence in this study, their ecological preference is obtained indirectly from the geochemical data obtained from the XRF and EA measurements, which helps to resolve this problem by providing indirect information about the ecological preferences of these ostracod species (Figure 5.11). On the basis of the analysis of ostracod assemblages, frequently fluctuated palaeoclimatic and palaeoenvironmental evolution

stages are recognized. By interpolating constant sedimentation rates between the dated horizons, the data suggests high lake level and the wettest phase from 8600 – 5400 cal yr BP, where lack of ostracod probably caused by two possible scenarios. The first may be due to poor calcite preservation, also supported by Cohen (1987) who observed an abrupt decease of $CaCO_3$, Mg and Sr content during the pronounced lake level rise in Lake Mobutu. Similarly, Cohen et al. (1983) also pointed out that the absence of ostracod assemblages is representative of carbonate-bicarbonate poor water. The second scenario may correlate with chemical dissolution of calcium carbonate related to organic matter decay. Organic acids and carbon dioxide generated out of this organic material by degradation can lower the pore water pH and dissolve sedimentary carbonates, including ostracod valves (Dean, 1999). Similarly, Alin and Cohen (2003) observed for Lake Tanganyika where sediments with high soil organic matter (SOM) concentrations have lower ostracod abundance.

In a freshwater lake such as Lake Chamo, ostracod species and abundance correlate well with changing lake depth and once the condition is changing in to dry periods, specifically from 5100-2400 cal yr BP, where the water is shallow, a more alkaline/saline habitat is dominated by a variety of ostracod fauna. As the geochemical proxy identified at this time interval (Figure 5.11), calcium carbonate is highly saturated, which agrees with the argument of Palacios-Fest et al. (1994) who found that many ostracods species occur in saturated or super saturated waters with calcium carbonate. Fossil ostracod assemblages were found at a shallower water depth in Lake Malawi where the lake water is saturated with respect to $CaCO_3$ (Cohen et al., 2007). In contrast, Atnafu and Russo (2004) reported diversified assemblages of ostracods in Lake Ziway and Langano which indicate low salinity environments but increased salinity due to evaporation which diminishes diversity.

The high level of calcite from around 5400 cal yr BP corresponds to an increase in ostracod valves. Their preservation could suggest high alkalinity, which would promote the preservation of diverse ostracod taxa who could tolerate a wide range of alkalinities and salinity. Apart from the three most widely distributed ostracod species, seven taxa, *G. angulata, O.* sp. type Chamo*, O. omercooperi, I. gibba and H.*cf. *brevisetosa*, occurred

frequently, but only at this restricted interval of time within the core. Two other rare species, *S. Clavularis* Sars *and P. bouvieri* are also restricted to this time interval (Figure 5.13). The presences of most of these taxa indicate that the lake level was at a minimum at this time and the presence of more saturated waters with respect to calcium carbonate.

The high dominance of *G. angulata*, making up to 95% of the ostracod fauna at 10.52 m, which is a transition stage, indicates the preference of this species to predominantly freshwater and lower salinity level. *G. angulata* has also been reported in large numbers in the modern fresh water environments of modern Lake Ziway and Langano, in sheltered habitats close to vegetation (Martens, 1990 b; Martens and Tudorancea, 1991). Martens and Tudorancea (1991) also mention that *D. stevensoni* and *G. angulata* need high O_2 concentrations to aerate the eggs and juveniles in their carapaces. Therefore, the preference for inhabiting littoral vegetation may help them to get enough O_2 during the photosynthesis process. *G. angulata, O. omercooperi, I. gibba, and S. minuta* are also tolerant of a wide range of alkalinities/salinity in both modern and fossil assemblage of Lake Ziway (Lowndes, 1932; Atnafu and Russo, 2004) and Lake Nakuru (Cohen et al., 1983). Cohen et al. (1983), which is particularly observed in that *I. gibba* is a truly estuarine adapted species. The dominancy of *H. giesbrechtii*, which makes up to 99% of the ostracod fauna between 2800 to 2400 cal yr BP is a good indication for the depth of the lake being at its minimum level, whilst its disappearance afterwards indicates relatively high lake level. Martens and Tudorancea (1991) observed the appearance of a temporary pool fauna, *H. giesbrechtii*, towards the beginning of the rainy season (April – May) when the depth of the Lake Ziway was at its minimum level. Rumes (2010) also noted the occurrence of *H. giesbrechtii*, which is found in temporary water bodies and is specifically associated with warm and turbid ponds devoid of littoral or aquatic vegetation in moderately saline waters in Southern Kenya.

This shallower alkaline-saline environment was interrupted by relatively brief episodes of higher precipitation and relatively high lake level in Unit 3. This climate shift indicated by relatively less saline / alkaline conditions is shown by the dominance of the three most dominant groups *D. stevensoni*, *Limnocythere* sp. and *C. africana*. The diversity decreases

significantly which may be due to under saturation of calcium carbonate during this fluctuated humid and short dry condition from around 2400 to 800 cal yr BP. Specifically, the high abundance of *D. stevensoni* at this time interval indicates the reoccurrence of predominantly freshwater and lower salinity levels of the lake water.

In Unit 4, rapid return of highly alkaline/ saline condition from 800 cal yr B.P to the present are indicated by relatively more diverse assemblages of ostracod fauna. The climate was getting warmer as more *Limnocythere* and other associated groups dominate towards the upper part of the core. The dominancy of *D. stevensoni* and *C. africana* towards the most upper part of the core is attributed to an increase in littoral vegetation after the reoccurrence of wetter periods between 2400 and 1850 and from 1500 to 800 cal yr B.P. Martens et al. (1997) also found that *D. stevensoni* predominantly occurs in shallow margins of fresh water lakes and can occur in a range of saline to even very saline conditions. The co-occurrence of *D. stevensoni* and *C. africana* in the modern and fossil assemblages in Lake Ziway indicate the preference of a low salinity lake environment with calm (sheltered) waters (Martens and Tudorancea, 1991; Atnafu and Russo, 2004), although in the recent Lake Katanda and Lake Kyaninga (Uganda) *C. africana* was found in a wide range of conductivities ranging from around 100µS/cm up to 5800µS/cm (Rumes, 2010).

The highly variability in occurrence and abundance indicates variation in palaeoecological affinities related to the lake chemistry, which also validated by the geochemical proxies from the XRF measurement. Most of the ostracods species assemblages from Lake Chamo were responding to highly fluctuating environmental variability and indicated variation in lake depths as a result of evapo-precipitation and salinity change. Similarly, Atnafu and Russo, (2004) examined ostracod assemblages in relation to salinity fluctuations in the Ziway-Shala basin, attributed to changes in climate. Cohen et al. (1983) also studied the palaeoecological and palaeochemical parameters of Eastern and Southern Africa ostracods based on fossil assemblages and typology and suggested a fluctuating alkaline / saline condition during Holocene.

The presence and absence of diatoms in the sediment record of Lake Chamo have palaeolimnological implications. The high abundance of diatom in Unit 1 clearly reflects an early - middle Holocene high stand of the lake and increase in precipitation and/or a decrease in evaporation in the region. This condition promotes the entrance of substantial dissolved silica in to the lake through increased runoff from the surrounding basin; as a result, Si concentration remains relatively high during wet climate and high precipitation, as also indicated in Lake Malawi (Johnson et al., 2011). The presence of high amounts of Si/Ti from the XRF measurement is supported by the presence of abundant and large round shaped diatoms as shown in Figure 5.12 C. These kinds of diatoms require large amounts of silica in order to build their large skeletal structure but under drought climatic condition (Unit 2), the dissolved silica flowing into the lake may have been buried in the sediment when lake level dropped below the elevation of its outlet or diluted during times of high carbonate precipitation (Johnson et al., 2011; Stone et al., 2011). This high carbonate precipitation in turn may have led to the dilution or the deterioration of diatom valves (Johnson et al., 2011) and could be a reason for the observed significant lower abundance of diatom in Unit 2. This is in agreement with the geochemical data (Figure 5.11) where the declining of silica corresponds with the presence of few and elongate diatom in this unit. The rectangular shaped and/ or elongate diatoms (Figures 5.12, A and B) need a small amount of silica to build up their body and could be the reason for their presence under lower amount of Si/Ti in Unit 2. The other line of evidence for the decline of Si/Ti ratio in the record of the sediments in Unit 2 may have been due to the decrease in preservation of biogenic silica at high temperature and pH (Burnett et al., 2011). In Unit 3 small increments of diatom abundance are observed either due to terrigenous Si input during flooding events in this unit or due to the reoccurrence of relatively deeper and more diluted waters. In Unit 4, low presence of diatoms reflecting highly fluctuating water depth and chemistry.

5.4.3. Biogeographic and climatic implications

Ostracods in Lake Chamo are the dominant microfauna, as found in other East African Rift Valley Lakes and very important information is generated from their assemblages to estimate the highly climatic fluctuations of the region. Major changes in ostracod faunas

and lake conditions correspond to regionally recognized indications of climate changes. The ostracod data recorded from Lake Chamo is successful in reconstructing the known high stands lake level during early Holocene in ERVL (Gillespie et al., 1983; Lamb, 2001; Chalié and Gasse, 2002) and other East Africa lakes (Richardson and Dussinger, 1986; Johnson et al., 1991) and clearly identified the different fluctuations of climate throughout the Holocene period. Although the sharp high peaks of Ca and Sr in Lake Chamo indicate the strongest aridity started at around 5100 cal yr BP, the high-resolution analysis of shifts in ostracod fauna clearly indicate that the dry condition had already started by around 5400 cal yr BP and the decline of lake level may have started 300 years earlier than the start of maximum aridity. This is because calcium carbonate precipitation could have been enhanced in shallow lakes after a high evapotranspiration process by high temperatures for long time periods but the calcium carbonate concentration could be enough to build up their large skeletal structure of ostracods. That is why the biological indicator (ostracod) indicated the earlier start of dry condition in this lake. This biological data is in a good agreement with the diatom-inferred salinity reconstruction in Lake Abiyata (Chalié and Gasse, 2002) which indicates the presence of shallow, saline conditions after 5400 cal yr BP. Similarly, an increase in $CaCO_3$ and high alkalinities/ salinity tolerant taxa in Lake Chamo suggest that the lake levels declined after around 5400 cal yr BP. Cohen et al. (1983) suggests the presence of fresh water conditions until about 8000 yr BP and higher alkalinity throughout the remainder of the Holocene inferred from ostracod typology of fossil record from Lake Nakuru (Kenya).

Table 5.2. The distribution of the identified species from Lake Chamo and their distribution in other zoogeographic region of East African lakes.

Species	Location		Distribution
	Recent	Fossil	
Darwinula stevensoni (Brady and Robertson, 1870)	Lake Ziway (Lowndes, 1932); Lake Turkana (Cohen, 1986), western Uganda crater lakes (Rumes, 2010)	Late Pleistocene and Holocene Ziway- Shala Basin (Atnafu and Russo, 2004), Late Quaternary of Lake Mobutu (Cohen, 1987), Late Holocene of Lake Tanganyika(Wells et al., 1999)	Europe, N& S America, Africa, Asia (Lindroth, 1952)
Candonopsis africana Klie, 1944	Lake Ziway (Martens, 1990b), Recent freshwater of Sudan (Martens, 1984), western Uganda crater lakes (Rumes, 2010), Lake Kivu & lake Kibuga (Lindroth, 1952)	Late Pleistocene and Holocene Ziway- Shala Basin (Atnafu and Russo, 2004)	Ethiopia (Martens, 1984, 1990 b; Atnafu and Russo, 2004),Uganda(Rumes, 2010),Central Africa (Lindroth, 1952)
Gomphocythere angulata Lowndes, 1932	Lake Ziway, Shala, Awassa (Lowndes, 1932; Martens, 1990 b), Lake Turkana (Cohen, 1986),	Late Pleistocene and Holocene Ziway- Shala Basin (Atnafu and Russo, 2004)	Central and East Africa (Abyssinia, L. Magera, L. Kibuga) (Lindroth, 1952)
Oncocypris omercooperi Lowndes, 1932	Lake Ziway (Lowndes, 1932; Martens, 1990 b),Serpent Lake, Zaquala River Kattere, Hora Harsadi , Mt Chillalu (Lowndes, 1932)		West Africa (Angola), central & East Africa (Abyssinia) (Lindroth, 1952),
Oncocypris sp. Type Chamo	Lake Katanda and Lake Kyaninga (Uganda) (Rumes, 2010).		(Uganda) (Rumes, 2010)
Ilyocypris gibba (Ramdohr, 1808) Brady & Norman, 1889	Lake Turkana (Cohen, 1986), recent freshwater of Sudan (Martens, 1984), in Kenyan lakes and ponds (Rumes, 2010)	Late Pleistocene and Holocene Ziway- Shala Basin (Atnafu and Russo, 2004)	Europe, North Africa (Algeria, together with French West Africa) ,East Africa , Middle East, North and south America, central Asia, China (Lindroth, 1952; Meisch , 2000).
Humphcypris cf.*brevisetosa* Martens 1997			(Ethiopia, Kenya, Zaire) (S.Africa)(Martens, 1997)

Stenocypris minuta Lowndes, 1931	Lake Ziway, (Lowndes, 1932; Martens, 1990 b), Mount Chillalu (Lindroth, 1952)		East Africa (Abyssinia/ Ethiopia) (Lindroth, 1952)
Heterocypris giesbrechtii (G.W.Muller, 1910)	Lake Ziway (Martens, 1990 b), recent freshwater of Sudan (Martens, 1984), in Kenyan lakes and ponds (Rumes, 2010)	Late Pleistocene and Holocene Ziway- Shala Basin (Atnafu and Russo, 2004)	Sudan (Martens, 1984), Kenya (Rumes, 2010)
Hemicypris intermedia (Lindroth, 1952)	Lake Turkana (Cohen, 1986), recent freshwater of Sudan (Martens, 1984), in Kenyan lakes and ponds (Rumes, 2010)	Late Quaternary of Lake Mobutu (Cohen, 1987)	Uganda, Democratic Republic of the Congo (Cohen 1987), Sudan (Martens, 1984), Kenya (Rumes, 20110)
Sclerocypris Clavularis Sars, 1924	Lake Turkana (Cohen, 1986), in Kenyan lakes and ponds (Rumes, 2010)	Holocene of Lake Bogoria, (Cabral et al.,2005), Late Quaternary of Lake Mobutu (Cohen, 1987)	Uganda, Democratic Republic of the Congo (Cohen 1987), Kenya and India (Cabral et al.,2005), South Africa (Lindroth, 1952)
Psedocypris bouvieri Daday, 1908	Lake Rukwa (Martens, 1990), in Kenyan lakes and ponds (Rumes, 2010)	Late Pleistocene and Holocene Ziway- Shala Basin (Atnafu and Russo, 2004)	Tanzania (Martens, 1990), Kenya (Rumes, 2010), Ethiopia (Atnafu and Russo, 2004)

The ostracod fauna in the time range between 5400 to 2400 cal yr BP in Lake Chamo are indicators of an important biogeography event with intense palaeoclimatic implications. *D. stevensoni*, *C. africana*, *G. angulata*, *I. gibba*, *H. giesbrechtii*, and *Pseudocypris* sp. are also found in Ziway- Shala Basin during the late Pleistocene and Holocene (Atnafu and Russo, 2004). Martens (1990 b) and Martens and Tudorancea (1991) also reported most of these taxa in the modern Lake Ziway. The study carried out on faunal-substrate associations in modern Lake of Turkana at different water depths reported the presence of *I. gibba*, *G.*

angulata, D. stevensoni and *H. intermedia* (Cohen, 1986). *D. stevensoni* fossil were also found in Lake Mobutu during the Late Quaternary (Cohen, 1987) and in Lake Tanganyika during the Late Holocene (Wells et al., 1999).

Some other taxa found in Lake Chamo like *S.minuta, D.stevensoni, G.angulata*, *O.omercooperi* were also found in Lake Ziway by (Lowndes, 1932). Lowndes (1932) noted that *O.omercooperi* has its widest distribution in Ethiopia (Table 5.2) and occurs in highly variable saline water. *O.omercooperi* occurs in association with *O.*sp. type Chamo. Unidentified *Oncocypris* species recorded from Lake Chamo, the first record in ERVL is also found most frequently in pelagic samples in Lake Katanda, Kyaninga, and Ekikoto (Uganda) (Rumes, 2010). *C. africana, I. gibba*, *H.intermedia,* and *H. giesbrechtii,* were also identified in the modern freshwater of Sudan (Martens, 1984 b). *H. intermedia* are a rare species, mostly found in the upper part of the core in Lake Chamo (Figure 5.13), although it is quite abundant in Lake Mobutu during the Late Quaternary (Cohen, 1987). This species was found in shallow environments with non-vegetated bottoms in the turbid water of modern Lake Turkana (Cohen, 1986). *Sclerocypris clavularis* Sars is very rare and its occurrence is restricted to between 3700 to 3200 cal yr BP in Lake Chamo, with fossils of this species found in juveniles form. The species is restricted to Plio-Quaternary (the last epoch of the tertiary period) deposits of Kenya, from Lakes Turkana and Holocene of Lake Bogoria (Cabral et al., 2005), although Cohen (1987) noted that *S. clavularis* Sars, was found in high abundance in Lake Mobutu during the Late Quaternary.

Generally, low lake-levels during the Mid-Late Holocene in the Ziway - Shala basin and Lake Chamo are inferred from fossil ostracod analysis. On the same time range, a moderate rise in the lake level which may have led to the joining of three lakes (Shala, Abiyata, and Langano) occurred at around 2,500 cal yr BP (Gillespie et al., 1983; Benvenuti et al., 2002) and was also recorded in ostracod assemblages by Atnafu and Russo (2004) and in this study. Ostracod assemblages also used as indicator of lake-level fluctuations during the late Holocene of Lake Tanganyika (Alin and Cohen, 2003), which predominantly reflects arid Late Holocene conditions with relatively brief episodes of higher precipitation. Similar lake levels are also recorded in Lake Chamo.

5.5 Conclusion

The Lake Chamo ostracod record, along with the geochemical record, show a relationship existed between species ecological dynamics and high climatic fluctuations in the region during the Holocene. Each ostracod species clearly indicates its own response to the environmental fluctuations. The change in ostracod assemblages is evaluated in terms of salinity level as a result of change in the evapo-precipitation, which is favored by climate change. The salinity level also has a strong correlation with water depth. The ostracod assemblage of Lake Chamo show that the lake was slightly saline and/or freshwater, which occurred throughout the record, is represented by the core section. The results of this study are compatible with other regional studies dealing with lake level and palaeoclimate in East Africa during the Holocene.

Geometric morphometrics analysis complements the classical morphological observations to get the most possible similarity for the identification of genus *Limnocythere* found in Lake Chamo, in comparison with other *Limnocythere* found in ERVLs and East African Lakes. Both approaches distinguished three types of *Limnocythere* in Lake Chamo. A recommendation is forwarded for the needs of further investigations on both phenological and morphological approaches to identify and understand this genus and its ecological and evolutionary processes for palaeoenvironmental reconstruction.

Chapter 6

6. Summary and Perspectives

The research for this doctoral thesis was performed on one of the Ethiopian Rift Valley Lakes; Lake Chamo, using a multidisciplinary approach, in order to understand pronounced environmental changes and climate variability during the Holocene, and to contribute new findings to current debate surrounding the abrupt and gradual termination of African Humid Period in East Africa. In this thesis the sediment record of Lake Chamo has been investigated for it's geophysical, geochemical, and palaeobiological properties to reconstruct the environmental and climatic history of the region and help to resolve current debate on the humid-arid transitions in East Africa. Specifically, this research underlines the importance of multi-proxy indicators to explore a range of potential proxies for the interpretation of the climate signals registered and stored in the sediment for the past 9000 years. In this multi-proxy study on the environmental and climatic history of Lake Chamo, several proxies show significant variation which could be sensitive for the prevailing climatic and environmental shifts. Although the palaeoenvironmental reconstructions from Lake Chamo cover a limited time period of 9,000 years, the multi-proxy data can be used to explain the wet-dry transition during the termination of AHP's and could contribute to understanding of human dispersal and cultural development at the Holocene, which may provide evidence for the CRC 806 project objective.

The geophysical properties of sediment sequences allowed the recognition of down core changes in mineral composition and the amount and variations in geochemical elements to be determined which in terms of the environmental and climatic changes in the region. In addition, high fire frequency periods were triggered by drier climatic conditions which promoted ignition and biomass burning which is in analogous with lower lake level. Therefore, long-term trends in fire frequencies and lake level fluctuation followed the same trend.

Chapter 6

The preliminary study on ostracod assemblages in Lake Chamo sediment revealed the importance of this proxy to assess changes in salinity and /or alkalinity in response to climate change. Ostracod response to climatic and environmental shift is quite promising although its interpretation sometimes challenging due to the scarce ecological information available in East Africa region. This study also utilized geometric morphometric and multivariate statistical analysis to identify *Limnocythere* species of Lake Chamo.

The results in this study serve to reconstruct past environmental changes for Lake Chamo catchment area and its region. Furthermore they helped to assess forcing factors including environmental, ecological and human impacts which are likely to account for signals recorded by the palaeoenvironmental records. Overall, the combined results presented in this thesis provide evidence for an environmental synopsis of the Holocene. In the following sections, the major environmental changes at different time periods through the Holocene are outlined based on the main results of this research work.

6.1 The Early-Middle Holocene wet episode

The early Holocene in the Lake Chamo record showed a response to warmer and wetter climatic conditions. The relative lower lightness (L*) values accompanied with its dark grey color revealed the presence of an organic-rich deposit in the lowermost sediment profile (8600 - 5100 cal yr BP). The relationship between the high Si/Ti ratio and high diatom presence, along with low calcium carbonate content of the sediments, represent a high lake level and more humid climatic conditions which occurred during the early Holocene. Macroscopic charcoal input, together with organo-geochemical analysis (BC quantity and quality by the BPCA method) allowed characterization of fire residues, which documented high fire intensity during early to mid Holocene, due to in-creased productivity, which led to increased fuel availability and promoted fire. Particularly, the fire temperature sensitive ratio of benzene polycarboxylated acids produced from BC (B5CA/B6CA ratio; Figure 4.2) provided evidence that woody or shrub vegetation was a source of BC during this time. Lake Chamo charcoal data show greater fire levels during

the early and late Holocene, whereas lower levels in the mid-Holocene, which is typical to all parts of Africa (Marlon et al., 2013). In Lake Chamo, palaeoclimate information has also been inferred from ostracod assemblages, combined with elemental composition from the XRF. The lower parts of the profile, until around 5400 cal yr BP, was characterised by negligible ostracods and, in contrast, predominantly consisted of diatoms. Indications for a wet early-mid Holocene are supported by data from other Ethiopian studies, including the Ziway–Shala basin (Grove et al., 1975; Gillespie et al., 1983), Lake Abhé (Gasse, 1977; Gasse and Street, 1978), Lake Ashenge (Marshall et al., 2009), Lake Abiyata (Chalié and Gasse, 2002), the Bale Mountains, Southern Ethiopia (Mohammed and Bonnefille, 1998), the Southeastern Ethiopia Highlands and adjoining rift margins (Asrat et al., 2007; Baker et al., 2010), and Northern Ethiopia (Berakhi et al., 1998; Dramis et al., 2003; Gebru et al., 2009; Terwilliger et al., 2011; Terwilliger et al., 2013).

6.2 Mid - Late Holocene transition

The sediment composition changes drastically to a pronounced peak of carbonate and Sr content, dramatic decline of charcoal and BC concentration, modest to high ostracod abundance and decline of the diatoms content in the mid-late Holocene transition period in Lake Chamo records. In Lake Chamo, variations in carbonate content during mid - Holocene are thought to be driven directly by changes in evaporative concentration, due to the shifting balance of rainfall and evaporation. The high calcium carbonate (obtained from both XRF and EA) and Sr content accompanied by relatively lighter sediment, particularly between 5100 until 4000 cal yr BP, are interpreted as indicating dry regional climate conditions. These events of drought are widely recognized in equatorial East African limnological records such as in Lake Turkana (Ricketts and Johnson, 1996), in Lake Edward (Russell and Johnson, 2005), and in Lake Tanganyika (Cohen et al., 2005). Marked and extended period of drought on a millennial scale at around 4000 cal yr BP is a common feature of tropical Africa (Gasse, 2000). Specifically, Lake Edward experienced a major drought during this period (Russell and Johnson, 2005) which is also recorded by a

dramatic declining of charcoal as a result of a devoid in vegetation cover, in response to prolonged regional drought in Lake Chamo. Dramatic decline in charcoal counts, high B5CA/B6CA ratio value and low fire temperature from Lake Chamo allow fire residues to be attributed to frequent burning of grass savannah in response to regional aridity. The response of East Africa savannah vegetation to this regional aridity is also apparent from an abrupt decline in arboreal pollen percentages in Lake Tilo (Lamb, 2001), in Burundi and on Mount Kenya (Jolly et al., 1994; Wooller et al., 2000) and from lowered C/N ratios and increased $\delta^{13}C$ data from Lake Tilo (Lamb et al., 2004).

Temperature increase resulted in the preservation of calcite with highest ostracod abundance and high fire frequency from 5100 to 4000 cal yr BP in Lake Chamo, showing a shift to more dry climatic conditions. Variations in the ostracod assemblages in Lake Chamo during this time suggest the ecosystem composition responded to warming climatic conditions. Therefore, the hydrological sensitivity of Lake Chamo lacustrine systems is directly linked to precipitation and evaporation, which in turn lead to changes in salinity and alkalinity. Specifically, high peaks of Ca and Sr at around 5100 cal yr Bp in Lake Chamo, an abrupt increase in $\delta^{18}O$ values at 4800 cal yr BP in Lake Tilo (Lamb et al., 2000), increments of $\delta^{18}O$ and $\delta^{13}C$ records of Lake Awassa at around 5500 cal yr BP (Lamb et al., 2002) and sharp decrease of Lake Ziway-Shala water level during 5700 – 5100 cal yr BP (Gillespie et al., 1983) potentially indicate the onset of aridity on a regional scale. In a broader context, lowering of lake levels from around 5500 cal yr BP onwards in tropical African sites (Stager et al., 1997) confirm this aridity. Gasse (2000) and Russell (2003 a) also indicated the transition from a wet Early Holocene to a more arid Late Holocene by 5500-5200 cal yr BP.

6.3 Late Holocene

The sediment sequences of Lake Chamo are valuable archives for Holocene environmental and climatic changes due to the presence of a continuous record, but, due to the lack of a precise chronology, particularly in the upper part of the core, the data can rarely be

interpreted in a straightforward manner with regards to the Late Holocene's environmental history. This study shows that the Late Holocene period was less humid than the Early-Mid Holocene. Based on the existing age model, the Lake Chamo sediment records wet periods from 2400 to 1850 cal yr BP and 1500 to 800 cal yr BP were interrupted by a short period of drier and warmer climatic conditions from 1850 to 1500 cal yr BP during the Late Holocene. The diversity of ostracod species decreases significantly during the fluctuating humid and dry condition at around 2400 to 800 cal yr BP. Generally, moderate values of all geochemical data and the high color L*– a*– b* data after 800 cal yr BP revealed the presence of dry conditions. The diverse assemblages of ostracod fauna also prevail the rapid return of highly alkaline/ saline condition as a result of this drier period. These environmental changes during the Late Holocene could be linked to changes in rainfall pattern in eastern Africa as a result of frequent and/or more intense ENSO events (Russell and Johnson, 2007).

In the uppermost part of the core the fluctuating input of clastic sediments is found to be due to changing intensity of anthropogenic land use in the lake's surroundings, including the clearance of natural vegetation. This caused increased inwash of clastic debris into the lake, especially during phases of relatively high rainfall, and is responsible for elevated values for MS, K, Ti, Si, and Fe particularly at around 1500 - 800 cal yr BP, and is associated with the first documented evidence of forest and vegetation disturbance. These peak values, interpreted as spikes of peak erosion, are caused by the evolving influence of population and livestock pressure. Differentiating the climatic variability, human impact, or a combination of both factors, remains difficult to estimate at this time, but the presence of high sedimentation rates towards the uppermost part of the record suggests the presence of human settlement and disturbance in the savanna ecosystem during the Late Holocene. The increase in charcoal influx and higher proportions of BC at approximately 2000 cal yr BP is associated with disturbance related to widespread anthropogenic ecosystem disturbance. In more recent times, development of pastures around the catchment of Lake Chamo has been the principal cause of deforestation throughout the region.

Chapter 6

A multi-proxy approach such as geophysical, geochemical, and palaeobiological (Charcoal and ostracods) investigation in Lake Chamo sediment was carried out, and the climate proxies extracted and interpreted from these analysis contribute to address the objectives of the study. Therefore, the results have provided an insight into the long-term development in understanding of driving mechanisms such as climate change, changing fire regimes, and changing intensities of human impact. The study provides a defined time period for the termination of the AHP with dramatic climate shift during the Early-Mid Holocene transition, which is known to have occurred in most of the East African region. The changes in ostracod assemblages indicate the species' ecological dynamics and their response to high levels of climatic fluctuations in the region during the Holocene.

6.4 Future research

The main results of this thesis suggest future directions for palaeoenvironmental research should be aimed at constraining the understanding of environmental dynamics in Ethiopia and, in a broader context, East Africa. Inclusion of additional and high-resolution records into future palaeoenvironmental research would provide evidence to distinguish regional and site-specific trends in the records. The isotopic and elemental analysis of ostracod shells, which is under investigations, will help to reconstruct the wet/dry variability and help to make detailed palaeoclimate estimates. In addition, the presence of a different kind of diatoms in Lake Chamo, and their palaeochemical proxies, could provide a complementary line of evidence for the ostracods assemblages which could provide an independent verification to increase the reliability of the evidence. Therefore, there is much potential for further work on diatoms in this core with high resolution spatial and temporal scales. Diatoms have good potential, especially for reconstruction of the lake level change, particularly in the hydrologically sensitive lakes of East Africa. There is a need for further studies to fill in the substantial data gaps which exist both spatially and temporally in East Africa. High resolution records deserve particular attention to undertake comparisons between sites and are keys to be able to differentiate between climatically- and

anthropogenically-induced changes in the past. Geometric morphometrics analysis complements the classical morphological observations and use of the coupled approach will help further ostracod taxonomic work to identify different group of ostracods before using them for ecological and evolutionary processes during palaeoenvironmental reconstruction.

References

Admassu, D., Ahlgren, I., 2000. Growth of juvenile tilapia, Oreochromis niloticus L. from Lakes Zwai, Langeno and Chamo (Ethiopian rift valley) based on otolith microincrement analysis. Ecology of Freshwater Fish 9, 127-137.

Alemayehu, T., Ayenew, T., Kebede, S., 2006. Hydrogeochemical and lake level changes in the Ethiopian Rift. Journal of hydrology 316, 290-300.

Alin, S.R., Cohen, A.S., 2003. Lake-level history of Lake Tanganyika, East Africa, for the past 2500 years based on ostracode-inferred water-depth reconstruction. Palaeogeography, Palaeoclimatology, Palaeoecology 199, 31- 49.

Assefa, E., Bork, H.-R., 2014. Deforestation and forest management in southern Ethiopia: investigations in the Chencha and Arbaminch areas. Environmental management 53, 284-299.

Assefa, E., Bork, H.-R., 2014. Dynamics and driving forces of agricultural landscapes in Southern Ethiopia–a case study of the Chencha and Arbaminch areas. Journal of Land Use Science, 1-16.

Assefa, E., Bork, H.-R., 2015. Farmers´ Perception Of Land Degradation And Traditional Knowledge In Southern Ethiopia–Resilience And Stability. Land Degradation & Development,doi:10.1002/ldr.2364

Assefa, E., Bork, H.-R., 2014. Long-Term Indigenous Soil Conservation Technology in the Chencha Area, Southern Ethiopia: Origin, Characteristics, and Sustainability. Ambio 43, 932-942.

Asrat, A., Baker, A., Mohammed, M.U., Leng, M.J., Calsteren, P.V., Smith, C., 2007. A high-resolution multi-proxy stalagmite record from Mechara, Southeastern Ethiopia: palaeohydrological implications for speleothem palaeoclimate reconstruction. Journal of Quaternary Science 22, 53-63.

Atnafu, B., Russo, A., 2004. Late Quaternary lacustrine ostracoda of the Ziway-Shala Basin (Ethiopia) as paleoenvironmental indicators. Bollettino della Socita Paeontologica Italiana 43, 235-266.

Arthur, W.K., Arthur, W.J., Curtis, C.M., Lakew,B., Lesur- Gebremariam, J., Ethiopia, Y. 2010. Fire on the Mountain: Dignity and Prestige in the History and Archaeology of the Borada Highlands in Southern Ethiopia. The Magazine of the Society for American Archaeology 10: 17-21.

References

Awulachew, S.B., 2006. Investigation of physical and bathymetric characteristics of Lakes Abaya and Chamo, Ethiopia, and their management implications. Lakes and Reservoirs: Research and Management 11, 133-140.

Baker, A., Asrat, A., Fairchild, I.J., Leng, M.J., Thomas, L., Widmann, M., Jex, C.N., Dong, B., van Calsteren, P., Bryant, C., 2010. Decadal-scale rainfall variability in Ethiopia recorded in an annually laminated, Holocene-age, stalagmite. The Holocene 20, 827-836.

Baker, A., Asrat, A., Fairchild, I.J., Leng, M.J., Wynn, P.M., Bryant, C., Genty, D., Umer, M., 2007. Analysis of the climate signal contained within $\delta^{18}O$ and growth rate parameters in two Ethiopian stalagmites. Geochimica et Cosmo-chimica Acta 71, 2975- 2988.

Baltanas, A., Brauneis, W., Danielopol, D.L., Linhart, J., 2003. Morphometric methods for applied ostracodology: tools for outline analysis of nonmarine ostracodes. Paleontological Society Papers 9, 101.

Baltanas , A., Danielopol, D.L., 2011. Geometric morphometrics and its use in ostracod research: a short guide. Joannea Geol. Paläont 11, 235-272.

Bard, K.A., Coltorti, M., DiBlasi, M.C., Dramis, F., Fattovich, R., 2000. The environmental history of Tigray (Northern Ethiopia) in the Middle and Late Holocene: A preliminary outline. African Archaeological Review 17, 65-86.

Belete, A., 2009. Climate Change Impact on Lake Abaya Water Level. Unpublished M.Sc thesis, Addis Ababa University, Ethiopia.

Benvenuti, M., Carnicelli, S., Belluomini, G., Dainelli, N., Di Grazia, S., Ferrari, G., Iasio, C., Sagri, M., Ventra, D., Atnafu, B., 2002. The Ziway–Shala lake basin (Main Ethiopian rift, Ethiopia): a revision of basin evolution with special reference to the Late Quaternary. Journal of African Earth Sciences 35, 247-269.

Berakhi, O., Brancuccio, L., Calderoni, G., Coltorti, M., Dramis, F., Umer, M., 1998. The Mai Maiken sedimentary sequence: a reference point for the environmental evolution of the highlands of northern Ethiopia. Geomorphology 23, 127-138.

Berke, M.A., Johnson, T.C., Werne, J.P., Schouten, S., Sinninghe Damsté, J.S., 2012. A mid-Holocene thermal maximum at the end of the African Humid Period. Earth and Planetary Science Letters 351, 95-104.

Blaauw, M., Christen, J.A., 2011. Flexible paleoclimate age-depth models using an autoregressive gamma process. Bayesian Analysis 6, 457-474.

Bond, W., Midgley, G., Woodward, F., 2003. What controls South African vegetation-climate or fire? South African Journal of Botany 69, 79-91.

References

Bond, W., Woodward, F., Midgley, G., 2005. The global distribution of ecosystems in a world without fire. New Phytologist 165, 525-538.

Bond, W.J., Silander Jr, J.A., Ranaivonasy, J., Ratsirarson, J., 2008. The antiquity of Madagascar's grasslands and the rise of C4 grassy biomes. Journal of Biogeography 35, 1743-1758.

Brodowski, S., Rodionov, A., Haumaier, L., Glaser, B., Amelung, W., 2005. Revised black carbon assessment using benzene polycarboxylic acids. Organic Geochemistry 36, 1299-1310.

Brown, E., Johnson, T., Scholz, C., Cohen, A., King, J., 2007. Abrupt change in tropical African climate linked to the bipolar seesaw over the past 55,000 years. Geophysical Research Letters 34.

Brown, E.T., Le Callonnec, L., German, C.R., 2000. Geochemical cycling of redox-sensitive metals in sediments from Lake Malawi: A diagnostic paleotracer for episodic changes in mixing depth. Geochimica et Cosmochimica Acta 64, 3515-3523.

Burnett, A.P., Soreghan, M.J., Scholz, C.A., Brown, E.T., 2011. Tropical East African climate change and its relation to global climate: a record from Lake Tanganyika, Tropical East Africa, over the past 90+ kyr. Palaeogeography, Palaeoclimatology, Palaeoecology 303, 155-167.

Cabral, M., Colin, J.-P., Carbonel, P., 2005. First occurrence of the genus Sclerocypris Sars, 1924 (Ostracoda) in the? Pleistocene of Western Europe (Portugal). Journal of Micropalaeontology 24, 169-170.

Chalié, F., Gasse, F., 2002. Late Glacial–Holocene diatom record of water chemistry and lake level change from the tropical East African Rift Lake Abiyata (Ethiopia). Palaeogeography, Palaeoclimatology, Palaeoecology 187, 259-283.

Chorowicz, J., 2005. The East African rift system. Journal of African Earth Sciences 43, 379-410.

Clark, J.S., Merkt, J., Muller, H., 1989. Post-Glacial Fire, Vegetation, and Human History on the Northern Alpine Forelands, South-Western Germany. Journal of Ecology 77, 897-925.

Cohen, A.S., 1987. Fossil ostracodes from Lake Mobutu (Lake Albert): palaeoecologic and taphonomic implications. Palaeoecology of Africa and Surrounding Islands. Balkema, Rotterdam, 271-281.

Cohen, A.S., 1986. Distribution and faunal associations of benthic invertebrates at Lake Turkana, Kenya. Hydrobiologia 141, 179-197.

References

Cohen, A.S., 2003. Paleolimnology, The History and Evolution of Lake Systems. Oxford university press, 241-247.

Cohen, A.S., Dussinger, R., Richardson, J., 1983. Lactstrine palaeochemical interpretations based on Eastern and Southern African Ostracods. Palaeogeography, Palaeoclimatology, Palaeoecology 43, 129 - 151.

Cohen, A.S., Palacios-Fest, M.R., Msaky, E.S., Alin, S.R., McKee, B., O'Reilly, C.M., Dettman, D.L., Nkotagu, H., Lezzar, K.E., 2005. Paleolimnological investigations of anthropogenic environmental change in Lake Tanganyika: IX. Summary of paleorecords of environmental change and catchment deforestation at Lake Tanganyika and impacts on the Lake Tanganyika ecosystem. Journal of Paleolimnology 34, 125-145.

Cohen, A.S., Stone, J.R., Beuning, K.R., Park, L.E., Reinthal, P.N., Dettman, D., Scholz, C.A., Johnson, T.C., King, J.W., Talbot, M.R., 2007. Ecological consequences of early Late Pleistocene megadroughts in tropical Africa. Proceedings of the National Academy of Sciences 104, 16422-16427.

Colombaroli, D., Verschuren, D., 2010. Tropical fire ecology across the African continent: A paleoecological perspective. PAGES news 18, 65-67.

Conedera, M., Tinner, W., Neff, C., Meurer, M., Dickens, A.F., Krebs, P., 2009. Reconstructing past fire regimes: methods, applications, and relevance to fire management and conservation. Quaternary Science Reviews 28, 555-576.

Conway, D., 2000. Some aspects of climate variability in the North East Ethiopian Highlands-Wollo and Tigray. SINET-Ethiopian Journal of Science 23, 139-161.

Corti, G., 2009. Continental rift evolution: from rift initiation to incipient break-up in the Main Ethiopian Rift, East Africa. Earth-Science Reviews 96, 1-53.

Croudace, I.W., Rindby, A., Rothwell, R.G., 2006. ITRAX: description and evaluation of a new multi-function X-ray core scanner. Special Publication-Geological Society of London 267, 51.

Crul, R., 1995. Limnology and hydrology of Lake Victoria. UNESCO/IHP-IV Project M-5.1, in Studies and Reports in Hydrology 53. UNESCO, Paris, France.

Dadebo, E., 2009. Filter-feeding habit of the African catfish Burchell, 1822 (Pisces: Clariidae) in Lake Chamo, Ethiopia. Ethiopian Journal of Biological Sciences 8, 15-30.

Dadebo, E., Mengistu, S., 2008. Feeding habits, ontogenetic dietary shift and some aspects of reproduction of the tigerfish hydrocynus forskahlii (Cuvier, 1819)(Pisces: Characidae) in Lake Chamo, Ethiopia. Ethiopian Journal of Biological Sciences 7, 123-137.

References

Daniau, A.-L., Bartlein, P. J., Harrison, S. P., Prentice, I. C., Brewer, S., Friedlingstein, P., Harrison-Prentice, T. I., Inoue, J., Izumi, K., Marlon, J. R., Mooney, S., Power, M. J., Stevenson, J., Tinner, W., Andrič, M., Atanassova, J., Behling, H., Black, M., Blarquez, O., Brown, K. J., Carcaillet, C., Colhoun, E. A., Colombaroli, D., Davis, B. A. S., D'Costa, D., Dodson, J., Dupont, L., Eshetu, Z., Gavin, D. G., Genries, A., Haberle, S., Hallett, D. J., Hope, G., Horn, S. P., Gebru, T., Katamura, F., Kennedy, L. M., Kershaw, P., Krivonogov, S., Long, C., Magri, D., Marinova, E., McKenzie, G. M., Moreno, P. I., Moss, P., Neumann, F. H., Norström, E., Paitre, C., Rius, D., Roberts, N., Robinson, G. S., Sasaki, N., Scott, L., Takahara, H., Terwilliger, V.,Thevenon, F., Turner, R., Valsecchi, V. G., Vannière, B., Walsh, M., Williams, N., Zhang, Y. 2012. Predictability of biomass burning in response to climate changes. Global Biogeochemical Cycles, Vol. 26, GB4007, doi:10.1029/2011GB004249.

Danielopol, D.L., Baltanás, A., Namiotko, T., Geiger, W., Pichler, M., Reina, M., Roidmayr, G., 2008a. Developmental trajectories in geographically separated populations of non-marine ostracods: morphometric applications for palaeoecological studies. Senckenbergiana lethaea 88, 183-193.

Darbyshire, I., Lamb, H., Umer, M., 2003. Forest clearance and regrowth in northern Ethiopia during the last 3000 years. The Holocene 13, 537-546.

Dean, W.E., 1999. The carbon cycle and biogeochemical dynamics in lake sediments. Journal of paleolimnology 21, 375-393.

Debret, M., Desmet, M., Balsam, W., Copard, Y., Francus, P., Laj, C., 2006. Spectrophotometer analysis of Holocene sediments from an anoxic fjord: Saanich Inlet, British Columbia, Canada. Marine geology 229, 15-28.

Debret, M., Sebag, D., Desmet, M., Balsam, W., Copard, Y., Mourier, B., Susperrigui, A.-S., Arnaud, F., Bentaleb, I., Chapron, E., 2011. Spectrocolorimetric interpretation of sedimentary dynamics: The new "Q7/4 diagram". Earth-Science Reviews 109, 1-19.

deMenocal, P., Ortiz, J., Guilderson, T., Adkins, J., Sarnthein, M., Baker, L., Yarusinsky, M., 2000. Abrupt onset and termination of the African Humid Period: rapid climate responses to gradual insolation forcing. Quaternary science reviews 19, 347-361.

Diro, G.T., Grimes, D., Black, E., O'Neill, A., Pardo-Iguzquiza, E., 2009. Evaluation of reanalysis rainfall estimates over Ethiopia. International Journal of Climatology 29, 67-78.

Diro, G.T., Black, E., Grimes, D., 2008. Seasonal forecasting of Ethiopian spring rains. Meteorological Applications 15, 73-83.

Dramis, F., Umer, M., Calderoni, G., Haile, M., 2003. Holocene climate phases from buried soils in Tigray (northern Ethiopia): comparison with lake level fluctuations in the Main Ethiopian Rift. Quaternary Research 60, 274-283.

References

Dwyer, E., Pinnock, S., Grégoire, J.-M., Pereira, J., 2000. Global spatial and temporal distribution of vegetation fire as determined from satellite observations. International Journal of Remote Sensing 21, 1289-1302.

Ebinger, C., Yemane, T., Harding, D., Tesfaye, S., Kelley, S., Rex, D., 2000. Rift deflection, migration, and propagation: Linkage of the Ethiopian and Eastern rifts, Africa. Geological Society of America Bulletin 112, 163-176.

Ebinger, C., Yemane, T., WoldeGabriel, G., Aronson, J., Walter, R., 1993. Late Eocene–Recent volcanism and faulting in the southern main Ethiopian rift. Journal of the Geological Society 150, 99-108.

Finch, J., Marchant, R., 2011. A palaeoecological investigation into the role of fire and human activity in the development of montane grasslands in East Africa. Vegetation History and Archaeobotany 20, 109-124.

Foerster, V., Junginger, A., Langkamp, O., Gebru, T., Asrat, A., Umer, M., Lamb, H., Wennrich, V., Rethemeyer, J., Nowaczyk, N., 2012. Climatic change recorded in the sediments of the Chew Bahir basin, southern Ethiopia, during the last 45,000 years. Quaternary International 274, 25-37.

Forester, R., 1988. Nonmarine calcareous microfossil sample preparation and data acquisition procedures. United States Geol Surv Tech Proceed HP-78 RI, 1-9.

Garcin, Y., Melnick, D., Strecker, M.R., Olago, D., Tiercelin, J.-J., 2012. East African mid-Holocene wet–dry transition recorded in palaeo-shorelines of Lake Turkana, northern Kenya Rift. Earth and Planetary Science Letters 331, 322-334.

Gasse, F., 1977. Evolution of Lake Abhe (Ethiopia and TFAI), from 70,000 BP. Nature 265, 42- 45.

Gasse, F., 2000. Hydrological changes in the African tropics since the Last Glacial Maximum. Quaternary Science Reviews 19, 189-211.

Gasse, F., Fontes, J.-C., 1989. Palaeoenvironments and palaeohydrology of a tropical closed lake (Lake Asal, Djibouti) since 10,000 yr BP. Palaeogeography, Palaeoclimatology, Palaeoecology 69, 67-102.

Gasse, F., Street, F., 1978. Late Quaternary lake-level fluctuations and environments of the northern Rift Valley and Afar region (Ethiopia and Djibouti). Palaeogeography, Palaeoclimatology, Palaeoecology 24, 279-325.

Gebremariam, B., 2007. Basin Scale Sedimentary and Water Quality Responses to External Forcing in Lake Abaya, Southern Ethiopian Rift Valley. PhD Thesis. Universität Siegen. CICD Series Vol.6.

References

Gebru, T., 2007. Vegetation history and palaeoenvironmental reconstruction from buried wood charcoal in northern Ethiopia (Tigray). Unpublished M.Sc thesis, Addis Ababa University, Ethiopia.

Gebru, T., Eshetu, Z., Huang, Y., Woldemariam, T., Strong, N., Umer, M., DiBlasi, M., Terwilliger, V.J., 2009. Holocene palaeovegetation of the Tigray Plateau in northern Ethiopia from charcoal and stable organic carbon isotopic analyses of gully sediments. Palaeogeography, Palaeoclimatology, Palaeoecology 282, 67-80.

Gillespie, R., Street-Perrott, F.A., Switsur, R., 1983. Post-glacial arid episodes in Ethiopia have implications for climate prediction. Nature 306, 680-683.

Glaser, B., Haumaier, L., Guggenberger, G., Zech, W., 1998. Black carbon in soils: the use of benzenecarboxylic acids as specific markers. Organic geochemistry 29, 811-819.

Grove, A., Street, F.A., Goudie, A., 1975. Former lake levels and climatic change in the Rift Valley of southern Ethiopia.The Geographical Journal 141, 177-194.

Halfman, J.D., Johnson, T.C., Finney, B.P., 1994. New AMS dates, stratigraphic correlations and decadal climatic cycles for the past 4 ka at Lake Turkana, Kenya. Palaeogeography, Palaeoclimatology, Palaeoecology 111, 83-98.

Hammer, Ø., Harper, D., Ryan, P., 2001. PAST: Paleontological Statistics Software Package for Education and Data Analysis Palaeontol. Electronica 4, 1-9.

Hammes, K., Schmidt, M.W.I., Smernik, R.J., Currie, L.A., Ball, W.P., Nguyen, T.H., Louchouarn, P., Houel, S., Gustafsson, O., Elmquist, M., Cornelissen, G., Skjemstad, J.O., Masiello, C.A., Song, J., Peng, P., Mitra, S., Dunn, J.C., Hatcher, P.G., Hockaday, W.C., Smith, D.M., Hartkopf-Froeder, C., Boehmer, A., Luer, B., Huebert, B.J., Amelung, W., Brodowski, S., Huang, L., Zhang, W., Gschwend, P.M., Flores-Cervantes, D.X., Largeau, C., Rouzaud, J.N., Rumpel, C., Guggenberger, G., Kaiser, K., Rodionov, A., Gonzalez-Vila, F.J., Gonzalez-Perez, J.A., de la Rosa, J.M., Manning, D.A.C., Lopez-Capel, E., Ding, L., 2007. Comparison of quantification methods to measure fire-derived (black/elemental) carbon in soils and sediments using reference materials from soil, water, sediment and the atmosphere. Global Biogeochemical Cycles 21, GB3016, doi:10.1029/2006GB002914.

Holmes, J.A., Chivas, A.R., 2002. The Ostracoda: applications in Quaternary research. Geophysical Monograph 131, American Geophysical Union, Washington, DC.

Jansen, J., Van der Gaast, S., Koster, B., Vaars, A., 1998. CORTEX, a shipboard XRF-scanner for element analyses in split sediment cores. Marine Geology 151, 143-153.

Jeltsch, F., Milton, S.J., Dean, W.R.J., Van Rooyen, N., Moloney, K.A. 1998. Modelling the impact of small-scale heterogeneities on tree-grass coexistence in semi-arid savannas. Journal of Ecology 86, 780-793.

References

Johnson, T.C., Halfman, J.D., Showers, W.J., 1991. Paleoclimate of the past 4000 years at Lake Turkana, Kenya, based on the isotopic composition of authigenic calcite. Palaeogeography, Palaeoclimatology, Palaeoecology 85, 189-198.

Johnson, T.C., Brown, E.T., Shi, J., 2011. Biogenic silica deposition in Lake Malawi, East Africa over the past 150,000 years. Palaeogeography, Palaeoclimatology, Palaeoecology 303, 103-109.

Jolly, D., Bonnefille, R., Roux, M., 1994. Numerical interpretation of a high resolution Holocene pollen record from Burundi. Palaeogeography, palaeoclimatology, palaeoecology 109, 357-370.

Junginger, A., 2011. East African climate variability on different time scales: The Suguta Valley in the African-Asian monsoon domain.Ph.D. Thesis, University of Potsdam, Germany. http://opus.kobv.de/ubp/volltexte/2011/5683/.

Junginger, A., Roller, S., Olaka, L.A., Trauth, M.H., 2014. The effects of solar irradiation changes on the migration of the Congo Air Boundary and water levels of paleo-Lake Suguta, Northern Kenya Rift, during the African Humid Period (15–5ka BP). Palaeogeography, Palaeoclimatology, Palaeoecology 396, 1-16.

Kebede, E., Mariam, Z.G., Ahlgren, I., 1994. The Ethiopian Rift Valley lakes: chemical characteristics of a salinity-alkalinity series. Hydrobiologia 288, 1-12.

Kibret, T., Harrison, A.D., 1989. The benthic and weed-bed faunas of Lake Awasa (Rift Valley, Ethiopia). Hydrobiologia 174, 1-15.

Klie, W., 1933. Die Ostracoden der Rift Tel Seen in Kenia. Internationale Revue der gesamten Hydrobiologie und Hydrographie 29, 1-14.

Klie, W., 1939. Ostracoden aus dem Kenia-Gebiet, vornhemlich von dessen Hochgebirgen. Internationale Revue der gesamten Hydrobiologie und Hydrographie 39, 99-161.

Kröpelin, S., Verschuren, D., Lézine, A.-M., Eggermont, H., Cocquyt, C., Francus, P., Cazet, J.-P., Fagot, M., Rumes, B., Russell, J., 2008. Climate-driven ecosystem succession in the Sahara: the past 6000 years. Science 320, 765-768.

Lamb, A.L., Leng, M.J., Lamb, H.F., Mohammed, M.U., 2000. A 9000-year oxygen and carbon isotope record of hydrological change in a small Ethiopian crater lake. The Holocene 10, 167-177.

Lamb, A.L., Leng, M.J., Lamb, H.F., Telford, R.J., Mohammed, M.U., 2002. Climatic and non-climatic effects on the δ18O and δ13C compositions of Lake Awassa, Ethiopia, during the last 6.5 ka. Quaternary science reviews 21, 2199-2211.

References

Lamb, A.L., Leng, M.J., Umer Mohammed, M., Lamb, H.F., 2004. Holocene climate and vegetation change in the Main Ethiopian Rift Valley, inferred from the composition (C/N and δ13C) of lacustrine organic matter. Quaternary Science Reviews 23, 881-891.

Lamb, H.F., 2001. Multi-proxy records of Holocene climate and vegetation change from Ethiopian crater lakes, Biology and Environment: Proceedings of the Royal Irish Academy. Jstor, pp. 35-46.

Lesur, J., Hildebrand, E.A., Abawa, G., Gutherz, X., 2013. The advent of herding in the horn of Africa: new data from Ethiopia, Djibouti and Somaliland. Quat. Int., 1e11.

Le Turdu, C., Tiercelin, J.-J., Gibert, E., Travi, Y., Lezzar, K.-E., Richert, J.-P., Massault, M., Gasse, F., Bonnefille, R., Decobert, M., 1999. The Ziway–Shala lake basin system, Main Ethiopian Rift: influence of volcanism, tectonics, and climatic forcing on basin formation and sedimentation. Palaeogeography, Palaeoclimatology, Palaeoecology 150, 135-177.

Lindroth, S., 1952. Taxonomic and Zoogeographical studies of the ostracod fauna in the inland waters of East Africa. Results of the Swedish East Africa Expedition 1948, Zoology, No.2.

Linhart, J., Brauneis, W., Neubauer, W., Danielopol, D.L., 2006. Morphomatica, Computer Program, version 1.6. http://palstrat.uni-graz.at/morphomatica/morphomatica_e.htm.

Long, C.J., Whitlock, C., Bartlein, P.J., 2007. Holocene vegetation and fire history of the Coast Range, western Oregon, USA. The Holocene 17, 917-926.

Lowndes, A.G., 1932. Report on the Ostracoda.Mr. Omer-Cooper's Investigation of the Abyssinian Fresh Waters (Dr. Hugh Scott's Expedition). Proceedings of the Zoological Society of London 102, 677-708.

Marlon, J.R., Bartlein, P.J., Daniau, A.-L., Harrison, S.P., Maezumi, S.Y., Power, M.J., Tinner, W., Vanniére, B., 2013. Global biomass burning: A synthesis and review of Holocene paleofire records and their controls. Quaternary Science Reviews 65, 5-25.

Marshall, M.H., Lamb, H.F., Davies, S.J., Leng, M.J., Kubsa, Z., Umer, M., Bryant, C., 2009. Climatic change in northern Ethiopia during the past 17,000 years: A diatom and stable isotope record from Lake Ashenge. Palaeogeography, Palaeoclimatology, Palaeoecology 279, 114-127.

Martens, K., 1984 a. Annotated checklist of the nom-marine ostracods (Curstacea, ostracoda) from the African inland waters. Zoologische dokumentatie-N20- documentation zoologique.

References

Martens, K., 1984 b. On the freshwater ostracods (Crustacea, Ostracoda) of the Sudan, with special reference to the Red Sea Hills, including a description of a new species. Hydrobiologia 110, 137-161.

Martens, K., 1990 a. Revision of African Limnocythere ss Brady, 1867 (Crustacea, Ostracoda), with special reference to the Rift Valley Lakes: morphology, taxonomy, evolution and (palaeo-) ecology. Archiv für Hydrobiologie. Supplementband. Untersuchungen des Elbe-AEstuars 83, 453-524.

Martens, K., 1990 b. Speciation and evolution in the genus Limnocythere BRADY, 1867 sensu strict (Crustacea, Ostracoda) in the East African Galla and Awassa basins (Ethiopia). Cour. Forsh- Inst.Senckenberg 123, 87-95.

Martens, K., Rossetti, G., Fuhrmann, R., 1997. Pleistocene and recent species of the family Darwinulidae Brady & Norman, 1889 (Crustacea, Ostracoda) in Europe. Hydrobiologia 357, 99-116.

Martens, K., Savatenalinton, S., 2011. A subjective checklist of the Recent, free-living non-marine Ostracoda (Crustacea). Zootaxa 2855, 1-79.

Martens , K., Tudorancea, C., 1991. Seasonally and spatial distribution of the ostracods of Lake Zwai, Ethiopia (Crustacea: Ostracoda). Freshwater Biology 25, 233-241.

McGee, D., deMenocal, P., Winckler, G., Stuut, J., Bradtmiller, L., 2013. The magnitude, timing and abruptness of changes in North African dust deposition over the last 20,000 yr. Earth and Planetary Science Letters 371-372,163-176.

Meisch, C., 2000. Freshwater Ostracoda of Western and Central Europe. In Schwoerbel, J. & P. Zwick (eds), Su¨ swasserfauna von Mitteleuropa, vol. 8/3. Akademischer Verlag Spektrum, Heidelberg, 522.

Mengistu, S., 2006. Status and challenges of Aquatic invertebrate Research in Ethiopia: A Review. Ethiopian Biological Science 5, 75 -115.

Mohammed, M., Bonnefille, R., 1998. A late Glacial/late Holocene pollen record from a highland peat at Tamsaa, Bale Mountains, south Ethiopia. Global and Planetary Change 16, 121-129.

Morrill, C., Overpeck, J.T., Cole, J.E., 2003. A synthesis of abrupt changes in the Asian summer monsoon since the last deglaciation. The Holocene 13, 465-476.

Moy, C.M., Seltzer, G.O., Rodbell, D.T., Anderson, D.M., 2002. Variability of El Niño/Southern Oscillation activity at millennial timescales during the Holocene epoch. Nature 420, 162-165.

References

Nicholson, S.E., 1996. A review of climate dynamics and climate variability in eastern Africa. In: The Limnology, climatology and paleoclimatology of the East African lakes (eds Johnson, T.C. & Odada, E.O.) Gordon & Breach, Amsterdam, 25-56.

Olaka, L.A., Odada, E.O., Trauth, M.H., Olago, D.O., 2010. The sensitivity of East African rift lakes to climate fluctuations. Journal of Paleolimnology 44, 629-644.

Paillard, D., Labeyrie, L., Yiou, P., 1996. Macintosh program performs time-series analysis. Eos, Transactions American Geophysical Union 77, 379-379.

Palacios-Fest, M.R., Cohen, A.S., Anadon, P., 1994. Use of ostracods as paleoenvironmental tools in the interpretation of ancient lacustrine records. Revista Espanola De Paleontologia 9, 145-164.

Park, L.E., Cohen, A.S., 2011. Paleoecological response of ostracods to early Late Pleistocene lake-level changes in Lake Malawi, East Africa. Palaeogeography, Palaeoclimatology, Palaeoecology 303, 71-80.

Power, M.J., Marlon, J., Ortiz, N., Bartlein, P., Harrison, S., Mayle, F., Ballouche, A., Bradshaw, R., Carcaillet, C., Cordova, C., 2008. Changes in fire regimes since the Last Glacial Maximum: an assessment based on a global synthesis and analysis of charcoal data. Climate Dynamics 30, 887-907.

Pyne, S.J., Andrews, P.L., Laven, R.D., 1996. Introduction to wildland fire. John Wiley and Sons, Inc., New York.

Reimer, P. J., Baillie, M. G. L., Bard, E., Bayliss, A. Beck, J. W., Blackwell, P. G., Ramsey, C. B., Buck, C. E., Burr, G. S., Edwards, R. L., Friedrich, M., Grootes, P. M., Guilderson, T. P., Hajdas, I., Heaton, T. J., Hogg, A. G., Hughen, K. A., Kaiser, K. F., Kromer, B., Mccormac, F. G., Manning, S. W., Reimer, R. W., Richards, D. A., Southon, J. R., Talamo, S., Turney, C. S. M., Van Der Plicht, J. M., Weyhenmeyer, C. E., 2009. IntCal09 and Marine09 radiocarbon age calibration curves, 0–50,000 years cal BP, Radiocarbon, 51, 1111–1150.

Renssen, H., Brovkin, V., Fichefet, T., Goosse, H., 2006. Simulation of the Holocene climate evolution in Northern Africa: the termination of the African Humid Period. Quaternary International 150, 95-102.

Rethemeyer, J., Fülöp, R.-H., Höfle, S., Wacker, L., Heinze, S., Hajdas, I., Patt, U., König, S., Stapper, B., Dewald, A., 2013. Status report on sample preparation facilities for 14C analysis at the new CologneAMS center. Nuclear Instruments and Methods in Physics Research Section B: Beam Interactions with Materials and Atoms 294, 168-172.

Richardson, J., Dussinger, R., 1986. Paleolimnology of mid-elevation lakes in the Kenya Rift Valley, Paleolimnology IV. Springer, pp. 167-174.

References

Ricketts, R., Johnson, T., 1996. Climate change in the Turkana basin as deduced from a 4000 year long δ O18 record. Earth and Planetary Science Letters 142, 7-17.

Rohlf, F.J., 2001. tpsDIG, Program version 1.43. Department of Ecology and Evolution,SAS Institute Inc. SAS/STAT ®9.2 User's Guide. Cary, NC: SAS Institute Inc.

Rome, D.R., 1962. Exploration hydrobiologique du Lac Tanganyika (1946–1947). 3. Ostracods. Institut Royal Sciences Natural Belgique, Brussels 1- 309.

Roth, P.J., Lehndorff, E., Brodowski, S., Bornemann, L., Sanchez-García, L., Gustafsson, Ö., Amelung, W., 2012. Differentiation of charcoal, soot and diagenetic carbon in soil: method comparison and perspectives. Organic Geochemistry 46, 66-75.

Rothwell, R., Rack, F., 2006. New techniques in sediment core analysis: an introduction. Geological Society Special Publication 267, 1-29.

Rucina, S.M., Muiruri, V.M., Kinyanjui, R.N., McGuiness, K., Marchant, R., 2009. Late Quaternary vegetation and fire dynamics on Mount Kenya. Palaeogeography, Palaeoclimatology, Palaeoecology 283, 1-14.

Rumes, B., 2010. Regional diversity, ecology and palaeoecology of aquatic invertebrate communities in East African lakes. Ph.D. Thesis. University of Gent, Belgium.

Russell, J.M., Johnson, T.C., 2005. A high-resolution geochemical record from Lake Edward, Uganda Congo and the timing and causes of tropical African drought during the late Holocene. Quaternary Science Reviews 24, 1375-1389.

Russell, J.M., Johnson, T.C., 2007. Little Ice Age drought in equatorial Africa: Intertropical Convergence Zone migrations and El Niño -Southern Oscillation variability. Geology 35, 21 - 24.

Russell, J.M., Johnson, T.C., Kelts, K.R., Laerdal, T., Talbot, M.R., 2003 a. An 11,000 year lithostratigraphic and paleohydrologic record from Equatorial Africa: Lake Edward, Uganda-Congo. Palaeogeography, Palaeoclimatology, Palaeoecology 193, 25-49.

Sars, G.O., 1928. An account of the Crustacea of Norway, with short descriptions and figures of all the species: IX. Ostracoda.

Schmidt, M.W., Skjemstad, J.O., Czimczik, C.I., Glaser, B., Prentice, K.M., Gelinas, Y., Kuhlbusch, T.A., 2001. Comparative analysis of black carbon in soils. Global Biogeochemical Cycles 15, 163-167.

Schütt, B., Förch, G., Bekele, S., Thiemann, S., 2002. Modern water level and Sediment accumulation changes of Lake Abaya, southern Ethiopia-A case study from the northern lake area. Water Resources and Environment Research 2, 418-422.

References

Schutt, B., Thiemann, S., 2006. Kulfo River, South-Ethiopia as the regulator of lake level changes in the Lake Abaya-Lake Chamo System, Zbl. Geol. Paläont. Teil I, 2004, 129-143.

Segele, Z.T., Lamb, P.J., 2005. Characterization and variability of Kiremt rainy season over Ethiopia. Meteorology and Atmospheric Physics 89, 153-180.

Segele, Z.T., Lamb, P.J., Leslie, L.M., 2009. Seasonal-to-interannual variability of Ethiopia/Horn of Africa monsoon. Part I: associations of wavelet-filtered large-scale atmospheric circulation and global sea surface temperature. Journal of Climate 22, 3396-3421.

Seleshi, Y., Zanke, U., 2004. Recent changes in rainfall and rainy days in Ethiopia. International Journal of Climatology 24, 973-983.

Shibru, S., Woldu, Z., 2006. Comparative floristic study on Mt. Alutu and Mt. Chubbi along an altitudinal gradient. Journal of the Drylands1, 8-14.

Soromessa, T., Teketay, D., Demissew, S., 2004. Ecological study of the vegetation in Gamo Gofa zone, southern Ethiopia. Tropical Ecology 45, 209-222.

Stager, J.C., Cocquyt, C., Bonnefille, R., Weyhenmeyer, C., Bowerman, N., 2009. A late Holocene paleoclimatic history of Lake Tanganyika, East Africa. Quaternary Research 72, 47-56.

Stager, J.C., Cumming, B., Meeker, L., 1997. A high-resolution 11,400-yr diatom record from Lake Victoria, East Africa. Quaternary research 47, 81-89.

Stager, J.C., Cumming, B.F., Meeker, L.D., 2003. A 10,000-year high-resolution diatom record from Pilkington Bay, Lake Victoria, East Africa. Quaternary Research 59, 172-181.

Stone, J.R., Westover, K.S., Cohen, A.S., 2011. Late Pleistocene paleohydrography and diatom paleoecology of the central basin of Lake Malawi, Africa. Palaeogeography, Palaeoclimatology, Palaeoecology 303, 51-70.

Stracke, A., 2008. From the photography to the digitalized outline suitable for MORPHOMATICA. Contribution To Geometric Morphometrics Ber. Inst. Erdwiss. K.-F.-Univ. Graz ISSN 1608-8166 Band 13 69.

Street, F.A., Grove, A., 1979. Global maps of lake-level fluctuations since 30,000 yr BP. Quaternary Research 12, 83-118.

Stuiver, M., Polach, H.A., 1977. Reporting of C-14 data–discussion. Radiocarbon 19, 355-363.

References

Stuiver, M., Reimer, P.J., 1993. Radiocarbon calibration program Calib Rev 6.0.0. Radiocarbon 35, 215 - 230.

Stuiver, M., Reimer, P.J., Reimer, R., 2005. CALIB Radiocarbon Cali¬bration (rev. 5.0.2). On-line Manual. http://radiocar¬bon.pa.qub.ac.uk/calib/manual/.

Talling, J., Talling, I.B., 1965. The chemical composition of African lake waters. Internationale Revue der gesamten Hydrobiologie und Hydrographie 50, 421-463.

Telford, R.J., Lamb, H.F., 1999. Groundwater-mediated response to Holocene climatic change recorded by the diatom stratigraphy of an Ethiopian crater lake. Quaternary Research 52, 63-75.

Terwilliger, V.J., Eshetu, Z., Disnar, J.-R., Jacob, J., Paul Adderley, W., Huang, Y., Alexandre, M., Fogel, M.L., 2013. Environmental changes and the rise and fall of civilizations in the northern Horn of Africa: An approach combining δD analyses of land-plant derived fatty acids with multiple proxies in soil. Geochimica et Cosmochimica Acta 111, 140-161.

Terwilliger, V.J., Eshetu, Z., Huang, Y., Alexandre, M., Umer, M., Gebru, T., 2011. Local variation in climate and land use during the time of the major kingdoms of the Tigray Plateau in Ethiopia and Eritrea. Catena 85, 130-143.

Thevenon, F., Williamson, D., Vincens, A., Taieb, M., Merdaci, O., Decobert, M., Buchet, G., 2003. A late-Holocene charcoal record from Lake Masoko, SW Tanzania: climatic and anthropologic implications. The Holocene 13, 785-792.

Tilahun, G., Ahlgren, G., 2010. Seasonal variations in phytoplankton biomass and primary production in the Ethiopian Rift Valley lakes Ziway, Awassa and Chamo–The basis for fish production. Limnologica-Ecology and Management of Inland Waters 40, 330-342.

Trauth, M.H., Maslin, M.A., Deino, A.L., Junginger, A., Lesoloyia, M., Odada, E.O., Olago, D.O., Olaka, L.A., Strecker, M.R., Tiedemann, R., 2010. Human evolution in a variable environment: the amplifier lakes of Eastern Africa. Quaternary Science Reviews 29, 2981-2988.

Umer, M., Lamb, H., Bonnefille, R., Lézine, A.-M., Tiercelin, J.-J., Gibert, E., Cazet, J.-P., Watrin, J., 2007. Late Pleistocene and Holocene vegetation history of the Bale mountains, Ethiopia. Quaternary Science Reviews 26, 2229-2246.

Vavra, W., 1891. Ostracoden Bohmns 58-62.

Vavra, W., 1897. Die Süsswasser-Ostracoden Deutsch-Ostafrikas. Deutsch Ost Afrika 4, 1-28.

References

Verschuren, D., 2002. Climate reconstruction from African lake sediments. http://www.gsf.fi/esf_holivar.

Verschuren, D., Laird, K.R., Cumming, B.F., 2000. Rainfall and drought in equatorial east Africa during the past 1,100 years. Nature 403, 410-414.

Verschuren, D., Tibby, J., Sabbe, K., Roberts, N., 2000. Effects of depth, salinity, and substrate on the invertebrate community of a fluctuating tropical lake. Ecology 81, 164-182.

Weber, M.E., 1998. Estimation of biogenic carbonate and opal by continuous non-destructive measurements in deep-sea sediments: application to the eastern Equatorial Pacific. Deep-Sea Research Part I 45, 1955-1975.

Weber, M.E., Tougiannidis, N., Kleineder, M., Bertram, N., Ricken, W., Rolf, C., Reinsch, T., Antoniadis, P., 2010. Lacustrine sediments document millennial-scale climate variability in northern Greece prior to the onset of the northern hemisphere glaciation. Palaeogeography, Palaeoclimatology, Palaeoecology 291, 360-370.

Weber, M.E., Niessen, F., Kuhn, G., Wiedicke, M., 1997. Calibration and application of marine sedimentary physical properties using a multi-sensor core logger. Marine Geology 136, 151-172.

Wells, T., Cohen, A.S., Park, L., Dettman, D., McKee, B., 1999. Ostracode stratigraphy and paleoecology from surficial sediments of Lake Tanganyika, Africa. Journal of Paleolimnology 22, 259-276.

Whitlock, C., Anderson, R.S., 2003. Fire history reconstructions based on sediment records from lakes and wetlands, Fire and Climatic Change in Temperate Ecosystems of the Western Americas. Springer, pp. 3-31.

Whitlock, C., Larsen, C.P.S., 2001. Charcoal as a fire proxy. In: J.P. Smol, H.J.B. Birks and W.M. Last (Editors), Tracking Environmental Change Using Lake Sediments. Volume 3: Terrestrial, Algal, and Siliceous Indicators. Kluwer Academic Publishers, Dordrecht, The Netherlands, 75-97.

Whitlock, C., Millspaugh, S.H., 1996. Testing the assumptions of fire-history studies: an examination of modern charcoal accumulation in Yellowstone National Park, USA. The Holocene 6, 7-15.

WoldeGabriel, G., Heiken, G., White, T.D., Asfaw, B., Hart, W.K., Renne, P.R., 2000. Volcanism, tectonism, sedimentation, and the paleoanthropological record in the Ethiopian Rift System. Special Papers-Geological Society Of America, 83-99.

References

WoldeGabriel, G., Yemane, T., Suwa, G., White, T., Asfaw, B., 1991. Age of volcanism and rifting in the Burji-Soyoma area, Amaro horst, Southern Main Ethiopian Rift: Geo-and biochronologic data. Journal of African Earth Sciences (and the Middle East) 13, 437-447.

Wolf, M., Lehndorff, E., Wiesenberg, G.L., Stockhausen, M., Schwark, L., Amelung, W., 2013. Towards reconstruction of past fire regimes from geochemical analysis of charcoal. Organic Geochemistry 55, 11-21.

Wooller, M.J., Street-Perrott, F., Agnew, A., 2000. Late Quaternary fires and grassland palaeoecology of Mount Kenya, East Africa: evidence from charred grass cuticles in lake sediments. Palaeogeography, Palaeoclimatology, Palaeoecology 164, 207-230.

Wooller, M.J., Swain, D.L., Ficken, K.J., Agnew, A., Street-Perrott, F., Eglinton, G., 2003. Late Quaternary vegetation changes around Lake Rutundu, Mount Kenya, East Africa: evidence from grass cuticles, pollen and stable carbon isotopes. Journal of Quaternary Science 18, 3-15.

Yirgu, G., Ebinger, C.J., Maguire, P.K.H., 2006. The Afar volcanic province within the East African Rift System: introduction. Geological Society, London, Special Publications 259, 1-6.

Yusuf, H., Treydte, A.C., Demissew, S., Woldu, Z., 2011. Assessment of woody species encroachment in the grasslands of Nechisar National Park, Ethiopia. African Journal of Ecology 49, 397-409.

Zolitschka, B., Mingram, J., Van Der Gaast, S., Jansen, J.F., Naumann, R., 2001. Sediment logging techniques, Tracking environmental change using lake sediments. Springer, pp. 137-153.

Appendix A

Images of the cores with thier field depths as taken by MSCL

Appendix B

Results of outline analyses performed for comparing the SEM pictures of *Limnocythere* in Lake Chamo and the valve outline with other *Limnocythere* species in different ERVLS and East African lakes

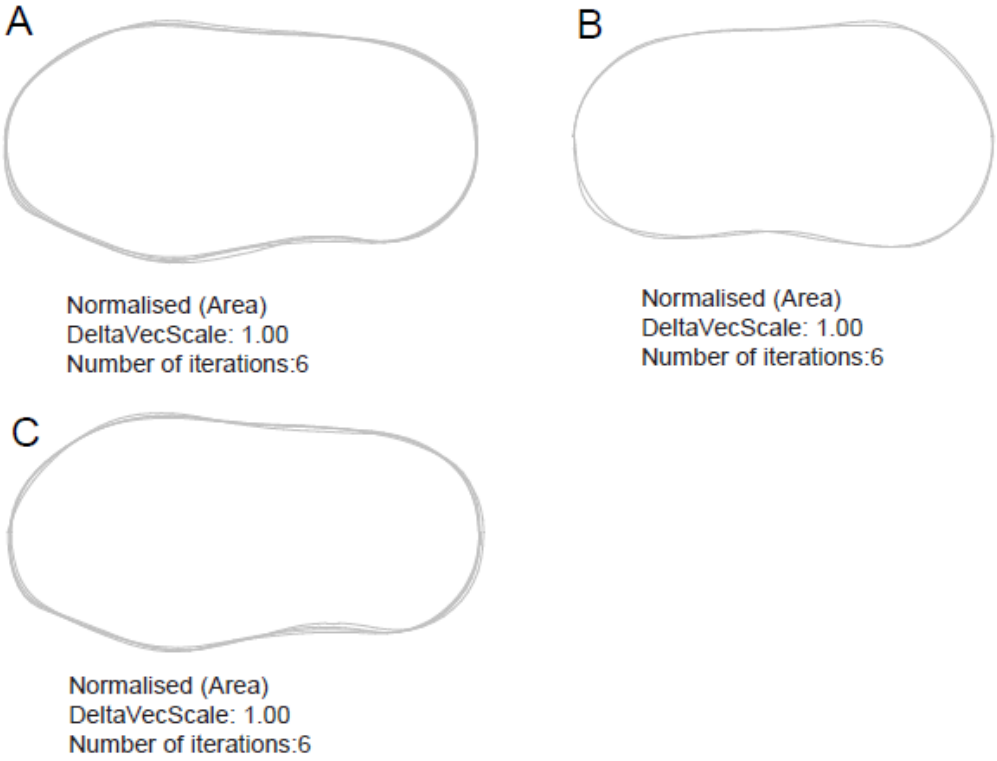

A. Outline analysis carried out on both right valves of male and left valves of female *L. africana* (A &B) and only right valve of male *L. minor* (C) and *Limnocythere* in Lake Chamo using a Geometric Morphometric approach. Comparison of mean outlines calculated for the species in "normalised for area" mode. The specimen cluster view for A [La_M_17_Q_RV_Ext vs. L1_M_TG2_40_RV_Ext, L1_M_TG2_41_RV_Ext, L1_M_TG2_43_RV_Ext], B [L a_F_17_P_LV_Ext and L2_F_TG4_10_LV_Ext], C [Lm_M_17_O_RV_Ext vs. L1_M_TG2_40_RV_Ext, L1_M_TG2_41_RV_Ext, L1_M_TG2_43_RV_Ext].

Appendix

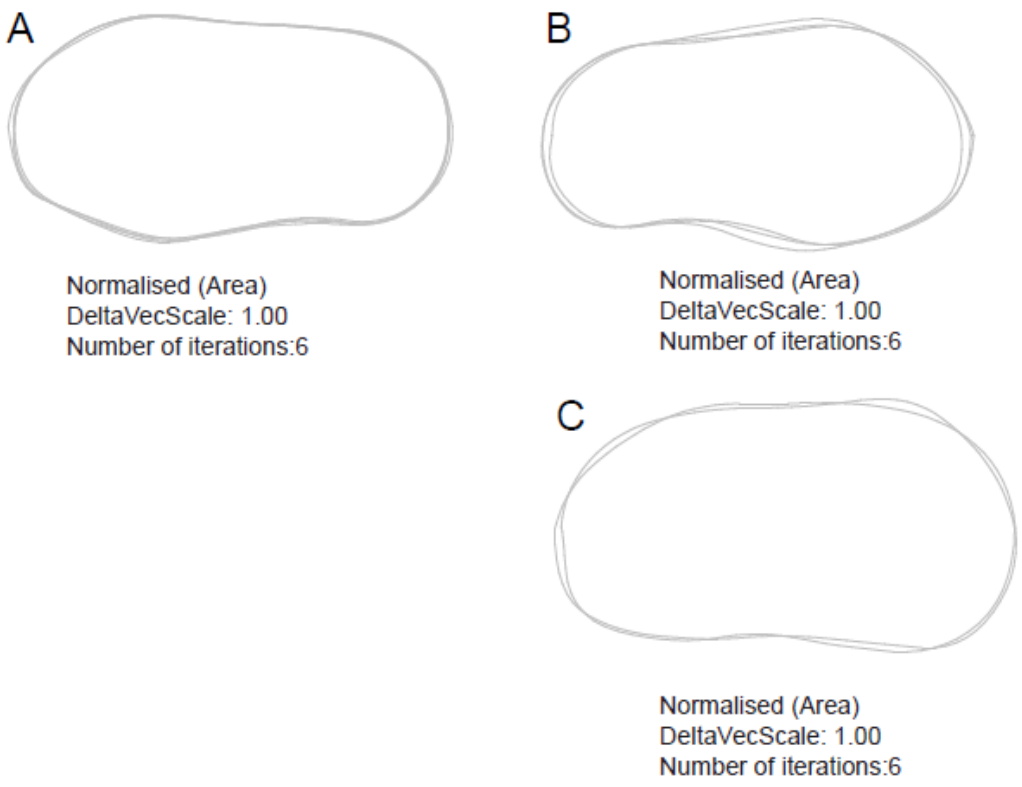

B. Outline analysis performed on both right and left valves of male and only left valves of female *L. borisi shalaensis* (Lake Langano) and *Limnocythere* in Lake Chamo using a Geometric Morphometric approach. Comparison of mean outlines calculated for the species in "normalised for area" mode. The specimen cluster view for A [Lbs_M_17_M_RV_Ext vs. L1_M_TG2_40_RV_Ext, L1_M_TG2_41_RV_Ext, L1_M_TG2_43_RV_Ext], B [L bs_M_17_L_LV_Ext vs. L1_M_TG4_ 1_LV_Ext], C [Lbs_F_17_N_RV_Ext vs. L2_F_TG4_10_LV_Ext].

Appendix

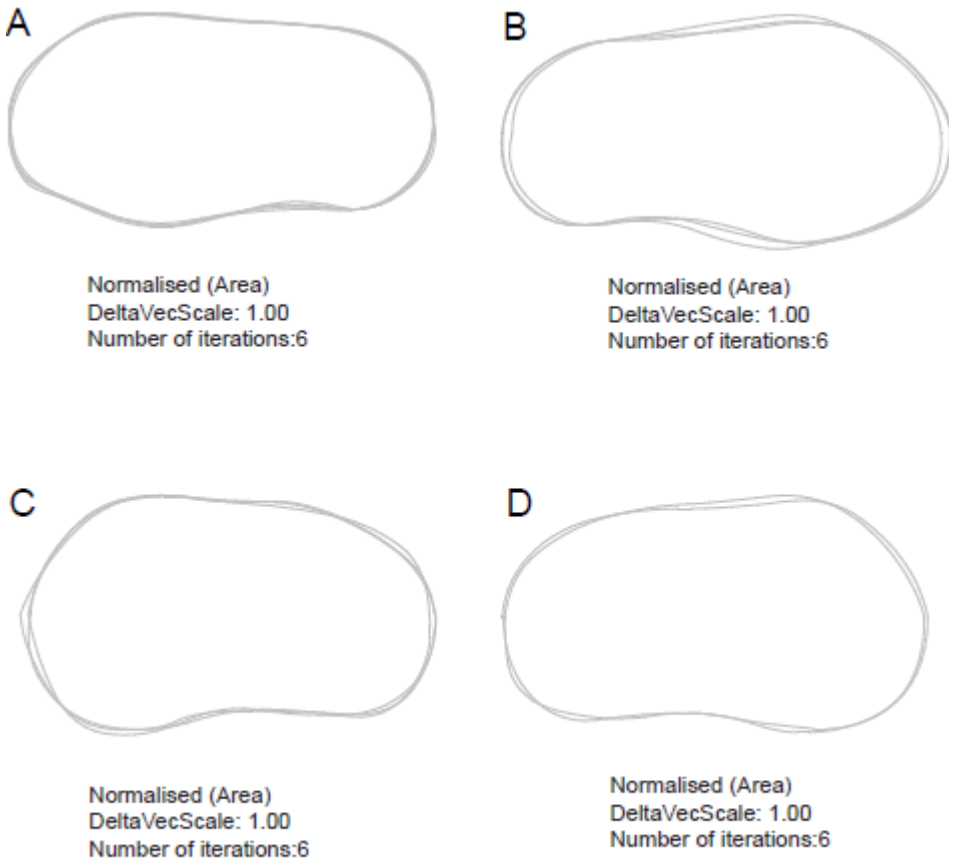

C. Outline analysis presented on both right and left valves of male and female *L. borisi borisi* and *Limnocythere* in Lake Chamo using a Geometric Morphometric approach. Comparison of mean outlines calculated for the species in "normalised for area" mode. The specimen cluster view for A [Lbb_M_17_A_RV_Ext vs. L1_M_TG2_40_RV_Ext, L1_M_TG2_41_RV_Ext, L1_M_TG2_43_RV_Ext], B [Lbb_M_17_B_LV_Ext vs. L3_M_TG4_21_LV_Ext, L3_M_TG4_23_LV_Ext], C [Lbb_F_17_E_RV_Ext vs. L2_F_TG4_7_RV_Ext, L2_F_TG4_9_RV_Ext], D [Lbb_F_17_F_LV_Ext vs. L2_F_TG4_10_LV_Ext].

Appendix

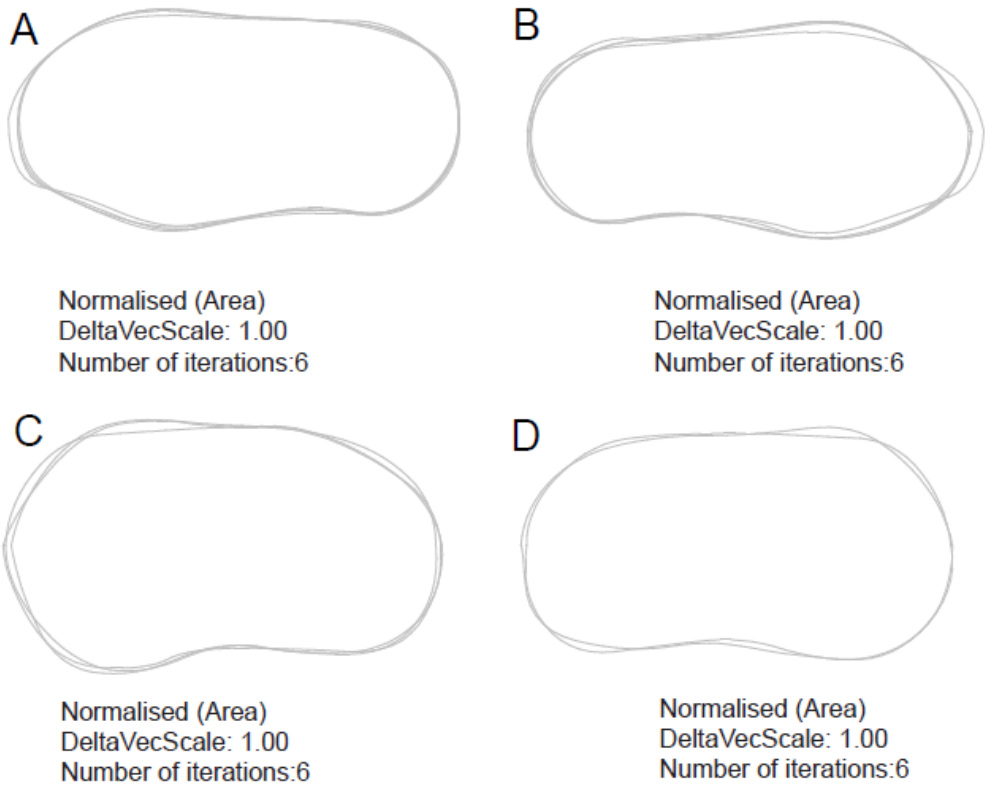

D. Outline analysis carried out on both right and left valves of male and female *L. borisi awassaensis* and *Limnocythere* in Lake Chamo using a Geometric Morphometric approach. Comparison of mean outlines calculated for the species in "normalised for area" mode. The specimen cluster view for A [Lba_M_19_D_RV_Ext vs. L1_M_TG2_40_RV_Ext, L1_M_TG2_41_RV_Ext, L1_M_TG2_43_RV_Ext], B [Lba_M_19_F_LV_Ext vs. L3_M_TG4_21_LV_Ext, L3_M_TG4_23_LV_Ext], C [Lba_F_19_E_RV_Ext vs. L2_F_TG4_7_RV_Ext, L2_F_TG4_9_RV_Ext], D [Lba_F_19_G_LV_Ext vs. L2_F_TG4_10_LV_Ext].

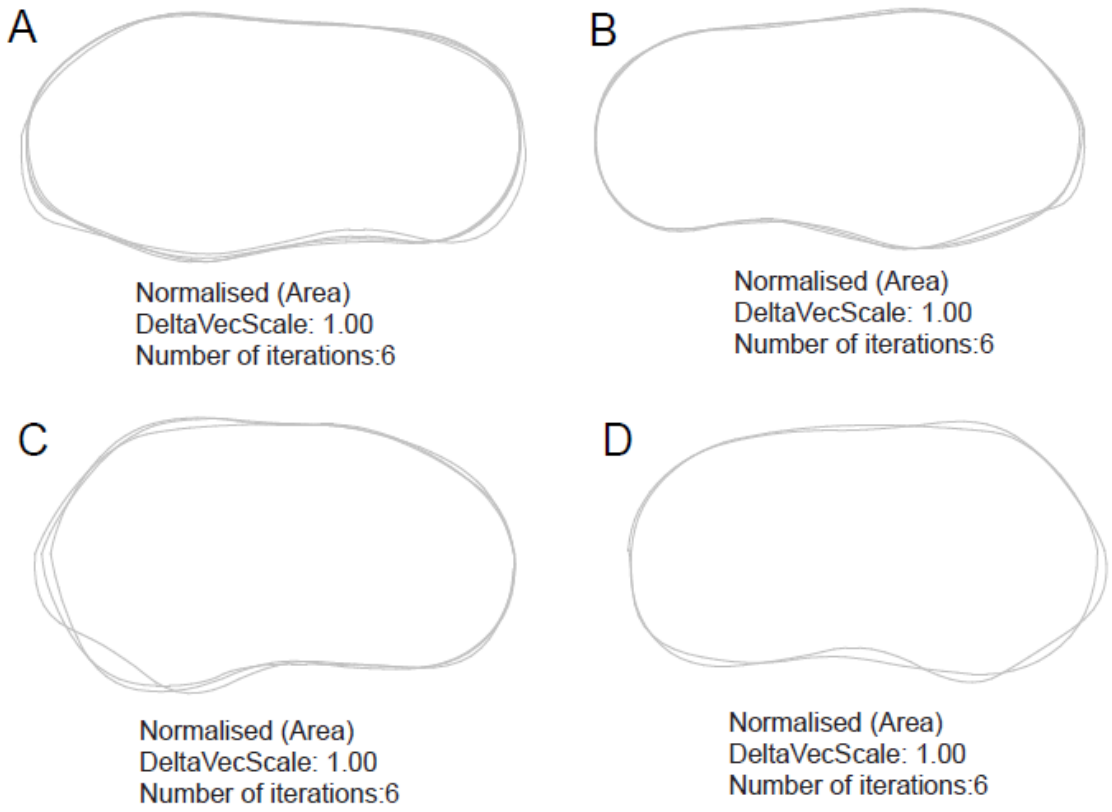

E. Outline analysis performed on both right and left valves of male and female *L.borisi shalaensis* (Lake Shala) and *Limnocythere* in Lake Chamo using a Geometric Morphometric approach. Comparison of mean outlines calculated for the species in "normalised for area" mode. The specimen cluster view for A [Lbs_M_18_P_RV_Ext vs. L1_M_TG2_40_RV_Ext, L1_M_TG2_41_RV_Ext, L1_M_TG2_43_RV_Ext], B [Lbs_M_18_Q_LV_Ext vs. L3_M_TG4_21_LV_Ext, L3_M_TG4_23_LV_Ext], C [Lbs_F_18_M_RV_Ext vs. L2_F_TG4_7_RV_Ext, L2_F_TG4_9_RV_Ext], D [Lbs_F_18_L_LV_Ext vs. L2_F_TG4_10_LV_Ext].

Appendix

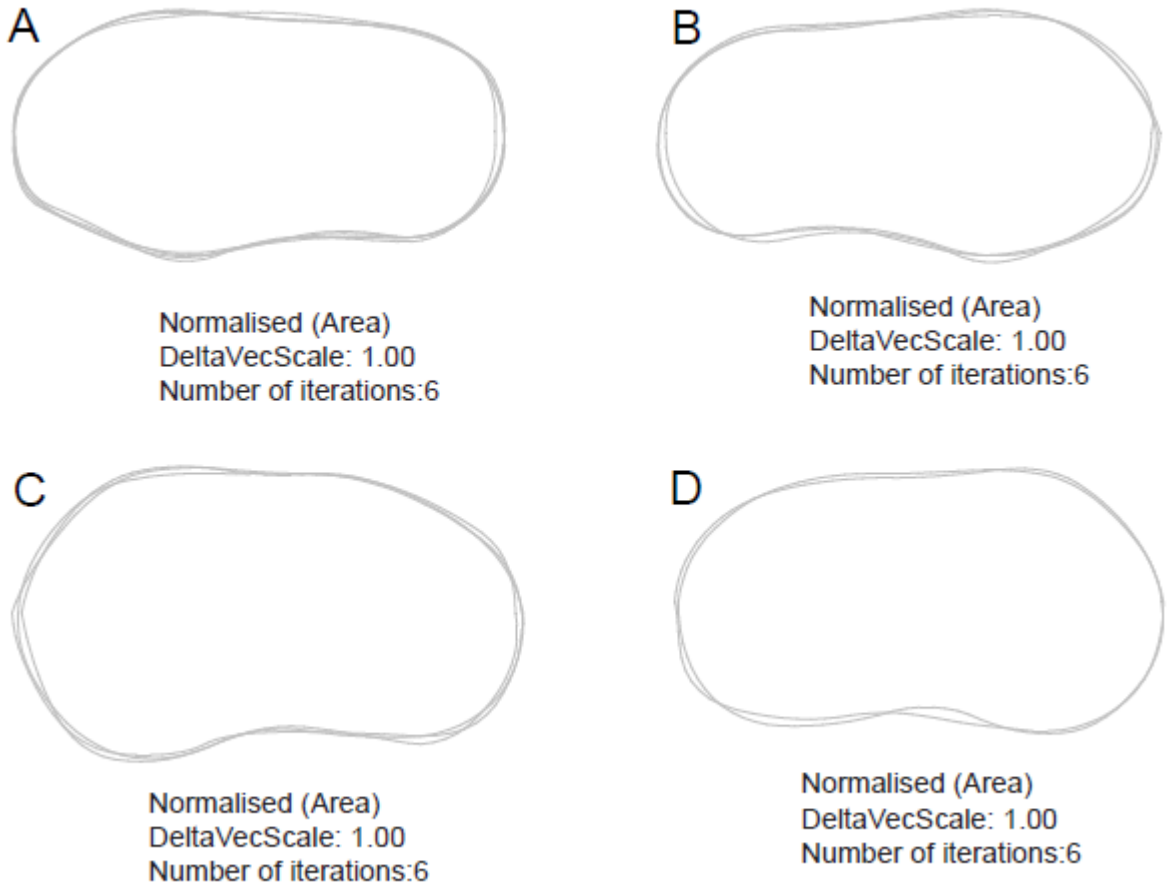

F. Outline analysis presented on both right and left valves of male and female *L. michaelseni Daday and L.dadayi* and *Limnocythere* in Lake Chamo using a Geometric Morphometric approach. Comparison of mean outlines calculated for the species in "normalised for area" mode. The specimen cluster view for A [Lm & Ld_M_19_N_RV_Ext vs. L1_M_TG2_40_RV_Ext, L1_M_TG2_41_RV_Ext, L1_M_TG2_43_RV_Ext], B [Lm & Ld_M_19_O_LV_Ext vs. L3_M_TG4_21_LV_Ext, L3_M_TG4_23_LV_Ext], C [Lm & Ld_F_19_S_RV_Ext vs. L2_F_TG4_7_RV_Ext, L2_F_TG4_9_RV_Ext], D [Lm & Ld_F_19_T_LV_Ext vs. L2_F_TG4_10_LV_Ext].

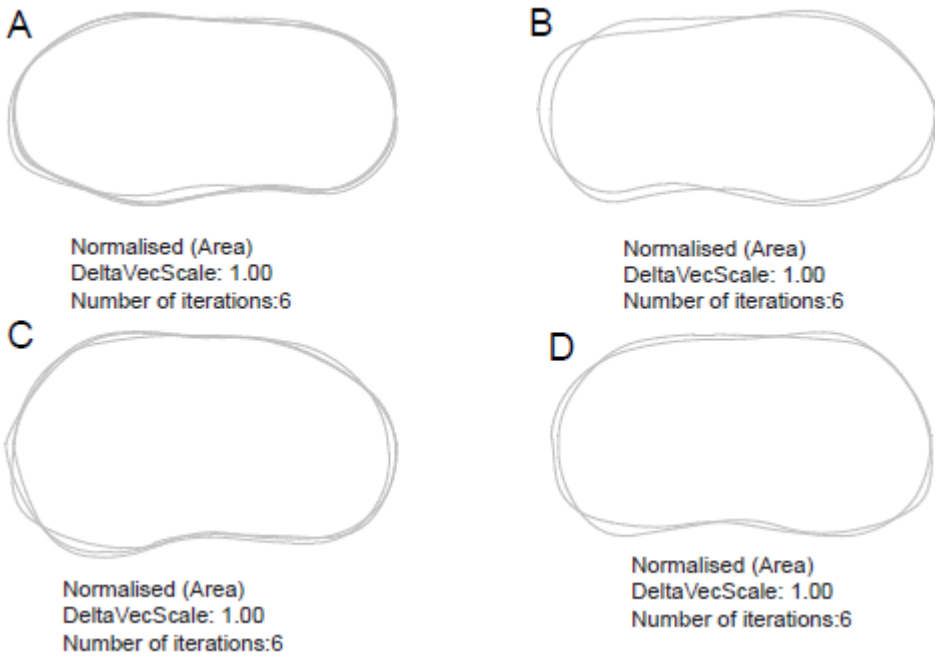

G. Outline analysis carried out on both right and left valves of male and female *L. thomasi langanoensis* and *Limnocythere* in Lake Chamo using a Geometric Morphometric approach. Comparison of mean outlines calculated for the species in "normalised for area" mode. The specimen cluster view for A [L tl_M_18_H_RV_Ext vs. L1_M_TG2_40_RV_Ext, L1_M_TG2_41_RV_Ext, L1_M_TG2_43_RV_Ext], B [L t l _M_18_G_LV_Ext vs. L1_M_TG4_ 1_LV_Ext], C [L t l_F_18_A_RV_Ext vs. L2_F_TG4_7_RV_Ext, L2_F_TG4_9_RV_Ext], D [L t l_F_18_B_LV_Ext vs. L2_F_TG4_10_LV_Ext].

Appendix

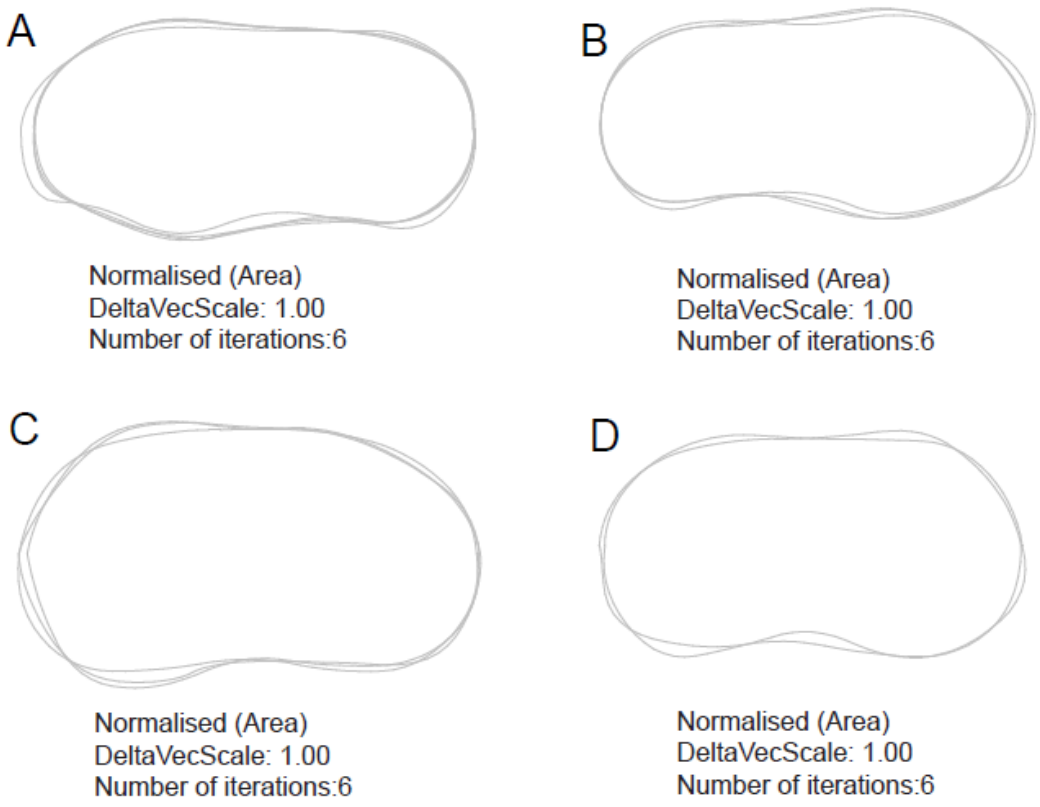

H. Outline analysis performed on both right and left valves of male and female *L. thomasi thomasi* and *Limnocythere* in Lake Chamo using a Geometric Morphometric approach. Comparison of mean outlines calculated for the species in "normalised for area" mode. The specimen cluster view for A [L tt_M_16_F_RV_Ext vs. L1_M_TG2_40_RV_Ext, L1_M_TG2_41_RV_Ext, L1_M_TG2_43_RV_Ext], B [L tt_M_16_G_LV_Ext vs. L3_M_TG4_21_LV_Ext, L3_M_TG4_23_LV_Ext], C [Ltt_F_16_K_RV_Ext vs. L2_F_TG4_7_RV_Ext, L2_F_TG4_9_RV_Ext], D [Ltt_F_16 _J_LV_Ext vs. L2_F_TG4_10_LV_Ext].

Erklärung

Ich versichere, dass ich die von mir vorgelegte Dissertation selbstständig angefertigt, die benutzten Quellen und Hilfsmittel vollständig angegeben und die Stellen der Arbeiteinschließlich Tabellen, Karten und Abbildungen-, die anderen Werken in Wortlaut oder dem Sinn nach entnommen sind, in jedem Einzelfall als Entlehnung kenntlich gemacht habe; dass diese Dissertation noch keiner anderen Fakultät oder Universität zur Prüfung vorgelegen hat; dass sie- abgesehen von unten angegebenen Teilpublikationen- noch nicht veröffentlicht worden ist sowie, dass ich eine solche Veröffentlichung vor Abschluss des Promotionsverfahrens nicht vornehmen werde. Die Bestimmungen der Promotionsordnung sind mir bekannt. Die von mir vorgelegte Dissertation ist von Prof. Dr. Frank Schäbitz betreut worden.

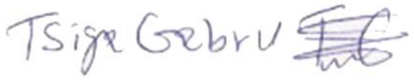

Köln, 2014

Tsige Gebru Kassa